UNIVERSITY OF CALIFORNIA
RIVERSIDE

Rescue of Intestinal Barrier Function Defects in PTPN2-Deficient Model Systems by the JAK-Inhibitor, Tofacitinib

A Dissertation submitted in partial satisfaction
of the requirements for the degree of

Doctor of Philosophy

in

Biomedical Sciences

by

Anica Dominique Pizarro Sayoc

March 2020

Dissertation Committee:
Dr. Declan F. McCole, Chairperson
Dr. Christian Lytle
Dr. David Lo

The Dissertation of Anica Dominique Pizarro Sayoc is approved:

_____

_____

_____

Committee Chairperson

University of California, Riverside

Acknowledgements

First, I would like to thank my PI and mentor Dr. Declan F. McCole for giving me the opportunity to work in the lab and making all of this possible. Thank you for taking a chance on me, giving me an awesome project, and for having faith in me. Thank you for teaching me how to be critical of my own work and those of others. You encouraged me to look at the world from different perspectives and not just take everything I read or see at face value (even if I still do). Most of all, thank you for your patience. You believe in me so much more than I believe in myself, and for that, I am truly grateful.

To Dr. Christian Lytle, thank you so much for always making sure I'm doing okay. Despite your busy administrative and teaching schedules, you always made time for your students. Your passion for intestinal physiology and metabolites is admirable. Thank you for teaching me how the humble gut does so much for us and that the simplest experiments are the ones that give us the most wisdom. Thank you for listening, for giving great advice, and for the unwavering support.

To Dr. David Lo, thank you for always sharing your newest and coolest findings with me. I learn so much from our meetings, and even when I can't keep up, you make sure you to explain concepts before moving on. Thank you for all the pep talks and your valuable input to my project during these last couple of years.

The McCole lab members, current and past, deserve a very big thank you. I appreciate all of your support, help, and friendship. Dr. Marianne Spalinger, I would not have finished this without you. I'm still star-struck that I get to work with you when I used to just cite your papers. Thank you so much for your willingness to help move my

project along and for teaching me what it's like to be high-throughput. You should've come to the lab sooner. Dr. Moorthy Krishnan, thank you for the guidance and mentorship, especially during my first few years in the lab. Thank you Rosie Alvarez for teaching me how to handle mice for the very first time. I treasured our time working in the McCole lab together and I will always miss working with you. For teaching me so much about lab and life, thank you. Dr. Ali Shawki, thank you for showing me how to do things the right way. You are meticulous and thorough when it comes to lab work and you give such great advice, too, about everything. Thank you for your wisdom. Vinicius Canale, you are a something else. Thank you for hearing me out and for showing me what perseverance, patience, and prayer can do. Thank you Pritha Chatterjee for always being so kind and encouraging. Even when both of our experiments are not working, you always show me the brighter side of things. To all of my mentees who have helped me run all the Western blots, process samples, and take inventory, a special thank you to Reyna Preciado, Jossue Jimenez, Kyle Gibson, Rebecca Hernandez, Christ Ordookhanian, and Madhumitha Pudukottai.

To my labmate since day 1, my fellow Disney fanatic: Dr. Stephanie King. Through the good times and really, really bad times, thank you for always being there for me, with me. I appreciate and admire you as a scientist, as a person, as a friend. A very huge thank you to Alina Santos for always checking up on me and offering to help me in lab. You're smart and hard-working and you're so considerate of others. Thank you for our talks, sticky notes, and texts with words of encouragement, which have helped me immensely through this last stretch of my PhD. To Parima Udompholkul, thank you for

all the laughs and all the snacks (which are so important!). You've taught me so much about how to have more confidence in myself and you helped me work through so many dilemmas. You are resilient and I admire you for your strength and generosity. Finally, to the strongest person I have ever met, Dr. Nancy Lainez. Thank you so much for being there, for listening, for understanding. I have leaned on you so many times for support and I'm so lucky and grateful for you and your friendship. Thank you for constantly reminding me that I'm not alone.

To my mentors, especially Dr. Ethan Chen and Dr. Mary Lorenson, thank you very much for all of the advice since the very beginning. I've always held my rotation in the Walker lab very dear to my heart. Thank you to Dr. Emma Wilson for being available in my times of crisis, to Dr. Monica Carson for empowering me regarding the Pizza Friday budget, to Dr. Djurdica Coss for troubleshooting tips and for allowing our lab to use her equipment (especially the precious plate reader!), and to my fellow BMSC students for all the great conversations we have together. Thank you also to the rest of the UCR Biomedical Sciences faculty and staff for their enthusiasm and support of BMSC students.

Thank you to our collaborators, Dr. Shujun (Lisa) Fan and Dr. Grant Butt from the University of Otago, New Zealand for the beautiful work on the colonoids. Thank you both for your time, hard work, and input on such a major part of the tofacitinib project.

I would like to thank my friends back home who never stop inviting me to outings despite years of limited availability. Thank you especially to my good friend Guia Panajon for this. I would also like to give a very big thank you to my loving family.

Mommy and Tito John, thank you for feeding Mike and me. Thank you for being patient with me and I hope I make you proud. To Kaye, Alex, Kuya, Carla, my second family Ninong Elmo, Ninang Chu, Kuya Allan, and Anna, thank you so much for pushing me to keep going and finish my degree. To my in-laws: Muchisimas gracias por todo y por sus apoyos. Los amo mucho. Lo siento que estoy siempre ocupada.

Finally, I would like to give a very special and sincere thank you to my loving husband. Thank you so much for supporting me throughout this whole journey. You have taken care of me and have been so patient. I could not have done this without you. Truly.

The text of this dissertation, in part, is a reprint of the material as it appears in *Inflammatory Bowel Diseases* (Chapters 2). The co-author Declan F. McCole listed in that publication directed and supervised the research that forms the basis for this dissertation.

ABSTRACT OF THE DISSERTATION

Rescue of Intestinal Barrier Function Defects in PTPN2-Deficient Model Systems by the JAK-Inhibitor, Tofacitinib

by

Anica Dominique Pizarro Sayoc

Doctor of Philosophy, Graduate Program in Biomedical Sciences
University of California, Riverside, March 2020
Dr. Declan F. McCole, Chairperson

The multifactorial etiology of inflammatory bowel disease (IBD), which consists of Crohn's disease (CD) and ulcerative colitis (UC), has posed significant challenges in the development of treatment options for affected patients. IBD therapeutics including steroids and immunosuppressive agents are focused on controlling symptoms of inflammation rather than targeting specific molecules. Despite the development of biologics such as anti-TNF (infliximab), representing a shift in IBD therapeutics, about half of IBD patients do not respond or lose response over time to conventional and biologic therapies, thus leaving IBD patients no options but to undergo surgery to resect affected regions of the intestine. Fortunately, small-molecule Janus kinase (JAK) inhibitors have shown promising results in patients with IBD. In particular, the pan-JAK inhibitor tofacitinib has been approved for the treatment of moderate-to-severe UC. Despite its effectiveness in inducing a clinical response and maintaining remission in UC

patients, little is known about which cells involved in gut homeostasis, including intestinal epithelial cells (IECs), are targeted. The aim of the work described in this dissertation is to elucidate if and how tofacitinib exerts its beneficial effects on IECs and epithelial barrier function.

Using IEC culture and human enteroids challenged with cytokine-induced barrier dysfunction, we show for the first time that tofacitinib can reduce barrier permeability through claudin-2 regulation and normalization of ZO-1 localization. Through cell culture and animal models we also show that the signaling and barrier defects associated with loss of activity of the IBD susceptibility gene, protein tyrosine phosphatase non-receptor type 2 (*PTPN2*), can be corrected by tofacitinib. Additionally, the compromised barrier function arising from disrupted crosstalk between macrophages and IECs induced by *PTPN2* loss was also reversed by tofacitinib treatment *in vivo* and *in vitro*.

Overall, the data in this dissertation show that tofacitinib can protect barrier integrity in IECs and reverse the consequences caused by a genetic defect in *PTPN2*. These data reveal the need for more specific IBD treatments on an individual basis. Tofacitinib may serve as a more effective treatment for IBD patients with *PTPN2* loss-of-function mutations, thus leading to longer periods of remission and better quality of life.

Table of Contents

List of Figures

Chapter 2

Chapter 3

List of Tables

Chapter 1: Introduction

Function and structure of intestinal epithelium

The intestinal epithelium plays a crucial role as a physical barrier in maintaining separation of the environment from the host. The intestinal epithelial cells (IECs) lining the entire mucosal surface of the intestines absorb nutrients and secrete fluid and factors through ion-coupled channels. New IECs originate from the stem cell niche residing at the bottom of the crypts then migrate up the villus as they differentiate into specific cell types. The crypt-villus axis constantly renews itself every 3-5 days as senescent cells undergo anoikis at the villus tip. The channels present in both the apical and basolateral regions of the cell tightly regulate the balance between fluid and electrolyte concentrations in and out of IECs .

Intestinal barrier function and permeability

The barrier function of the intestinal epithelium depends on multiple factors. The epithelial cells themselves physically serve as a barrier. Commensal bacteria fend off opportunistic and pathogenic microbes and provide factors necessary for IEC growth and function. The mucus layer also provides a matrix to keep luminal contents distant from the IECs and lubricate the mucosa to protect it from mechanical stress. Cell junctional protein complexes connect neighboring IECs together while regulating paracellular passage of electrolytes, fluid, and macromolecules. Although the microbial and chemical barriers contribute greatly to intestinal integrity, this dissertation will mainly focus on tight junction proteins as the regulators of intestinal epithelial barrier function.

The net functions of the pore, leak, and unrestricted barriers ultimately dictate how permeable or "leaky" the epithelial barrier is. Each with their own charge- and size-selective properties, the expression and proper localization of proteins that make up junctional complexes collectively dictate the integrity of the barrier.

Pore pathway of permeability

The pore-pathway of permeability allows for the paracellular passage of fluid and electrolytes. Functional assessment of the pore barrier is conducted by measuring the transepithelial electrical resistance (TER) across a monolayer of IECs which indicates the net flux of all ions across the epithelium [1],[2]. The main and primary regulators of the pore pathway are the claudin family of tetraspan membrane proteins. There are 24 claudins, each with their own unique function and regulation, which are expressed in various epithelial tissues throughout the body. This dissertation will focus on the expression and function of claudins in the intestine. Claudins 1 and 4 have barrier-sealing properties that restrict the paracellular passage to cations, while claudins 2 and 15 have pore-forming properties and increase permeability to cations [3]. Claudin-2 also enhances water efflux through its biophysical properties in acting as a *de facto* 'water channel'. This is clinically relevant since fluid secretion can contribute to diarrhea, the main symptom of IBD, and biopsies from patients with active IBD express higher levels of claudin-2 compared to non-inflamed controls [4]. Although the function of claudin-2 to form pore channels is physiologically important, its upregulation has been suggested as a biomarker for IBD [5].

Leak pathway of permeability

The leak pathway of permeability allows for the paracellular passage of macromolecules such as bacterial proteins. Unlike the pore pathway, the leak pathway is not charge-selective [6]. Paracellular passage of tracers or probes such as the fluorescein isothiocyanate-fluorescently-labeled 4kDa dextran (FD4), over time, can serve as a direct measure of macromolecular permeability across the leak barrier [1],[2]. Four of the tight junction proteins regulating this pathway will be discussed in this dissertation, include zonula occludens-1 (ZO-1), JAM-A, occludin, and tricellulin. ZO-1 is not a transmembrane protein, but instead stabilizes and binds tight junction proteins to the actin cytoskeleton and is required for the regulation and assembly of tight junction proteins [7],[8]. Depletion of ZO-1 in MDCK cells resulted in increased barrier defects for larger solutes without affecting flux through claudin pores [8]. Junctional Adhesion Molecule (JAM-A) is another tight junction protein that regulates macromolecular permeability. Cells with a transient knockdown of JAM-A exhibited reduced TER, while colonic mucosal sheets from JAM-A knockout mice had increased FD4 flux [9]. Occludin was the first identified transmembrane protein and contributes to the paracellular seal of the epithelium [7],[10]. It has 4 transmembrane domains and requires binding to ZO-1 in order to be localized at tight junctions [7],[10]. Tricellulin, which belongs to the same family of transmembrane proteins as occludin (MARVEL: MAL and related *proteins* for vesicle trafficking and membrane link), also restricts passage of larger solutes without affecting ion permeability [11]–[13]. Although it has overlapping functions with

occludin, it is primarily localized at tricellular contacts, but can localize to bicellular junctions to compensate for loss of occludin [11]–[14].

Unrestricted pathway of permeability

Lastly, the unrestricted pathway of intestinal permeability can also be assessed as an indicator of epithelial damage or apoptosis [2]. Independent of tight junctions, large proteins and bacteria can pass through this pathway, which usually occurs in severe intestinal inflammation and robust epithelial injury [2]. Passage of larger probes, such as the Rhodamine B-labeled 70kDa dextran (RD70), can serve as a functional assessment of impaired barrier function due to epithelial damage.

Tight junction localization

In addition to the expression of proteins that make up the tight junction complex, the localization of tight junction proteins is absolutely crucial to their function. The pro-inflammatory cytokine IFN-γ induces tight junction disassembly in an *in vitro* model by internalizing tight junction proteins via macropinocytosis [15]. Additionally, increased FD4 permeability by IFN-γ was correlated, not with a decrease in ZO-1 protein expression, but mislocalization [16]. The phosphorylation of myosin light chain (MLC) contracts the perijunctional actomyosin ring, which pulls on the tight junction proteins thereby increasing the paracellular space between IECs resulting in increased paracellular permeability [17]. Furthermore, as an IEC is shed from the villus tip, it sends signals to adjacent cells to contract actin-myosin rings, which directs tight junction proteins to the

basal surface of the apoptotic cell to rapidly re-establish the epithelial layer and maintain the barrier, even when large numbers of cells are apoptosing [2],[18]. These results suggest that permeability can be altered independent of tight junction protein expression, and that the regulation of the tight junction complex is highly dynamic. Even if "holes" or "gaps" are presented by mislocalization of tight junction proteins, in normal conditions, these appearances are transient and rare [13]. A reduced number of tight junction strands between cells does not mean this is an open vertical path for solutes and fluid [13]. The overall net result of tight junction protein expression, interaction, and localization determines barrier function.

Inflammatory bowel disease (IBD)

Inflammatory bowel disease (IBD), referring to two main conditions Crohn's disease (CD) and ulcerative colitis (UC), is a chronic, remitting and relapsing condition affecting the gastrointestinal tract. IBD has been reported to affect 3.5 million people in North America and Europe, and is on the rise, with increasing incidence rates in Africa, Asia, and South America where IBD has not been previously observed [19]. Clinical symptoms of IBD include abdominal pain, weight loss, loss of appetite, fever, anemia due to blood loss, and diarrhea. Poorer quality of life has been reported in both adult and pediatric patients with IBD, compared to healthy controls [20]. The cost of care for IBD, which includes therapeutics, emergency room visits, hospitalizations, and surgeries have added up to an average of $22,987 paid claims per year and $2,213 out-of-pocket costs per year, amounts that are 2-3-fold higher compared to non-IBD patients [21]. It is during

the first year after diagnosis that IBD patients incurred the most costs [21]. Reduced work productivity and school absenteeism are also higher in IBD patients [22],[23].

The etiology of IBD is multifactorial, involving genetics, the immune system, the epithelial barrier, and gut microbial flora, as drivers of the disease [24]. Environmental factors such as diet, lifestyle, smoking, and the use of antibiotics also affect the interplay between these factors and can act as triggers to initiate or exacerbate symptoms [24]. Because of this, there is currently no cure for IBD, but with the huge financial and life-long burden it entails, it is crucial to continue improving our understanding of IBD.

Crohn's disease

Despite sharing similar features, differences in the histopathology of CD and UC make each condition distinct. Crohn's disease (CD) is characterized by "skip lesions", which can occur anywhere in the gastrointestinal tract [25]–[27]. The patchy inflammation observed in CD is transmural, thus affecting all layers of the intestinal wall [25]–[27]. CD is marked by macrophage recruitment and granuloma formations in the gut [25]–[27]. Gross features include a "cobblestoning" appearance and thickened wall of the intestine [25]–[27]. Focal crypt distortion has also been observed in CD [25]–[27]. CD is mediated primarily by T-helper type 1 (Th1)/Th17 immune responses characterized by high IFN-γ levels in intestinal tissues [28],[29]. Th1 cells secrete cytokines, such as IFN-γ, and are effective against intracellular virus and bacteria infections that grow in macrophages [30].

Ulcerative colitis

Ulcerative colitis (UC) almost exclusively affects a continuous area in the distal regions of the colon [25],[26],[31]. Histologically, UC affects only the intestinal mucosa [25],[26],[31]. The clinical manifestation of UC is characterized by large recruitment of neutrophils and formation of ulcerations, appearing as pseudopolyps, and dysplasia [25],[26],[31]. Diffuse, continuous distortion and atrophy of crypts, leading to shortened colon and lumen narrowing is typical of UC [25],[26],[31]. UC has been associated with a T-helper type 2 (Th2) response mediated by natural killer T cells producing IL-13, which has cytotoxic effects on HT29 IECs [32]. Th2 cells secrete cytokines, including IL-13, which upregulate antibody production and protect against parasitic infections [30].

Pediatric IBD

About 20% of IBD patients were diagnosed under the age of 18 [33],[34]. Although they make up a fraction of IBD patients, they are the most difficult to treat since, in addition to symptoms mentioned previously, physiological and emotional complications are most vulnerable during childhood [34]. Primarily, failure to thrive has been the major issue [35], especially in children diagnosed with IBD below the age of 5. Vitamin and nutrient deficiencies are common in these patients due to intestinal malabsorption and chronic inflammation. Bone health in pediatric patients is also impaired due to chronic inflammation, and has been correlated with increased serum levels of the pro-inflammatory cytokine IL-6 [36]. This is criticial since most adult bone mass is achieved by adolescence, putting patients at risk for bone fractures later in life

[35]. In addition, clinical manifestations of pediatric IBD can vary, with children and adolescents presenting with extraintestinal symptoms that may lead to a misdiagnosis, thus resulting in delay of treatment. Children and adolescents with IBD also suffer psychosocially, as depression and anxiety positively correlate with disease activity [37],[38]. Overall strategies for pediatric IBD patients are therefore aimed at eliminating symptoms to restore normal growth and improve quality of life [35].

IBD and immune function

The abnormal and robust immune response to microbial flora and environmental antigens is characteristic of IBD. This is thought to be due to the imbalance between anti- and pro-inflammatory immune cells and mediators which results in a drastic immune response [39]. The cytokines that mediate immune cell activation, recruitment, and amplification of cytokine production dictate the environment for intestinal homeostasis or inflammation [40],[41]. The infiltration of both innate and adaptive immune cells including macrophages, neutrophils, dendritic cell, and T cells into the gut lamina propria is followed by the release of pro-inflammatory cytokines. Interferon-gamma (IFN-γ) released by T cells are increased in tissues from CD patients [42]–[44]. Tumor necrosis alpha (TNF-α) secreted by multiple cell types such as macrophages, T cells, dendritic cells, and fibroblasts, in turn cause pro-inflammatory cytokine production and inhibition of M2 macrophages as well as IEC death and impaired barrier function [40].

Macrophages are an essential part of the innate immune system that play key roles in mucosal homeostasis in the gut [45],[46]. As part of the largest immune component in

the body, intestinal macrophages underlying the epithelial cells remove debris and invading pathogenic bacteria, as well as communicate with other immune cells to help coordinate specific responses. Macrophages produce anti-inflammatory cytokines such as IL-10, which act on T cells to suppress colitis [47]. Macrophages that are recruited to the site of inflammation in the gut secrete cytokines IL-6, TNF-α, and IL-1β [48]. Complexities of the effects of IL-6 have to be noted considering that classically-activated macrophages (CAM, M1) treated with IL-6 secreted more pro-inflammatory IL-1β upon exposure to bacterial lipopolysaccharide (LPS) but also promote IL-10 secretion in alternatively-activated macrophages (AAM, M2) [49]. Recruited or resident tissue macrophages in the gut interact intimately with IECs and therefore regulate intestinal epithelial function also through direct communication via hetero-cellular gap junctions [50].

JAK-STAT signaling in IBD

The Janus kinase (JAK)-signal transducer and activator of transcription (STAT) pathway translates extracellular signals to cellular functions [51]. There are four members of the JAK family of non-receptor kinases: JAK1, JAK2, JAK3, and tyrosine kinase 2 (TYK2). Downstream effector STATs include STAT1, STAT3, STAT4, STAT5a/b, and STAT6. Upon binding of a cytokine to its respective receptors, JAKs associated with these receptors are brought in close proximity to each other and are phosphorylated via auto- or trans-phosphorylation by other JAKs. JAKs also phosphorylate cytosolic regions of the receptors, which then serve as docking sites for STATs. JAKs then phosphorylate

docked STATs, which dimerize, translocate to the nucleus, and serve as transcription factors for specific genes [51].

The JAK-STAT signaling pathway mediates and converts extracellular stimuli, from a variety of cytokines (small proteins produced mainly by cells), to the nucleus to carry out cellular response and functions [39],[51]. These functions include cell growth, survival, proliferation, differentiation, migration, and immune functions. Genome-wide association studies have identified that mutations in JAK2, TYK2, and STAT3 are associated with increased IBD susceptibility risk [52]. Common cytokines associated with IBD signal through the JAK-STAT pathway, including IL-6, IL-10, and IFN-γ [53]. Thus, the JAK-STAT signaling pathway is an important contributor to the pathogenesis of IBD, and by extension, an important target for therapeutic intervention.

IBD treatments

Treatments for IBD currently include steroids, immunosuppressants, and biologics. These treatments are meant to control inflammation and have been successful in that aspect of IBD to some extent. Steroids and immunosuppressants relieve inflammation and pain, but are broad-acting and lack specificity. Biologics such as anti-TNF antibodies, were intended to alleviate the effects of pro-inflammatory cytokine TNF-α (upregulated in IBD) which activates and recruits immune cells, damages epithelial cells, and promotes the production of more pro-inflammatory cytokines [54]. Other biologics include antibodies against adhesion molecules, such as α4β7, which immune cells need to adhere to endothelial cells in the gut before infiltrating the lamina

propria underlying the IECs [54]. Unfortunately, one-third to half of the patients with IBD do not respond well or lose response over time to these treatments due to the development of antibodies against these biologics [55],[56]. In addition, these biologics are administered intravenously or subcutaneously, and are significantly more expensive than conventional therapies. Non-compliance from patients to go to a facility to receive these treatments therefore jeopardizes the effectiveness of these therapeutics [55].

Small-molecule Janus kinase (JAK) inhibitors have been developed as small molecule alternatives for the treatment of IBD [57]. In particular, tofacitinib has shown greater efficacy in inducing a clinical response and maintaining remission than placebo in clinical trials [58], and therefore has been FDA-approved for the treatment of moderate-to-severe UC. In addition, as an orally-administered drug, tofacitinib is not immunogenic, has a tolerable safety profile, and is less expensive than biologics, thus making it more affordable and more patient-friendly with respect to administration [55].

After oral administration, peak plasma concentrations of tofacitinib are reached within 0.5-1 hour. Tofacitinib has a half-life of about 3 hours, although steady state concentrations are achieved in 24-48 hours after twice daily administration. Tofacitinib citrate has an oral bioavailability of 74%, with protein binding of 40% predominantly to albumin. Tofacitinib is cleared from the body via hepatic metabolism (70%, primarily by CYP3A4) and renal excretion (30%) of the parent drug. In a radiolabeled tofacitinib study in humans, more than 65% of the total circulating radioactivity was found to be unchanged tofacitinib and 35% to be 8 tofacitinib metabolites. The pharmacologic activity of tofacitinib is attributed mainly to the parent molecule [59].

Although tofacitinib has been shown to relieve macroscopic features of IBD in clinical trials, little is known about how it directly affects IECs and other cell types responsible for gut homeostasis.

IBD and barrier function

Compromised intestinal barrier function marked with increased barrier permeability is an early critical event and hallmark of chronic diseases, such as IBD [2],[60]–[62]. The main function of the intestinal epithelial barrier is to separate the environment (luminal components) from the host. When the intestinal barrier is compromised, it can lead to unregulated flux of ions and water into the lumen, which contributes to diarrhea, and increase the access of microbial products and food antigens into the underlying tissue, which could initiate or further propagate inflammation. In turn, due to the inflammation caused by the immune system's intolerance to bacterial proteins or antigens, damage occurs to the IECs. Because of this, intestinal permeability has been considered as an important early step in IBD pathogenesis as well as a functional predictor of the disease course of IBD [62]–[65]. Increased permeability has even been found to precede inflammation [66]. Regardless, measurement of intestinal permeability is not included as common practice in the diagnosis of IBD.

***PTPN2* in IBD**

In general, IBD is thought to be an inappropriate immune response to the normal gut flora in genetically-susceptible individuals. There are currently 201 gene loci with

231 distinct single nuclei polymorphisms (SNP) identified to increase susceptibility to IBD, most of which affect the interaction between IECs and the immune system, microbiome, and environmental factors [52],[67]–[69]. One of these genes is the protein tyrosine phosphatase non-receptor type 2 (*PTPN2*), which encodes for the T cell protein tyrosine phosphatase (TCPTP).

Protein phosphorylation is a post-translational modification and serves as a mechanism by which enzyme function can quickly be activated or deactivated. The balance in activity between kinases and phosphatases regulate specific cell functions during homeostasis and inflammation [70]. SNPs in the gene locus of *PTPN2* have been linked to type I diabetes, celiac disease, CD and UC [24],[67],[71]. Two isoforms of PTPN2 exist: the 45kDa isoform (TC-45), with a nuclear localization signal, can shuttle in and out of the nucleus, and the 48kDa isoform (TC-48) which is bound to the endoplasmic reticulum [72],[73]. As a tyrosine phosphatase, PTPN2 targets and deactivates a number of tyrosine kinases such as the epidermal growth factor receptor (EGFR), insulin receptor (IR) β, and members of the Janus kinase-signal transducer and activator of transcription (JAK-STAT) signaling pathway, specifically, JAK1, JAK3, STAT1, STAT3, STAT5 and STAT6 [73]–[77]. PTPN2 therefore negatively regulates signaling pathways activated by pro-inflammatory cytokines, such as IFN-γ and IL-6 [78],[79]. Early studies from our lab found that IECs deficient in PTPN2 possessed elevated basal and cytokine-induced STAT1 and STAT3 phosphorylation [79]–[81]. Additionally, these cells had an underlying barrier defect, with lower TER and higher FD4 permeability, both of which were worsened by treatment with the inflammatory

cytokine, IFN-γ [79]–[81]. Our lab has shown that the effect on pore barrier permeability is partly due to STAT1-dependent upregulation of pore-forming tight junction protein claudin-2 [81]. Therefore, by regulating the JAK-STAT signaling pathway activated by IFN-γ, PTPN2 protects the integrity of intestinal epithelial barrier.

Unlike in humans, only TC-45 is expressed in mice. *Ptpn2* is not embryonic lethal, but at about post-natal day 10, mice deficient in *Ptpn2* (constitutive knockout [KO]) mice start developing wasting disease: runted, lethargic, display hunching, have shut eyes, and diarrhea [82],[83]. Constitutive *Ptpn2* KO mice have lower hematocrit levels, severe anemia, splenomegaly, and succumb to systemic inflammation at week 3-5 of age [82],[83]. *Ptpn2* heterozygous (Het) mice, which have only one PTPN2 allele compared with wildtype (WT) littermates, are phenotypically normal, and do not display overt signs of disease [82],[83].

In animal models, susceptibility to intestinal inflammation and epithelial recovery responses are typically assessed using the dextran sulfate sodium (DSS)-induced colitis model in which mice are given 3-10% DSS in the drinking water for 5-10 days and allowed to recover for a 3-10 days [84]. Chemical injury by DSS causes direct IEC damage and impairs mucosal healing, which results in barrier dysfunction. Upon DSS-induced colitis, *Ptpn2* Het mice had worse disease severity (greater loss in body weight, colon length, higher histopathological scores) compared to DSS-treated WT controls [85]. Additionally, whole colons of untreated *Ptpn2* Het mice display higher levels of JAK1, JAK3, STAT1, and STAT3 phosphorylation, which were further enhanced after DSS treatment, in comparison to untreated and DSS-treated WT controls [85]. This

increased sensitivity to DSS suggests that missing one allele of *Ptpn2* is sufficient to "prime" the immune system to respond more readily to environmental factors which could lead to a more severe immune response, such as that seen in DSS-treated *Ptpn2* Het animals [85]. Interestingly, however, IEC-specific deletion of *Ptpn2* does not influence the severity of DSS-induced colitis due to potential compensation by increased proliferation in these mice [86].

Other experimental colitis studies performed on animal models with cell-specific knockout of *Ptpn2* have provided valuable insight on which cell types may be responsible for increased sensitivity in *Ptpn2*-deficient mice. After being injected with *Ptpn2*-deficient T cells then subjected to DSS, *Rag2* KO mice developed more severe colitis coupled with intestinal dysbiosis of commensal bacteria, compared to controls [87]. Myeloid-specific (LysMCre) knockout of *Ptpn2* also aggravated acute DSS-induced experimental colitis with worse endoscopic and histology scores, marked with higher epithelial damage and immune cell infiltration compared to WT counterparts [88]. Overall, these studies demonstrate the crucial role of PTPN2 in regulating inflammatory cytokine signaling associated with IBD pathophysiology.

By modulating the activation of signaling pathways that affect intestinal permeability, therapeutic strategies can be focused on maintaining the integrity of the epithelial barrier in the gut. Knowing specific IBD patients' genetic profiles may therefore improve the effectiveness of treatments.

Chapter 2: The JAK-Inhibitor Tofacitinib Rescues Human Intestinal Epithelial Cells and Colonoids from Cytokine-Induced Barrier Dysfunction

Anica Sayoc-Becerra[1], Moorthy Krishnan, PhD[1], Shujun Fan, PhD[2], Jossue Jimenez[1], Rebecca Hernandez[1], Kyle Gibson[1], Reyna Preciado[1], Grant Butt, PhD[2] and Declan F. McCole, PhD[1]

[1]Division of Biomedical Sciences, School of Medicine, University of California, Riverside, CA 92521, USA.

[2]Department of Physiology, School of Biomedical Sciences, University of Otago, Dunedin, New Zealand.

A version of this chapter is published in *Inflammatory Bowel Diseases*, 2019.

Introduction

Inflammatory bowel disease (IBD) is comprised of the chronic inflammatory conditions, Crohn's disease (CD) and ulcerative colitis (UC), in which the immune system mounts an abnormal response to normal constituents in the gastrointestinal tract in events driven by both genetic and environmental risk factors. Damage to the intestinal epithelium or disruption of the apical tight junctions, can compromise the ability of the epithelium to serve as a barrier between luminal contents and the underlying tissues [89]–[92]. Tight junctions connect neighboring intestinal epithelial cells (IECs), in concert with adherens junctions, and act as a selective barrier to paracellular solute permeability [90]–[92]. Reconfiguration of tight junctions, through removal or insertion of specific proteins, can increase intestinal permeability [89],[90],[93]. This facilitates dysregulated fluid and electrolyte transport, which can contribute to one of the main clinical symptoms of IBD, diarrhea [89],[90],[93]. Changes in expression or localization of tight junction proteins can also increase access of bacterial products into the lamina propria, which can trigger inappropriate immune responses and contribute to the pathogenesis of IBD [90],[93]. Permeability is an important parameter of intestinal homeostasis as increases in intestinal permeability have been shown to precede colonic inflammation in humans and animal models of colitis [66],[94],[95].

Paracellular permeability can feature both charge- and size-selective dependent or independent events and these functional characteristics of 'pore' and 'leak' barrier defects respectively, are in general regulated by different assemblies of tight junction proteins and associated signaling pathways [1]. The claudin family of transmembrane

proteins is a major structural component of the tight junction that are both size- and charge-selective for the passive paracellular movement of fluid and solutes [91],[92],[96]. One prominent member of this family is claudin-2 which can function directly as a water channel, but also forms cation-selective pores thus making the epithelial barrier more permissive to paracellular flux of fluid and cations, predominantly Na^+, which can decrease the electrical resistance across the epithelium [97]–[99]. This TJ protein is clinically-relevant since claudin-2 expression is increased in IBD and is regarded as a biomarker of increased paracellular permeability to electrolyte flux [89],[100],[101]. Claudin-2 is upregulated by several pro-inflammatory cytokines, including interferon-gamma (IFN-γ), and its induction is partly dependent on STAT1 binding to the claudin-2 promoter to regulate transcriptional expression [81]. Apart from claudins which predominantly regulate ion and water flux, the transmembrane proteins occludin and tricellulin help control paracellular passage of larger, uncharged solutes [12],[13],[102]. In addition to transmembrane proteins, peripheral membrane proteins, such as zonula occludens 1 (ZO-1), play crucial roles in both the assembly and regulation of tight junctions [62]. This is accomplished, at least in part, by their multiple domains that allow them to act as scaffolding proteins through interactions with other integral or regulatory proteins, including various claudins, occludin, and actin [10],[103],[104]. Further increasing the versatility of these structures is that the proteins comprising this complex conglomeration are highly dynamic. Thus, a typical feature of barrier dysfunction is altered membrane localization or increased internalization of tight junction proteins, in the presence or absence of changes in overall expression [105]–[107]. Therefore,

appropriate localization of tight junction associated proteins, such as ZO-1, is an essential factor in the maintenance of the epithelial barrier.

There are currently 231 independent SNPs in 200 gene loci, associated with the risk of onset of IBD, most of which are involved in regulating the immune system's interaction with IECs and microbial flora [24],[52],[68]. A number of these genes are involved in regulating the JAK-STAT pathway, which can be activated by several cytokines involved in IBD, including IFN-γ whose expression by $CD4^+$ T-lymphocytes is increased in inflamed intestinal tissues from CD patients compared with control subjects [24],[42]. The effects of IFN-γ are mediated primarily through the Janus kinase-signal transduction and transcription (JAK-STAT) signaling pathway, with specificity for activation of JAK1 and JAK2 [51]. Phosphorylated levels of their downstream targets STAT1 and STAT3 are elevated in CD patients compared with controls [108]. In addition, IFN-γ reduces epithelial barrier function by decreasing electrical resistance across intestinal cell monolayers and increasing permeability to macromolecules *in vitro* [109]–[113].

Inhibitors of JAK-STAT signaling have emerged as a new therapeutic focus in IBD. Tofacitinib (Xeljanz®, CP-690550), an orally-administered pan-JAK inhibitor was originally approved for the treatment of rheumatoid arthritis [114]. Tofacitinib is now FDA-approved for the treatment of moderate-to-severe UC and has been studied in Phase 2 clinical trials in CD [58],[115],[116]. Tofacitinib is a reversible, competitive small molecule inhibitor that binds to the adenosine triphosphate (ATP) binding site in the catalytic cleft of the kinase domain of JAKs. Tofacitinib structurally mimics ATP without

the triphosphate group, thus, by binding to the ATP site, it inhibits the phosphorylation and activation of JAK thereby preventing the phosphorylation and activation of downstream STAT proteins. Tofacitinib functions intracellularly and possesses high *in vitro* passive permeability consistent with intracellular entry by transcellular diffusion [114]. While studies on JAK-STAT signaling therapeutics have focused on immune cell targets and clinical primary endpoints, it is poorly understood how these agents affect IEC functions, such as the increase in intestinal permeability associated with IBD. In this study, we investigated whether tofacitinib exerts a direct beneficial effect on IEC barrier function and if it can rescue tight junction modifications caused by an IBD-relevant inflammatory cytokine, IFN-γ.

Materials and Methods

Materials

Human recombinant IFN-γ (Roche, Mannheim, Germany), tofacitinib (MedChemExpress, Monmouth Junction, NJ; Selleckchem, Houston, TX) and dimethyl sulfoxide (DMSO; Sigma-Aldrich, St. Louis, MO) were obtained from the sources indicated. IFN-γ was used at a concentration of 1000 U/ml, equivalent to 50 ng/ml, unless otherwise stated.

Cells

Human T_{84} and HT-29 IECs were grown in Dulbecco's modified Eagle's Medium/Ham's F-12 50:50 Mix (Corning, Tewksbury, MA) and McCoy's 5A medium

(Corning, Tewksbury, MA), respectively, supplemented with 10% heat-inactivated fetal bovine serum (Gibco, Waltham, MA) 1% L-glutamine (Invitrogen, Carlsbad, CA) and 1% penicillin (100 U/ml)/streptomycin (100 μg/ml) (Corning, Tewksbury, MA). Cells were cultured on standard cell culture plates or transwell membranes (0.4μm pore size, 1.12cm^2 surface area, Corning, Tewksbury, MA) in a 37°C incubator maintained at 5% CO_2/air mix. IECs were serum-deprived overnight prior to treatments with tofacitinib, DMSO and/or IFN-γ. For cells grown on transwells, tofacitinib and DMSO were administered to the apical compartment and IFN-γ was added to the basolateral compartment. IFN-γ was administered at a concentration (1000 U/ml; 24 hours) previously shown to decrease TER without causing damage to the epithelial monolayer [81].

Determination of Epithelial Monolayer Resistance and Paracellular Permeability

Transepithelial electrical resistance (TER) of T_{84} monolayers grown on transwells was measured using the EVOM2 Epithelial Voltohmmeter (World Precision Instruments, Sarasota, FL) and chopstick electrode set for EVOM2 (World Precision Instruments, Sarasota, FL). The average of three measurements per transwell was calculated and expressed in Ohms.cm^2.

Macromolecular paracellular permeability was measured as the flux of 4-kilodalton fluorescein isothiocyanate-dextran (4kDa FITC-dextran; FD4) (Sigma-Aldrich, St. Louis, MO) across polarized T_{84} monolayers. Following TER measurements, cells were washed twice with and equilibrated in PBS with $CaCl_2$ and $MgCl_2$ for 30

minutes at 37°C. FD4 at a final concentration of 1mg/ml was added to the apical compartment of the monolayers. After 2 hours of incubation at 37°C, 50µL of the basolateral solution was sampled in duplicate and fluorescence was detected using a microplate reader (Promega, Madison, WI). Based on relative fluorescence units (RFU), FD4 concentrations were calculated against a standard curve and expressed as percent change from untreated cells.

Preparation of Whole Cell Protein Lysates

At the end of the experimental period, cells were washed twice with ice-cold PBS. Ice-cold RIPA lysis buffer (50mM Tris-Cl pH 7.4, 150mM NaCl, 1% NP-40, 0.5% sodium deoxycholate, 0.1% SDS) supplemented with protease (Roche, Mannheim, Germany) and phosphatase inhibitors (sodium orthovanadate, Phosphatase Inhibitor Cocktail 2 and 3, Sigma-Aldrich, St. Louis, MO) was added and cells were incubated at 4°C for 15 minutes. Cells were scraped into microcentrifuge tubes and sonicated on ice at 30% amplitude, 10 s ON/OFF intervals for 20-40 s using the Q125 Sonicator (QSonica Sonicators, Newtown, CT). Cell lysates were centrifuged at 16,200 x *g* for 10 minutes to remove insoluble material and supernatants were collected into new microcentrifuge tubes. An aliquot of each sample was used to determine protein concentration using Pierce™ BCA Protein Assay Kit reagents (ThermoFisher Scientific, Waltham, MA). Protein content was adjusted with lysis buffer to ensure the same amount of total protein in each sample, and then mixed with loading buffer (60mM Tris-Cl pH 6.8, 2% SDS, 5%

β-mercaptoethanol, 0.01% bromophenol blue, 10% glycerol). All samples were boiled at 95°C for 10 minutes and loaded on SDS-polyacrylamide gels for Western blotting.

Western Blot Analysis

Whole cell proteins were resolved on 7% or 11% SDS-PAGE gels at 100V at room temperature then transferred onto polyvinylidene difluoride membranes (EMD Millipore, Darmstadt, Germany) for 2 hours at 250mA in 4°C. Membranes were blocked with 5% nonfat milk in TBS-T (Tris-buffered saline with 0.1% Tween-20) for 1 hour at room temperature, followed by further incubation with claudin-2 (1:1000, #32-5600, Invitrogen, Camarillo, CA), claudin-1 (1:1000, #51-9000, Thermo Fisher Scientific, Rockford, IL), claudin-4 (1:1000, #32-9400, Invitrogen, Camarillo, CA), claudin-15 (1:1000, #32-9800, Invitrogen, Frederick, MD), ZO-1 (1:1000, #61-7300, Thermo Fisher Scientific, Waltham, MA), occludin (1:1000, #71-1500 for T_{84} cells, Invitrogen, Carlsbad, CA; #40-4700 for the colonoids, Rockford, IL), tricellulin/marvel D2 (1:1000, ab203567, Abcam, Cambridge, MA), phospho-JAK1 (1:1000, #3331, Cell Signaling Technology, Danvers, MA), JAK1 (1:1000, #3344, Cell Signaling Technology, Danvers, MA), phospho-STAT1 (1:500, #9167, Cell Signaling Technology, Danvers, MA), STAT1 (1:1000, #9175, Cell Signaling Technology, Danvers, MA), phospho-STAT3 (1:1000, #9145, Cell Signaling Technology, Danvers, MA), STAT3 (1:1000, #9139, Cell Signaling Technology, Danvers, MA) and β-actin (1:8000, #A5316, Sigma-Aldrich, St. Louis, MO) primary antibodies overnight at 4°C. The following day, membranes were subjected to 5-minute washes (x5), or 3 quick rinses followed by 5-minute washes (x3),

with TBS-T, then incubated with peroxidase-conjugated secondary antibodies (goat anti-mouse (#115-036-062) or goat anti-rabbit (#111-036-045); Jackson Immunoresearch Laboratories, Inc. West Grove, PA) diluted at 1:5000 in 1% nonfat milk in TBS-T for 1 hour at room temperature. This was followed by 5-minute washes (x5), or 3 quick rinses followed by 5-minute washes (x3), with TBS-T. Membranes were then incubated with SuperSignal™ West Pico PLUS Chemiluminescent Substrate solution (ThermoFisher Scientific, Waltham, MA) according to manufacturer's directions and exposed to film (LabScientific Inc., Highlands, NJ). Densitometric analysis of the blots was performed using ImageJ software [117].

Claudin-2 Promoter Luciferase Reporter Assay

Claudin-2 promoter activity assay was performed in HT-29 IECs as previously described [81]. Briefly, a gene construct spanning the -900bp to +112bp region of the human *CLDN2* gene promoter (Integrated DNA Technologies, Coralville, IA) was cloned into the pGL3-Basic Luciferase Reporter Vector (Promega, Madison, WI) using the restriction enzymes NheI and KpnI. The sequence of the product was confirmed using sequencing analyses.

HT-29 cells were grown in 12-well cell culture plates until ~60% confluence was reached. The following day, cells were co-transfected with the *CLDN2* promoter-luciferase reporter construct and a reference construct containing *Renilla reniformis* luciferase (pRL) and the HSV-thymidine kinase (TK) promoter (Promega, Madison, WI) using Effectene® Transfection Reagent kit (Qiagen, Hilden, Germany) per manufacturer's

instructions. Twenty-four hours later, cells were pre-treated with tofacitinib or DMSO for 1 hour followed by IFN-γ for 24 hours. Luciferase activities were measured using the Dual-Luciferase® Reporter Assay System (Promega, Madison, WI) and a Glomax Multidetection System (Promega, Madison, WI). Firefly luciferase activity was normalized to *Renilla* luciferase activity.

ZO-1 and Occludin Immunofluorescence

After experimental treatments, T_{84} IECs grown on glass coverslips were washed twice with PBS, fixed with ice-cold methanol for 10 minutes at -20°C, then washed three times with PBS. Fixed cells were permeabilized with 0.5% Triton X-100 in PBS for 30 minutes at room temperature then washed again with PBS three times. After blocking with 10% normal donkey serum (Jackson Immunoresearch Laboratories, Inc. West Grove, PA) diluted in 0.04% PBS-Tween 20 (PBS-T) for 1 hour at room temperature, cells were stained with ZO-1 (#61-7300, ThermoFisher Scientific, Waltham, MA) or occludin (#71-1500, Invitrogen, Carlsbad, CA) primary antibody diluted at 1:200 in 1% NDS in PBS-T overnight at 4°C. Fixed cells were then washed five times with PBS-T followed by incubation with Alexa 488-conjugated donkey anti-rabbit secondary antibody (#711-545-152, Jackson Immunoresearch Laboratories, Inc. West Grove, PA) diluted at 1:200 in 1% PBS-T for 1 hour at room temperature. Stained cells were washed five times with PBS-T, once with PBS, then mounted in ProLong™ Gold Antifade Mountant with DAPI (Invitrogen, Carlsbad, CA) prior to visualization.

Images for ZO-1 immunofluorescence were captured using a Leica DM5500 microscope attached with a DFC365 FX camera using a 63x oil immersion objective with an additional 2x digital zoom. Individual images were converted into tiff files with the LAS-AF Lite software and Adobe Photoshop was used to create the final figures. The number of intercellular gaps per treatment was determined in 8 images per coverslip covering 4 different fields of view.

Z-stack images of occludin immunofluorescence were obtained using a CSU-X-1 spinning-disk confocal imager (Yokogawa, Japan) attached to a Zeiss Axio Observer inverted microscope (Carl Zeiss, Thornwood, NY). Original magnification of 63x was used. Micro-Manager Imaging Software (Molecular Devices, Sunnyvale, CA) was used to control the hardware (confocal microscope and the Prim 95B digital camera). Avi movie files were generated from z-stack images using ImageJ [117].

Human Colonoid Cultures

Epithelial derived colonic organoids (colonoids) were grown from crypts isolated from biopsy samples obtained from transverse colon of patients undergoing elective colonoscopy, primarily for colon cancer screening. Written informed consent was obtained before specimen collection and studies were approved by the Health and Disabilities Ethics Committee (New Zealand, Ethics No. 13/STH/155). The following protocols for colonoid isolation and culture were adapted from methods established by Sato, et al. [118]. The biopsy samples were collected in ice-cold DMEM/F12 medium containing antibiotics (1% Penicillin/Streptomycin, Normacin, 0.1 mg/ml, Fungizone, 2.5

μg/ml and Gentamycin 50 U/ml) and 5% FBS. They were then rinsed with PBS (x2), followed by PBS plus 10 mM DTT, before being transferred to ice-cold chelation media (PBS plus 8 mM EDTA, pH 7.5). Following 60 minutes of incubation on ice in the chelation media, the samples were transferred to fresh PBS containing 5% FBS (Gibco®, Thermo Fisher Scientific, NZ) and shaken vigorously to dislodge the crypts. The tissues were allowed to settle and the supernatant containing the crypts collected. This was repeated until shaking failed to release further crypts. The crypts were then pelleted (40 *g*, 2 minutes, 4°C), rinsed in basic culture media (Dulbecco's Modified Eagle Medium [DMEM]/F12 containing penicillin (100 U/ml)/streptomycin (100 μg/ml) and 5% FBS). They were then suspended in Matrigel™, transferred to 24-well plates (Thermo Fisher Scientific, Waltham, MA) and incubated at 37°C for 10 minutes to polymerize the Matrigel™. The crypts were then overlaid with the stem cell culture media (Table 2.1) and maintained at 37°C in a 5% CO_2/air mix. The initial structures that develop have a poorly differentiated squamous epithelium and are referred to as colonospheres [119]. By day 4-6, these structures differentiate into columnar epithelial colonoids and cultures consist primarily of differentiated colonoids by day 12-14. The culture media was replaced every 48 hours and the colonoids amplified by passaging every 7 days. When amplifying organoids, 10μM ROCK inhibitor (Merck, Kenilworth, NJ, USA) was included in the growth media. During experiments, this was omitted. All experiments used colonoids (≥ day 12) from passage 2-8 only.

Table 2.1: Human Colonoid Culture Media Components

Reagent	Stock Conc.	Final Conc.	µl per 50 ml	Supplier	Catalog No.
N2	100X	1X	250	Invitrogen	#17502048
B27	50X	1X	500	Invitrogen	#17504044
Nicotinamide	250 mM	10 mM	1000	Sigma	#N0636
N-acetyl-L-cysteine	500 mM	1 mM	50	Sigma	#A9165
LY 2157299	1 mM	500 nM	25	AxonMedChem	#1491
SB 202190	1 mM	10 µM	250	Sigma	#S7067
PGE_2	10 µM	0.01 µM	25	Sigma	#P0409
hu EGF	100 µg/ml	50 ng/ml	12.5	Invitrogen	#PHG0311
Noggin	100 µg/ml	100 ng/ml	25	PeproTech	#120-10C
Gastrin	1 mg/ml	1 µg/ml	25	Pharmaco	3006/1
Wnt3A conditioned media		50%	25,000		
Rspo conditioned media		10%	5000		
Advanced DMEM/F12			17,037.5	Invitrogen	#12634-010
Glutamax	100X (200 mM)	1X	250	Invitrogen	25030-081
Hepes	1M	10 mM	250	Sigma	#H0887
Pen/Strep		1%	250	Invitrogen	15140-122
[a]gentamycin	10 mg/ml	50 µg/ml	N/A	Invitrogen	15710064
[a]fungizone	250 µg/ml	0.25-2.5 µg/ml	N/A	Invitrogen	109434.01
Normocin	50 mg/ml	0.1 mg/ml	50	Integrated Science	ant-nr-1
[b]ROCK inhibitor	1 mM	10 µM	N/A	Merck	#688000-1mg

[a] Reagents were added in the media only during sample collection.

[b] Reagents were added only when passaging colonoids.

Measurement of FITC Flux in Human Intestinal Colonoids

Colonoids from patients were amplified from the initial biopsy so that 4 wells were available from each patient at the same passage. After 12 days of culture, two wells of colonoids served as controls while IFN-γ (50 ng/ml) was added to the two remaining wells. Six hours after the addition of IFN-γ, tofacitinib (16.7μM) was added to one of the control wells and one of the wells to which IFN-γ had been added. Further additions of tofacitinib (16.7μM) were made after 24 hours and 48 hours.

The relative permeability of the colonoids was measured by adding 0.1 mg/ml of FD4 to the growth media then measuring the FD4 flux into colonoids with well-developed columnar epithelium 24 hours later. The fluorescence intensity in the mid-point of the organoid lumen was determined by carrying out a series of optical slices through each organoid using a Zeiss 710 LSM confocal microscope (GmbH, Jena, Germany) as previously described [120]. The fluorescence intensity was then converted to concentration using standard curves created from log serial dilutions of FD4 in growth media. Surface area and volume of the colonoids were calculated from the measured radius to allow calculation of the FD4 flux ($ng/cm^2.h$).

Statistical Analysis

Data are presented as means ± SEM or fold change from untreated controls for a series of *n* biological replicates or in the case of colonoids, patients. Statistical analysis was performed by analysis of variance (ANOVA) using GraphPad Prism 6.0 software

(GraphPad Software, La Jolla, CA). *P* values ≤ 0.05 were considered statistically significant.

Results

Acute treatment of tofacitinib restricts IFN-γ activation of JAK1-STAT1 signaling in intestinal epithelial cells

To confirm that tofacitinib was capable of interrupting phosphorylation of JAK1 and its downstream target, STAT1, by IFN-γ in IECs, T_{84} cells grown in regular 6-well plates were treated with vehicle DMSO or tofacitinib for 1 hour prior to exposure to IFN-γ for 30 minutes (for JAK1 activation) or 1 hour (for STAT activation) (schematic shown in Figure 2.1A). Whole-cell protein lysates were collected, subjected to Western blotting and probed for the proteins indicated. Although the decrease in JAK1 phosphorylation in resting cells treated with tofacitinib did not reach statistical significance, tofacitinib (50μM) pre-treatment significantly reduced IFN-γ-induced JAK1 phosphorylation in T_{84} cells ($P < 0.05$, $n = 3$; Figure 2.1B). As a downstream target of JAK1, STAT1 phosphorylation levels were significantly reduced by acute treatment of tofacitinib compared with untreated cells and completely blocked IFN-γ-induced STAT1 phosphorylation ($P < 0.001$, $n = 3$; Figure 2.1C). Similar results were observed with the phosphorylation levels of STAT3, another mediator of JAK signaling ($P < 0.05$, $P < 0.001$, $n = 4$; Figure 2.1D). These data indicate that, *in vitro*, tofacitinib can prevent cytokine-induced JAK-STAT activation in IECs.

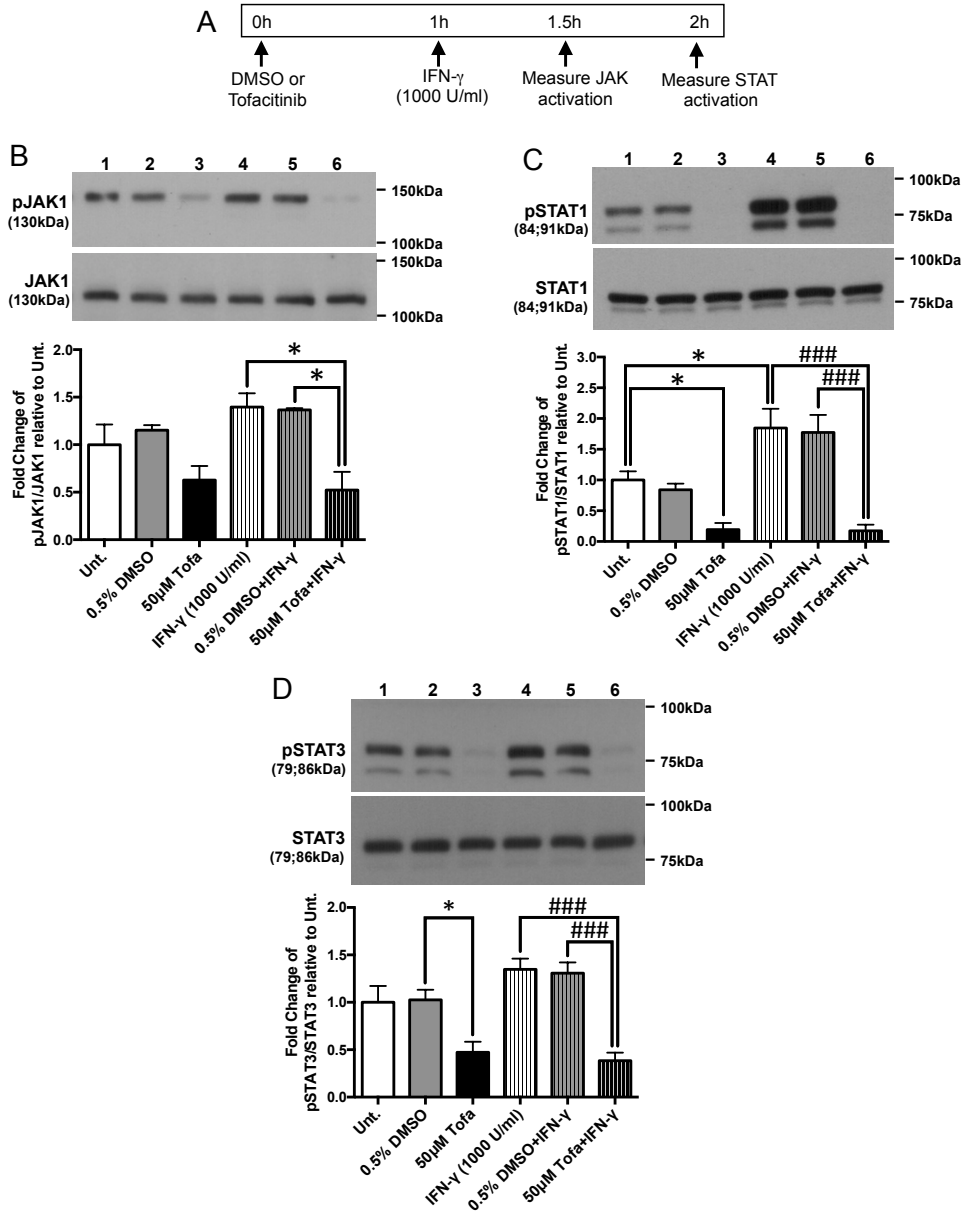

Figure 2.1: Tofacitinib pre-treatment prevented IFN-γ-induced JAK1, STAT1, and STAT3 phosphorylation in IECs *in vitro*.

(A) Schematic of the acute prevention protocol for tofacitinib to determine JAK-STAT activation in IECs. T_{84} IECs were treated with vehicle (DMSO) or tofacitinib (Tofa, 50μM) for 1h followed by IFN-γ (1000 U/ml) treatment for either 30min (for JAK activation) or 1h (for STAT activation). Cells were lysed and protein extracts were subjected to Western blotting for the proteins indicated. Densitometric analysis was performed and normalized to (B) pJAK1/JAK1, (C) pSTAT1/STAT1, and (D) pSTAT3/STAT3 levels of each replicate's respective untreated (Unt.) controls (* $P < 0.05$, ### $P < 0.001$, $n = 3$-4).

Tofacitinib prevents IFN-γ-induced barrier dysfunction in intestinal epithelial cells in vitro

IFN-γ is known to disrupt IEC tight junction composition and increase paracellular permeability to electrolytes and macromolecules.[28, 54] To test whether tofacitinib protected against IFN-γ-stimulated increases in permeability, T_{84} IECs were grown on transwells and apically treated with tofacitinib or vehicle (DMSO) with or without subsequent basolateral treatment with IFN-γ, (schematic shown in Figure 2.2A). After 24 hours, there was no significant difference in TER between untreated, DMSO-treated and cells treated with tofacitinib alone at increasing concentrations of 2μM, 10μM and 50μM (Figure 2.2B). While IFN-γ decreased TER, this was unaltered by DMSO. However, tofacitinib prevented the IFN-γ-induced decrease in TER in a dose-dependent manner ($P < 0.001$, $P < 0.0001$, $n = 3$; Figure 2.2B). In addition, tofacitinib pre-treatment prevented the IFN-g-induced increase in FD4 permeability compared with DMSO pre-treated cells ($P < 0.0001$; $n = 3$; Figure 2.2C). Moreover, DMSO or tofacitinib alone had no effect on FD4 permeability. These results indicate that tofacitinib exerts a protective effect against cytokine-induced paracellular permeability to electrolytes and macromolecules.

Early intervention with tofacitinib partially rescues the drop in TER but fully restores the increase in FD4 permeability induced by IFN-γ in IECs in vitro

To test the therapeutic effects of tofacitinib on barrier function, polarized T_{84} IECs grown on transwells were first treated with basolateral IFN-γ (1000 U/ml) followed

by two apical doses of tofacitinib (16.7μM each) or vehicle DMSO at two time points (6 hours and 18 hours post-IFN-γ treatment) to mimic twice daily clinical administration (schematic shown in Figure 2.2D). Twenty-four hours after IFN-γ treatment, TER and FD4 permeability were measured. Again, there were no differences in TER between untreated cells and cells treated with either DMSO or tofacitinib alone. However, the drop in TER induced by IFN-γ, which was unaffected by DMSO, was partially restored by tofacitinib ($P < 0.0001$, $n = 3$; Figure 2.2E). Moreover, the increase in FD4 permeability induced by IFN-γ was fully rescued by treatment with tofacitinib ($P < 0.01$, $n = 3$; Figure 2.2F). These data suggest that early intervention of tofacitinib is able to differentially rescue modes of IFN-γ-induced barrier dysfunction.

Tofacitinib reverses the FD4 permeability increase induced by IFN-γ in human colonic organoids

To more accurately reflect the complex, three-dimensional structure of the intestinal epithelium, which contains both a stem cell niche and other differentiated epithelial cell types surrounding a single luminal compartment, the effect of tofacitinib on permeability was determined using human colonoids, which are 3-D human colonic organoids with a mature columnar epithelium. Figure 2.3A shows a representative panel of optical slices through one colonoid, the mid-point of which is where FD4 signal intensity was measured. After 72 hours, IFN-γ treatment resulted in a 3-4-fold increase in FD4 influx into the colonoids from the bathing media, as shown in Figure 2.3B. The addition of tofacitinib rescued the IFN-γ-induced increase in FD4 flux, while yielding no

effect on the basal flux ($P < 0.01$, $n = 4$; Figure 2.3B). Changes in expression of tight junction proteins regulating the leak pathway can alter paracellular FD4 permeability across a monolayer of intestinal cells [105]. To better understand if changes in FD4 permeability seen in Figure 2.3B were due to altered tight junction protein expression, colonoids were harvested and processed for Western blotting. Figure 2.3C shows that the protein expression of ZO-1 and occludin were unaltered in organoids subjected to these treatments.

Similar to observations seen in human organoids, none of the treatment conditions had a significant impact on the protein expression of ZO-1, occludin and another transmembrane MARVEL family protein, tricellulin, in T_{84} monolayers subjected to the treatments in Figure 2.2A and 2.2D ($n = 4$; Figure 2.4). These results imply that the effects of IFN-γ and tofacitinib on FD4 permeability across the epithelium are likely not due to alterations in the expression of these tight junction proteins.

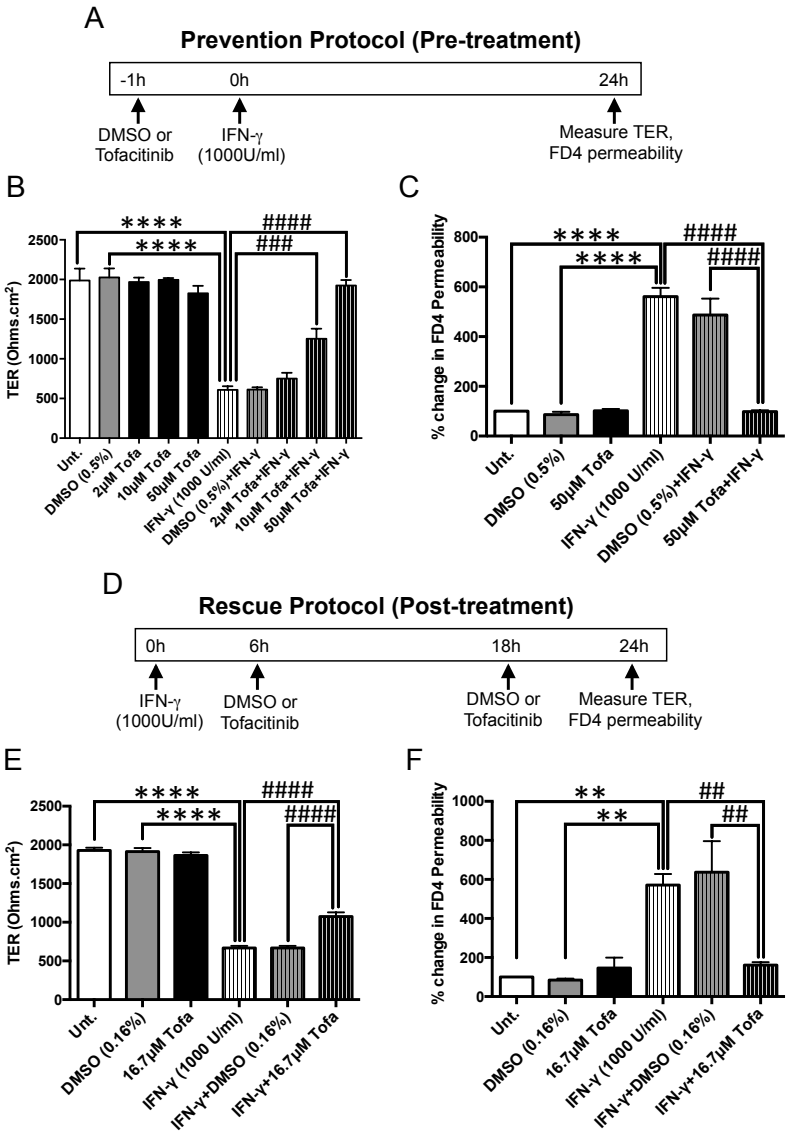

Figure 2.2: Tofacitinib prevents and rescues IECs against IFN-γ-induced barrier dysfunction.

(A) Schematic of the prevention protocol (Pre-treatment): T_{84} IECs grown on transwells were treated with varying concentrations of tofacitinib apically for 1h followed by basolateral administration of IFN-γ (1000 U/ml) for 24h. DMSO was used as a vehicle control. (B) TER and (C) FD4 permeability were measured 24h post-IFN-γ. (**** $P <$ 0.0001, ### $P < 0.001$, #### $P < 0.0001$, $n = 3$). (D) Schematic of the rescue protocol (Post-treatment): Therapeutic effects of tofacitinib were studied by treating T_{84} IECs post-IFN-γ treatment (1000 U/ml) with tofacitinib (16.7μM) apically at two time points (6h and 18h) to mimic twice daily clinical administration. Again, DMSO was used as a vehicle control. (E) TER and (F) FD4 permeability were measured 24h after IFN-γ treatment. (**** $P < 0.0001$, ** $P < 0.01$, #### $P < 0.0001$, ## $P < 0.01$, $n = 3$).

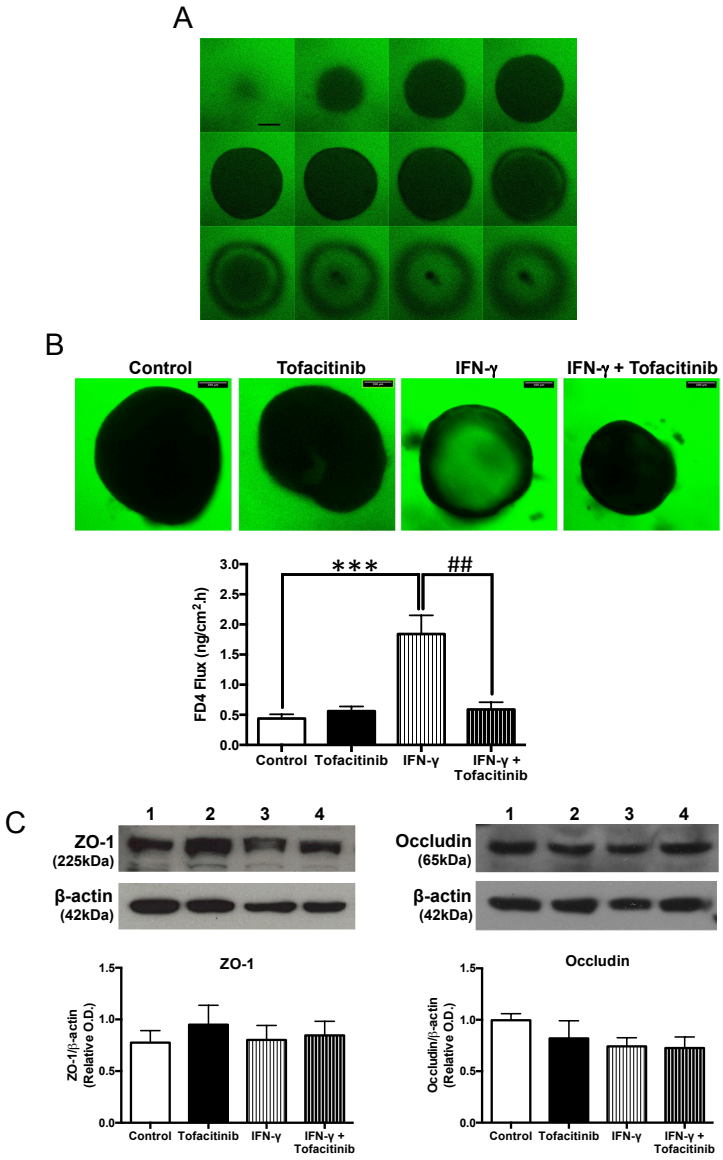

Figure 2.3: Tofacitinib rescues the permeability increase induced by IFN-γ in human colonic organoids.

(A) Representative series of optical slices through a human colonoid bathed in growth media containing 0.1 mg/ml FD4. Scale bar = 100 μm. (B) Following a rescue protocol, human colonoids cultured for 12d were treated with IFN-γ (50ng/ml, administered in the bathing media). Tofacitinib (16.7μM, administered in the bathing media) was added 6h-, 24h- and 48h-post IFN-γ treatment. FD4 flux across colonoid epithelium normalized to surface area of colonoids was measured 72h after IFN-γ administration. (*** $P < 0.001$, ## $P < 0.01$, $n = 4$). (C) Colonoids were harvested, lysed, and subjected to Western blotting for ZO-1 and occludin. Representative blots and densitometric analysis for ZO-1 and occludin are shown.

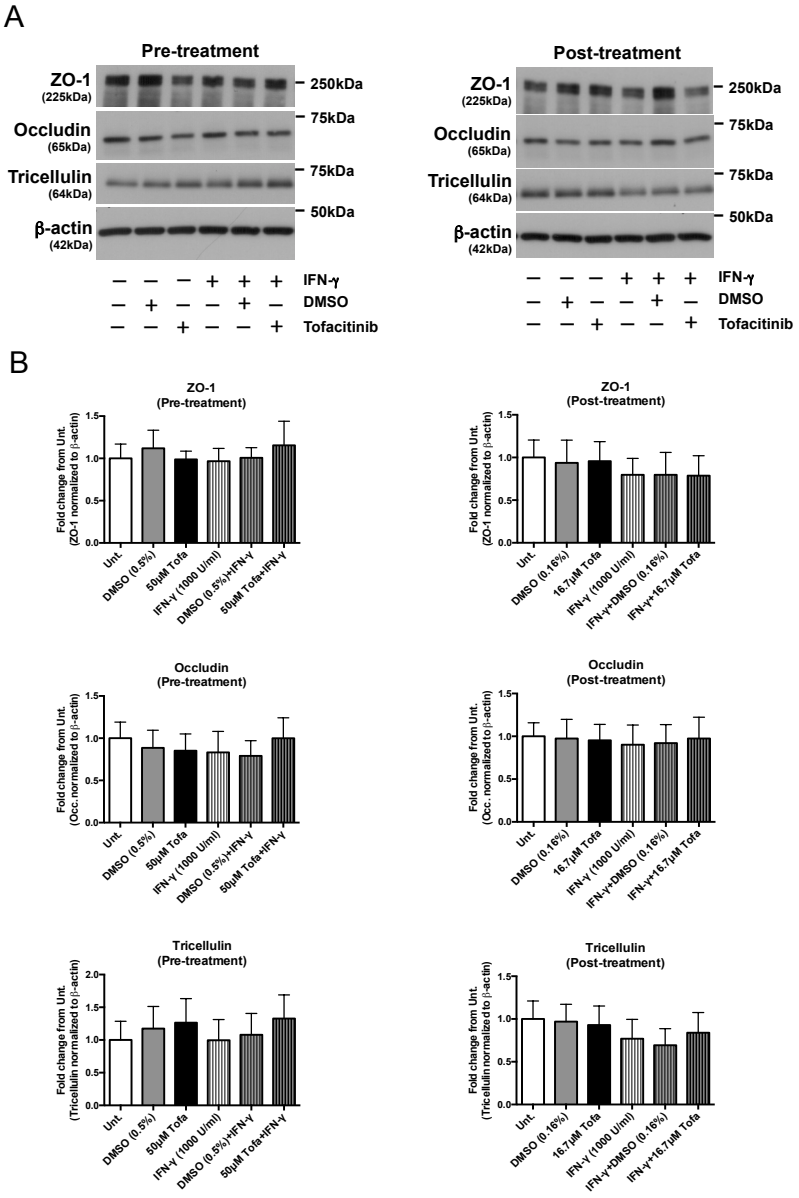

Figure 2.4: Tofacitinib does not alter protein expression of tight junction proteins involved in macromolecule permeability.

Pre-treatment: T_{84} cells grown in transwells were pre-treated with DMSO or tofacitinib (50μM) for 1h prior to IFN-γ (1000 U/ml) treatment for 24h. Post-treatment: T_{84} cells grown in transwells were first treated with IFN-γ (1000 U/ml) followed by two doses of DMSO or tofacitinib (16.7μM) at 6h and 18h post-IFN-γ administration. Twenty-four hours after IFN-γ exposure, cells were lysed, processed for Western blotting and probed for the proteins indicated. (A) Representative blots probed for ZO-1, occludin, tricellulin and β-actin. (B) Quantification of densitometric analysis normalized to untreated controls from four independent experiments ($n = 4$).

Tofacitinib protects the epithelial barrier by restricting IFN-γ induced ZO-1 relocalization

Having ruled out changes in tight junction protein expression by tofacitinib, to determine the mechanism(s) behind the protective effects of tofacitinib against the IFN-γ-induced increase in FD4 permeability seen in Figure 2.2C, T_{84} cells seeded on glass coverslips were treated with tofacitinib or DMSO for 1 hour, followed by IFN-γ treatment for 24 hours. Assessment of ZO-1 staining in fixed cells revealed that IFN-γ treatment caused increased formation of intercellular gaps that disrupted the regular chickenwire pattern seen in untreated and DMSO-treated cells (Figure 2.5A). The intercellular gaps were observed less frequently in cells pre-treated with tofacitinib, as quantified in Figure 5B. Similar observations were seen in cells treated with tofacitinib 6 hours and 18 hours post-IFN-γ challenge (Figure 2.5C) as quantified in Figure 2.5D. In staining for occludin in IFN-γ-treated cells, z-stack imaging revealed that these intercellular gaps were restricted to the apical portion of the cell monolayer and do not span the height of the IECs. A representative movie of a gap (available at *Inflammatory Bowel Diseases* online [16]), assessed by membrane occludin staining though z-stack imaging, confirms apical localization of the gap. These data suggest that the beneficial effects of tofacitinib in reducing FD4 permeability in this model system are likely due to normalizing localization of TJ proteins, including ZO-1, rather than by affecting their overall expression.

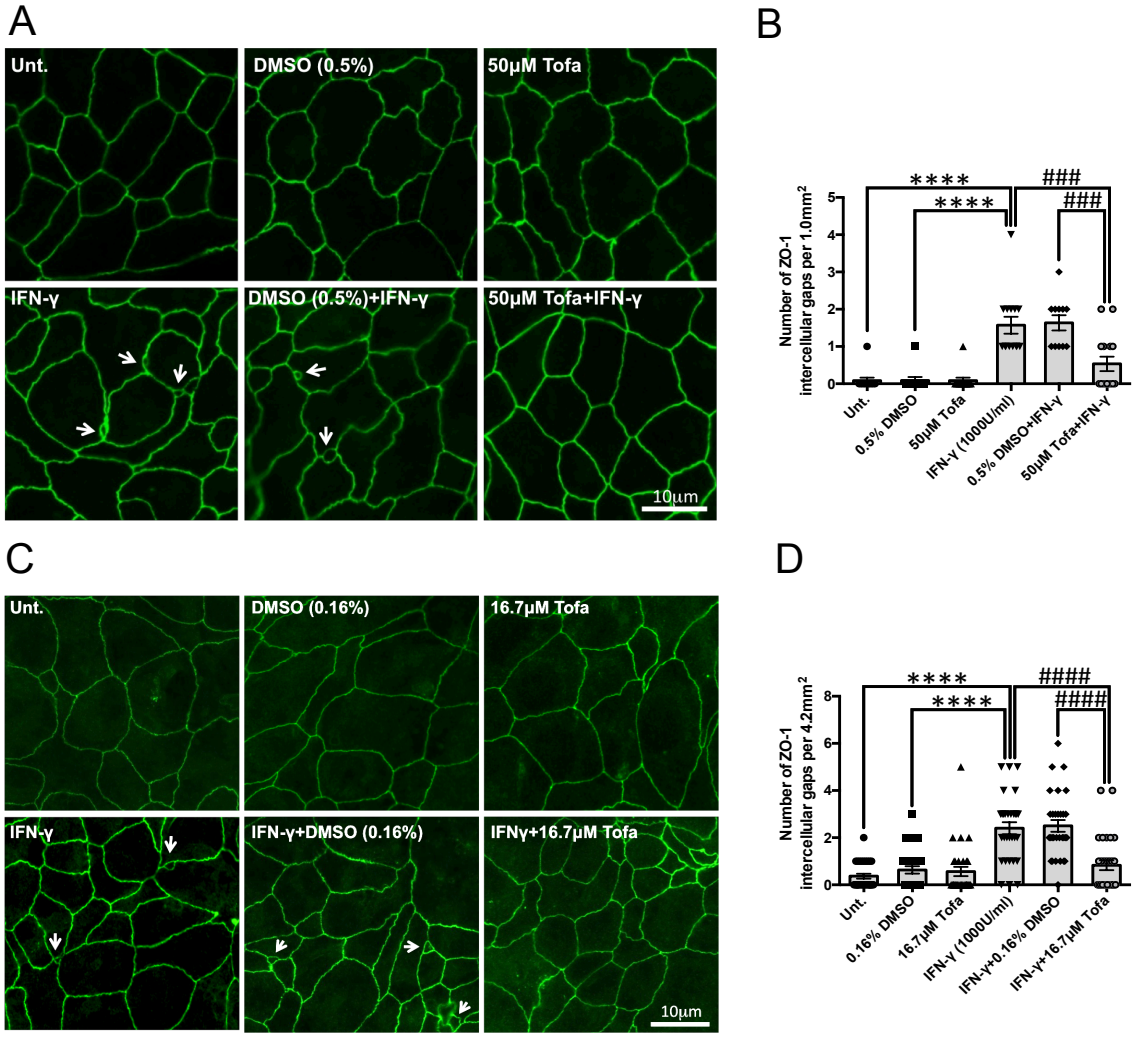

Figure 2.5: Tofacitinib reduces the number of apical intercellular gaps via ZO-1 rearrangement/localization caused by IFN-γ.

(A) Pre-treatment: T_{84} cells grown on coverslips pre-treated with tofacitinib or DMSO for 1h followed by IFN-γ (1000 U/ml, 24h) treatment were stained for ZO-1 and visualized via immunofluorescence microscopy. (B) Average number of intercellular gaps in 5 fields of view per condition from three independent pre-treatment experiments (**** $P <$ 0.0001, ### $P < 0.001$, ## $P < 0.01$, $n = 3$). (C) Post-treatment: ZO-1 staining in cells treated with tofacitinib or DMSO at 6h and 18h post-IFN-γ (1000 U/ml, 24h) treatment. (D) Number of intercellular gaps taken in 10 fields of view per condition from three independent post-treatment experiments (**** $P < 0.0001$, ### $P < 0.001$, $n = 3$). White arrows indicate intercellular gaps.

Tofacitinib restricts IFN-γ induced claudin-2 promoter activity and protein expression

To identify the mechanism(s) by which tofacitinib reduced the drop in TER caused by IFN-γ treatment, protein lysates were collected from polarized T_{84} IECs treated with tofacitinib, or DMSO, with or without IFN-γ exposure using the 'prevention' and 'rescue' protocols described in Figures 2.2A and 2.2D, respectively. Lysates were then subjected to Western blotting and probed for the expression of the cation selective pore-forming tight junction protein, claudin-2. After 24 hours, IFN-γ increased claudin-2 levels more than two-fold from untreated and DMSO-treated controls ($P < 0.001$, $n = 3$; Figure 2.6A). Conversely, tofacitinib pre-treatment prevented the IFN-γ-induced increase in claudin-2 protein levels *in vitro* ($P < 0.05$, $n = 3$; Figure 2.6A). When administered after IFN-γ exposure, tofacitinib could only partially normalize claudin-2 protein levels ($P < 0.05$, $n = 3$; Figure 2.6B). To identify the mechanism of claudin-2 upregulation affected by tofacitinib, we examined its effects on claudin-2 gene transcription given that the claudin-2 promoter contains a STAT-binding motif, and we previously demonstrated in HT-29 IECs expressing a claudin-2 promoter-luciferase construct, that following IFN-γ treatment, STAT1 binds to the claudin-2 promoter to induce its transcription [81]. In this study, HT-29 cells pre-treated with tofacitinib 1 hour before IFN-γ exposure for 24 hours displayed reduced claudin-2 promoter activity compared with cells challenged with IFN-γ alone or pre-treated with DMSO ($P < 0.001$, $n = 4$; Figure 2.6C). The tofacitinib-induced changes in claudin-2 protein levels suggest that tofacitinib reduces the changes in TER induced by IFN-γ, at least in part, through claudin-2 regulation. In addition to claudin-2, other members of the claudin family also contribute to changes in TER across

an epithelium. Claudin-1 and claudin-4 are known to tighten the barrier and increase TER, whereas overexpressing claudin-15 decreases TER and increases paracellular flux of cations, similar to claudin-2 [121]. However, protein expression of these claudins did not significantly change with tofacitinib or IFN-γ treatments (Figure 2.7), thus suggesting that the effects seen in TER are most likely mediated by the changes in claudin-2 expression.

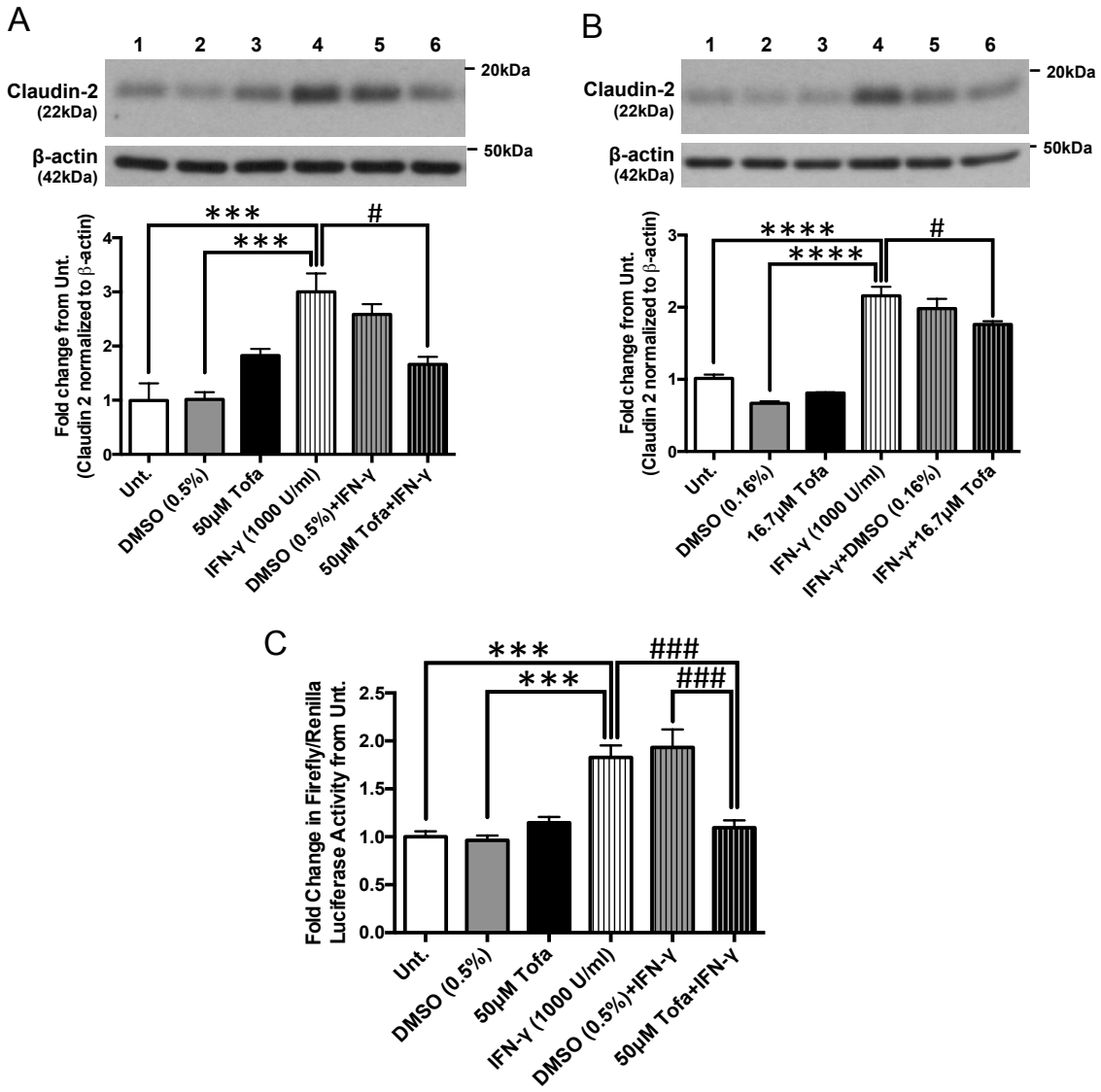

Figure 2.6: Tofacitinib restricts IFN-γ-induced claudin-2 protein expression and promoter activity.

(A) Pre-treatment: Claudin-2 protein expression was determined in T_{84} IECs pre-treated with tofacitinib or DMSO 1h prior to IFN-γ treatment for 24h and quantified using densitometric analysis and normalized to untreated controls. (*** $P < 0.001$, # $P < 0.05$, $n = 4$). (B) Post-treatment: Claudin-2 protein expression was determined in T_{84} cells treated with tofacitinib or DMSO 6h and 18h post-IFN-γ exposure and quantified using densitometric analysis and normalized to untreated controls. (**** $P < 0.0001$, # $P < 0.05$, $n = 3$). (C) Pre-treatment: Claudin-2 promoter activity was measured using a luciferase reporter assay on HT-29 IECs subjected to the treatment schedule outlined in Figure 1A. (*** $P < 0.001$, ### $P < 0.001$, $n = 4$).

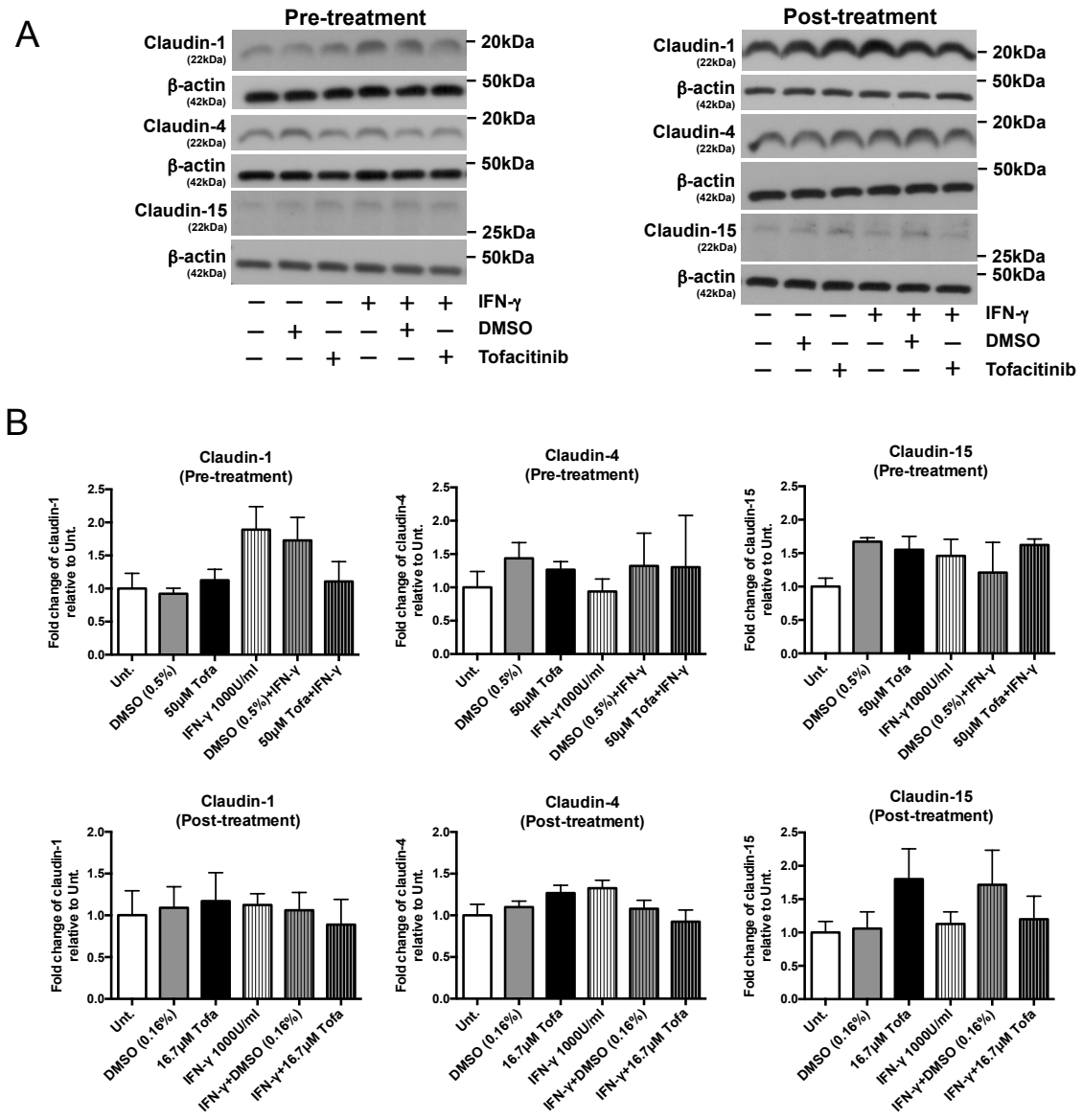

Figure 2.7: No significant changes in protein expression of claudins -1, -4, and -15 were found with any of the treatments *in vitro*.

T84 monolayers were subjected to vehicle (DMSO), tofacitinib and IFN-γ treatments following the 'prevention' and 'rescue' protocols. Cells were lysed, whole-cell protein lysates were processed, subjected to Western blotting, and probed for claudin-1, claudin-4 and claudin-15. (n = 3-4).

Discussion

Tofacitinib is a selective inhibitor of members of the JAK family kinases and demonstrates strong selectivity for JAK1 and JAK3 >>> JAK2 > tyrosine kinase 2 (TYK2) [114]. By inhibiting JAK phosphorylation, tofacitinib inhibits recruitment of downstream STAT family members by activated JAK1 and thus interrupts these signaling cascades, thereby reducing STAT-dependent activation of inflammatory genes (Figure 8) [51],[114]. Tofacitinib has proven to be an effective therapeutic agent in treating several chronic inflammatory diseases and has been FDA-approved for the treatment of rheumatoid arthritis, psoriasis, and more recently, ulcerative colitis [58],[116]. In phase 3 clinical trials, remission at 52 weeks occurred in up to 40.6% of UC patients who received 10mg of tofacitinib twice daily, compared with 11.1% in the placebo group [58]. At the same time, mucosal healing at 52 weeks occurred in 45.7% of patients on tofacitinib compared with 13.1% in those receiving placebo [58]. Although one of the primary endpoints of this study was mucosal healing, the direct effects of tofacitinib on the critical mucosal cell type comprising the intestinal barrier is unknown.

In this study, we showed that tofacitinib exerts a direct effect on IECs *in vitro* by inhibiting cytokine-induced JAK1-STAT1/3 activation. The timing of IFN-γ exposure was optimized for either maximal JAK1 or STAT1/3 phosphorylation and tofacitinib reduced IFN-γ stimulated p-JAK1, pSTAT1 and pSTAT3 to levels comparable to controls. Moreover, tofacitinib was not only capable of preventing permeability increases caused by IFN-γ, but also rescued epithelial monolayers from IFN-γ-induced increases in barrier permeability. Treating IECs with tofacitinib prior to IFN-γ challenge prevented

the dramatic decrease in TER and FD4 permeability enhancement. This suggests that tofacitinib inhibition of JAKs prior to exposure to a pro-inflammatory mediator is sufficient to maintain the barrier's integrity. This may have relevance to the clinical efficacy of tofacitinib in potentially limiting the epithelial barrier-disrupting effects of newly secreted inflammatory cytokines at the start of a flare in disease activity. The capacity of tofacitinib to rescue the permeability defect caused by IFN-γ in primary human colonoids further supports the evidence of a direct beneficial effect of tofacitinib on the intestinal epithelium. Human colonoids better recapitulate the microenvironment of IECs as they are grown in three-dimensional orientation, thus retaining both the structure and variety of epithelial cell subtypes of the colonic crypt [122]–[125]. Of note, while the same concentration of tofacitinib used for cell culture studies was able to rescue the increase in FD4 permeability caused by IFN-γ in colonoids, this was studied over a longer time period of exposure in colonoids than cell lines. Collectively, these data indicate that tofacitinib rescued barrier function using both epithelial model systems thus further validating the efficacy of this agent in normalizing barrier function.

We have attempted to discriminate between the two principal forms of permeability that are regulated by specific tight junction alterations, namely the size- and charge-selectivity of electrolyte flux as measured by TER (pore pathway), and the size but non-charge-selective permeability characterized by FD4 permeability (leak pathway) [6]. While increased involvement of the leak pathway can also lead to a reduction in TER, this functional parameter of permeability often correlates with changes in the expression of claudin family proteins, with increased expression of claudin-2 contributing

directly to reduced TER due to increased flux of Na^+ and water.[8, 11, 19, 23, 51, 52] We previously demonstrated that STAT1 binding is partly responsible for the IFN-γ-induced increase in claudin-2 promoter activity and mutation of the STAT-binding domain eliminates IFN-γ induced *CLDN2* promoter activity [81]. Our current data indicate that the inhibitory effect of tofacitinib on claudin-2 upregulation is at least partly attributed to inhibition of the *CLDN2* promoter (Figure 2.8). In agreement with our previous findings, this inhibitory effect is likely due to reduced STAT1-mediated transcription of claudin-2 since STAT1 is a substrate of activated JAK1. While we previously demonstrated that STAT1 binds to the *CLDN2* promoter to increase *CLDN2* expression via a STAT-binding motif, involvement of other STATs, specifically STAT6, in the regulation of claudin-2 expression by the inflammatory cytokine IL-13, has also been demonstrated [81],[101],[126]–[128]. However, our data do contrast with prior studies indicating that pharmacological inhibitors of STAT1 were unable to alleviate the IFN-γ-induced reduction in TER [113],[129]–[131]. Data from the same group suggested that following IFN-γ treatment, STAT1 promoted STAT5b activation, which formed a complex with Fyn Src kinase and PI3-kinase, to serve as a mediator of IFN-γ-induced barrier dysfunction, specifically macromolecule horseradish peroxidase translocation, in T_{84} monolayers [126]. These studies highlight how STAT proteins have versatile and complex roles in barrier function regulation, which can be context-dependent.

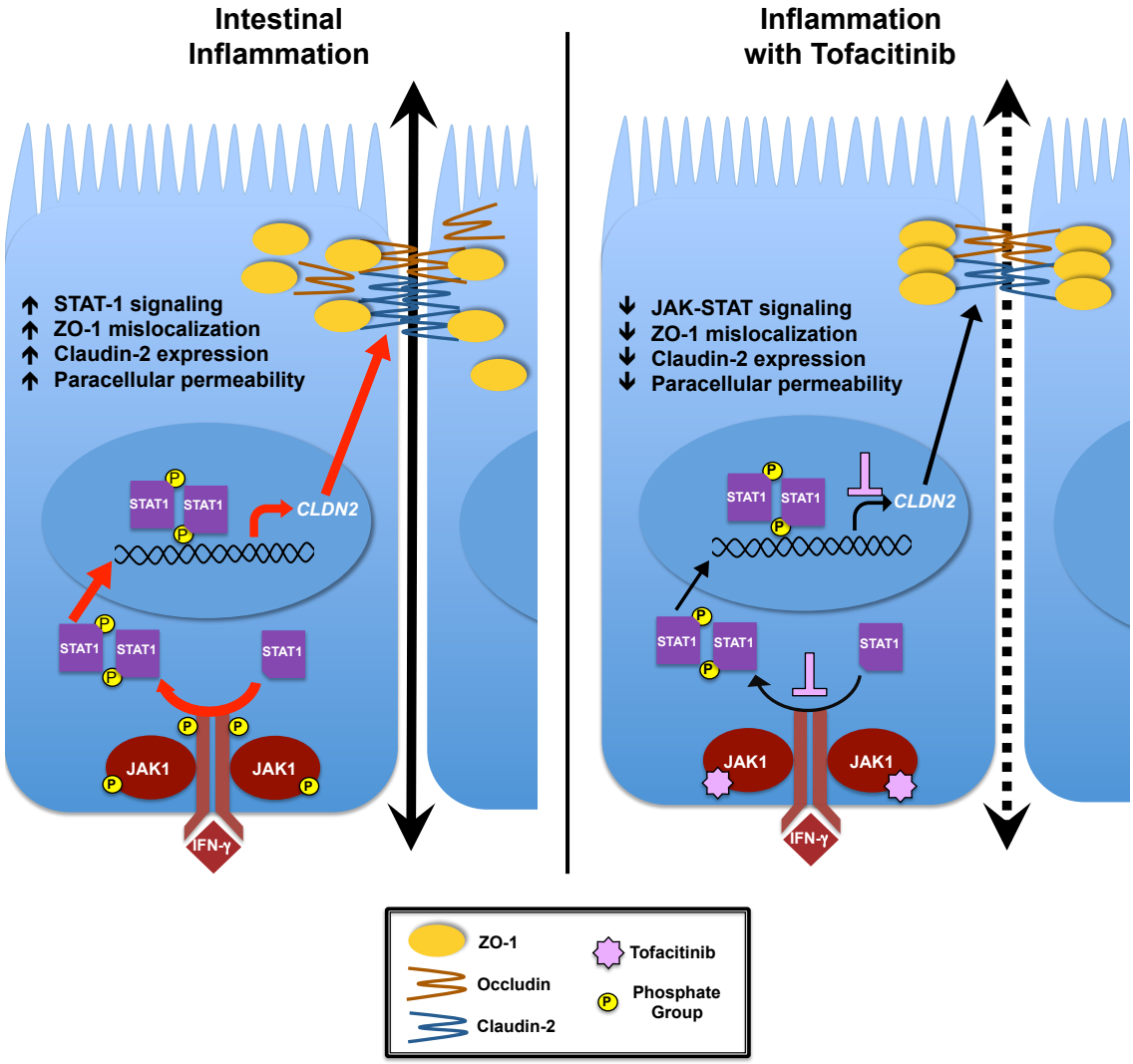

Figure 2.8: The protective effect of tofacitinib on IFN-γ-induced barrier dysfunction.

During inflammation in which cytokines such as IFN-γ are released and bind to their receptors on epithelial cells, JAK1 proteins are brought in close proximity to each other and are activated. These in turn phosphorylate cytokine receptors which serve as docking sites for STAT proteins, which are then activated by JAK1 proteins. Phosphorylated STATs dimerize, translocate to the nucleus and serve as transcription factors for specific genes, such as claudin-2. Upon IFN-γ treatment, claudin-2 expression is upregulated and ZO-1 mislocalizes to form intercellular gaps. As a small molecule inhibitor, when tofacitinib binds to the ATP-binding site of JAK proteins, the first step of the signaling cascade is stopped, therefore preventing and/or reducing the detrimental effects of IFN-γ on the intestinal epithelial barrier (summarized in right-hand panel; broken arrow reflects reduced paracellular permeability *vs*. inflammation alone shown in left-hand panel).

IFN-γ is a recognized modulator of the tight junction localization and expression of occludin and ZO-1 [15],[79],[109]–[112]. In the present study, we did not observe a significant difference in the expression levels of ZO-1, occludin or another member of the MARVEL family of transmembrane proteins involved in restricting macromolecular permeability, tricellulin, after IFN-γ treatment for 24 hours [12],[13],[102]. This suggests that the IFN-γ-induced increase in FD4 permeability, and thus the normalizing effect of tofacitinib on FD4, are likely not mediated by changes in overall protein expression of ZO-1, occludin or tricellulin. Instead, the inhibitory effect of tofacitinib on FD4 permeability is likely due to changes in tight junction protein localization. This was supported by ZO-1 relocalization data and the decreased frequency of intercellular gaps observed with ZO-1 immunofluorescence staining in cell monolayers treated with tofacitinib. Indeed, IFN-γ-induced alterations in barrier permeability and tight junction protein relocalization may partially be due to remodeling or internalization of these tight junction proteins from the plasma membrane into a subapical cytosolic compartment, as previously described [15].

Our study also showed that early intervention with tofacitinib during exposure to IFN-γ can fully rescue the increase in FD4 permeability, yet only partially mitigated the decrease in TER. This partial restoration correlates with our finding that claudin-2 protein expression levels did not return to those of untreated and DMSO-treated controls in the rescue protocol studies. A potential explanation could be that tofacitinib is unable to fully reverse the sequence of signaling events leading to increased claudin-2 and TER loss as opposed to its apparent capacity to arrest signaling modalities targeting junction proteins

involved in the 'leak' barrier defect, and thus reverse the increase in FD4 permeability caused by IFN-γ.

The concentration of tofacitinib used here to study barrier and JAK/STAT signaling effects on IECs are relatively higher compared with those used in other studies. For instance, tofacitinib at 30nM and 100nM reduced cytokine-induced STAT1 phosphorylation in $CD4^+$ T cells and fibroblast-like synoviocytes, respectively [132],[133]. However, this discrepancy could be attributed to the different cell types studied as in our experience intestinal epithelial cell lines are not as sensitive to inflammatory cytokines or pharmacological inhibitors as other cell types. Moreover, as shown in Figure 2B, the lowest dose of 2μM tofacitinib used did not produce a barrier-protecting effect against IFN-γ in IEC monolayers suggesting that in this experimental system, higher concentrations of tofacitinib are required to modulate downstream effector responses in readouts such as barrier function. Of note however, in our studies tofacitinib was administered at 2.6mg (16.7μM) or 7.8mg (50μM) which is within the dosage range of 5 or 10 mg given to ulcerative colitis patients [58],[134].

In summary, we have demonstrated that the JAK inhibitor, tofacitinib, is capable of both protecting against, and rescuing, the deleterious effects of IFN-γ on intestinal epithelial permeability using both cell line and human organoid model systems. Patients with ulcerative colitis who received tofacitinib for 8 weeks had significantly higher clinical response rates and lower Mayo endoscopic subscores compared with those receiving placebo [58],[134]. Additionally, those who received tofacitinib had higher remission rates at 52 weeks compared with those receiving placebo [58]. Our results

suggest that part of the clinical benefits of tofacitinib in treating ulcerative colitis patients may accrue from reducing the activity of JAK-activated signaling pathways that disrupt tight junction protein composition in IECs. While tofacitinib has been demonstrated to promote mucosal healing, we propose that part of its efficacy may also lie in its ability to restore normal mucosal barrier function as reflected by the normalization of permeability to macromolecules and reduced electrolyte flux.

Chapter 3: JAK Inhibition by Tofacitinib Rescues Barrier Dysfunction and JAK1-STAT1 Signaling Defects in *PTPN2*-deficient Intestinal Epithelial Cells *In Vitro* and Preserves the Barrier Integrity in an *Ex Vivo* Model System

Introduction

The chronic and relapsing nature of inflammatory bowel disease (IBD) decreases quality of life and can lead to devastating and at times life-threatening complications in IBD patients. The two types of IBD, Crohn's disease (CD) and ulcerative colitis (UC), have the highest prevalence rates in Europe and North America with accelerating incidence rates in developing countries [19]. IBD is a chronic condition in which the immune system mounts an abnormal response to normal flora in the gastrointestinal tract and is marked with abdominal pain, diarrhea, skip lesions in CD, and ulcers in UC. The damage to the intestinal epithelium from chronic inflammation can compromise its ability to serve as a selective physical barrier separating luminal contents from underlying lamina propria [96]. Altered expression and/or localization of specific tight junction proteins, can increase intestinal permeability, which has been shown to precede inflammation [66] and predict relapse in IBD [65]. This allows dysregulated ion and fluid transport as well as increased access of bacterial products and toxins into the lamina propria, which can trigger inappropriate immune responses and contribute to the pathogenesis of IBD [135].

Tofacitinib (CP-690,550), an orally-administered JAK inhibitor has been FDA-approved for the treatment of chronic inflammatory conditions and has been FDA-

approved for the treatment of moderate-to-severe UC [58]. While pre-clinical studies on therapeutics targeting the JAK-STAT pathway have focused on immune cell targets, it is poorly understood how this pathway affects IECs and how it contributes to altered IEC functions, such as impaired barrier function associated with IBD. We have recently shown that tofacitinib can reduce cytokine-induced barrier dysfunction in IECs *in vitro* [16].

The etiology of IBD has a significant genetic component that has not been widely exploited for therapeutic targeting. There are currently 201 candidate genes associated with risk of onset of IBD, most of which are involved in regulating the immune system's interaction with IECs and microbial flora [24],[52],[67],[136]. A number of these genes are involved in regulating the Janus kinase-signal transduction and activator of transcription (JAK-STAT) pathway, which can be activated by cytokines involved in IBD [24]. One of the major negative regulators of JAK-STAT signaling is T cell protein tyrosine phosphatase (TCPTP) encoded by the IBD candidate gene, protein tyrosine phosphatase nonreceptor type 2 (*PTPN2*). As a phosphatase, it regulates the JAK-STAT signaling pathway with substrates including JAK1, JAK3, and STAT1 [74],[79]. Loss-of-function mutations in *PTPN2* increase the risk of IBD [71] and transient knockdown of *PTPN2* in IEC lines leads to a further increase in permeability coupled with STAT1 and STAT3 activation following treatment with the IBD-associated pro-inflammatory cytokine IFN-γ [79].

We have also shown that IECs stably expressing shRNA against *PTPN2* have an underlying barrier dysfunction [80] and that tofacitinib can normalize barrier dysfunction

in parental T84 cells treated with pro-inflammatory cytokine IFN-γ [16]. Our main goal in this study was to determine if tofacitinib can correct JAK-STAT signaling defects and barrier dysfunction in *PTPN2*-deficient epithelial cell and animal models. Here, we show that tofacitinib can correct the elevated basal and cytokine-induced JAK1-STAT1 signaling and barrier defects in IECs lacking *PTPN2*. These studies were also aimed at determining if effects of tofacitinib can be recapitulated *in vivo* or *ex vivo* in *Ptpn2*-deficient mice or tissues. Moreover, I show that constitutive *Ptpn2* knockout (KO) mice display elevated levels of intestinal JAK-STAT activation and increased macromolecular permeability compared to their wildtype (WT) and *Ptpn2* heterozygous (Het) littermates. Although increased pSTAT1/STAT1 levels in IECs isolated from tamoxifen-inducible villin-Cre $Ptpn2^{fl/fl}$ mice ($Ptpn2^{\Delta IEC}$) were observed, these mice did not display an underlying increase in intestinal permeability. In conflict with earlier work from our lab, constitutive *Ptpn2* Het mice did not show an *in vivo* barrier defect compared to WT littermates and thus we were unable to determine the effectiveness of tofacitinib treatment in correcting a barrier defect *in vivo* in this mouse model. However, studies on isolated mouse tissues treated with tofacitinib *ex vivo* show that tofacitinib preserves barrier integrity in the *Ptpn2* Het intestine. In summary, tofacitinib can reverse JAK-STAT signaling defects and protect the barrier in *PTPN2*-deficient model systems.

Materials and Methods

Materials

Tofacitinib (MedChemExpress) and vehicle dimethylsulfoxide (DMSO, 0.5%, Sigma) were used in *in vitro* and *ex vivo* studies. Interferon-gamma (IFN-γ) at 100 U/ml (50ng/ml) was used in cell culture. Forskolin (Fsk, Sigma-Aldrich) and carbachol (carbamoylcholine chloride, CCh, Sigma-Aldrich) were used in the Ussing chambers experiments. Tofacitinib citrate (Selleckchem), methylcellulose (Sigma), and Tween-20 (Fisher) were used to make gavage solutions used in *in vivo* studies.

Analysis of JAK-STAT Signaling Upon Acute Treatment with Vehicle, Tofacitinib, and IFN-γ

To determine the effect of acute tofacitinib treatment on basal JAK1-STAT1 phosphorylation, HT-29 IECs stably expressing scrambled control shRNA (CTL) or shRNA targeted against *PTPN2* (KD) [80] were treated with vehicle (DMSO 0.5%) or tofacitinib (50μM) for 2 hours then washed twice with ice-cold PBS prior to cell lysis by RIPA buffer (50 mM Tris-Cl pH 7.4, 150 mM NaCl, 1% NP-40, 0.5% Na-deoxycholate, 0.1% SDS supplemented with protease (Roche) and phosphatase inhibitors (sodium orthovanadate, Phosphatase Inhibitor Cocktail 2 and 3, Sigma-Aldrich) and incubation at 4°C for 15 min.

The effect of tofacitinib treatment on acute cytokine-stimulated JAK-STAT activation was also determined in HT-29 CTL and *PTPN2* KD cells first treated with vehicle (DMSO 0.5%) or tofacitinib (50μM) for 1 hr followed by IFN-γ (1000 U/ml;

50ng/ml) exposure for 1 hr. Cells were washed twice with ice-cold PBS prior to cell lysis by RIPA buffer, as mentioned above.

Assessment of Barrier Function *In Vitro*

Polarized human IEC lines HT-29.cl19a and Caco-2BBe transduced with scrambled control shRNA (CTL) or shRNA against *PTPN2* (KD), as previously described [80], were used in these experiments. Cells were switched to serum-free media overnight, treated apically with 0.5% DMSO or 50μM tofacitinib with or without subsequent basolateral exposure to IFN-γ (100 U/ml; 5ng/ml). After 24 hours, transepithelial electrical resistance (TER) was measured using an epithelial volthommeter (EVOM2, World Precision Instruments) and companion chopstick electrodes (World Precision Instruments). TER is indicated as the average of 3 measurements per well and expressed as Ohms.cm^2. Cells were washed twice with PBS with $MgCl_2$ and $CaCl_2$ then equilibrated in 37C for 30 min. Leak barrier permeability was assessed by adding of 1mg/ml 4kDa fluorescein isothiocyanate (FITC)-dextran (FD4) apically to each well then sampling the basolateral compartment after 2 hrs to measure the amount of FD4 that has passed across the monolayers, as described previously [16]. Fluorescence was measured using a plate reader (Promega) and FD4 concentration was determined against a standard curve. Cells were then washed and lysed with RIPA as mentioned above.

Preparation of Whole Cell Lysates for Western Blotting

After lysis, cells were scraped into microcentrifuge tubes and homogenized by sonication on ice at 30% amplitude, at 10-second on/off intervals for 40 seconds using the Q125 Sonicator (QSonica) then centrifuged at 16,200 x g for 10 min at 4°C. Supernatants were collected and quantified using the Pierce BCA Protein Assay Kit (ThermoFisher Scientific). Equal protein concentration of each sample was mixed with loading buffer (60 mM Tris-Cl pH 6.8, 2% SDS, 5% β-mercaptoethanol, 0.01% bromophenol blue, 10% glycerol) to make loading samples, which were then incubated at 95°C for 10 min and stored in -20°C prior to Western blotting.

Western Blotting

Prepared lysates were loaded on 7% or 11% SDS-polyacrylamide gels and ran at 100 V for 1hr 40 min at room temperature then transferred onto polyvinylidene difluoride (PVDF) membranes (EMD) for 2 hours at 250mA in 4°C. PVDF membranes were rinsed 3x with Tris-buffered saline with 0.1% Tween-20 (TBS-T), then blocked with 5% milk in for 1 hr at room temperature prior to overnight incubation with primary antibodies (Table 3.1). Blots were rinsed 3x with TBS-T followed by 5 min washes (3x), then incubated with secondary antibodies horseradish peroxidase-conjugated goat anti-mouse (#115-036-062) or goat anti-rabbit (#111-036-045) IgG secondary antibodies (Jackson Immunoresearch Laboratories) diluted at 1:5000 or 1:2500, respectively in 1% milk in TBS-T for 1 hr at room temperature. Blots were again rinsed 3x with TBS-T followed by 5 min washes (3x). Membranes were then incubated with SuperSignal West Pico PLUS

Chemiluminescent Substrate solutions (ThermoFisher Scientific) per manufacturer's instructions then exposed to film (LabScientific Inc.). Densitometric analysis was performed using ImageJ [117].

Table 3.1: Primary antibodies used for Western blotting

Primary Antibodies	Host	Provider	Catalog No.	Dilution
ZO-1	Rabbit	Thermo Fisher Scientific (Rockford, IL)	61-7300	1:1000
Occludin	Rabbit	Thermo Fisher Scientific (Rockford, IL)	71-1500	1:1000
Phospho-JAK1 (Tyr 1022/1023)	Rabbit	Cell Signaling Technology (Danvers, MA)	#3331	1:1000
Total JAK1	Rabbit	Cell Signaling Technology (Danvers, MA)	#3344	1:1000
Phospho-STAT1 (Tyr 701)	Rabbit	Cell Signaling Technology (Danvers, MA)	#9167	1:1000
Total STAT1	Rabbit	Cell Signaling Technology (Danvers, MA)	#9175	1:1000
TCPTP (anti-mouse)	Mouse	Medimabs (Quebec, Canada)	MM-0018	1:500
TCPTP (anti-human)	Mouse	EMD Millipore (San Diego, CA)	PH03L	1:500
β-actin	Mouse	Sigma Aldrich (St. Louis, MO)	A5316	1:5000

Mice

Mice were housed in specific pathogen-free conditions, unless otherwise stated, under ambient temperature with a 12-hr light, 12-hr dark cycle. All protocols for animal care, use, and euthanasia were approved by the University of California, Riverside Institutional Animal Care and Use Committee in accordance with the National Institute of Health guidelines. Naïve 3 wk old BALB/c wildtype, *Ptpn2* constitutive heterozygous and knockout mice were used for both *in vivo* and *ex vivo* studies. Adult and 3wk old BALB/c wildtype and *Ptpn2* heterozygous mice housed in a conventional vivarium were used for tofacitinib citrate *in vivo* studies.

Adult and 3 wk old transgenic *Ptpn2*$^{fl/fl}$ mice bearing tamoxifen-inducible Cre-recombinase under the villin promoter (villin-Cre-ERT2) were also used in experiments. To induce targeted deletion of *Ptpn2* in villin-expressing cells (primarily consisting of the gut epithelium), mice were given intraperitoneal injection of tamoxifen (Sigma) dissolved in corn oil (Sigma) at 10mg/ml and administered at a dose of 50mg/kg body weight (50μL per 10g BW), once daily for 5 consecutive days. After 3 or 4 wks, barrier function was assessed, IECs were isolated, and tissues were harvested from mice. *Ptpn2*$^{fl/fl}$ mice that did not express Cre-recombinase, treated also with tamoxifen, were used as controls.

Tissue Collection and Intestinal Epithelial Cell (IEC) Isolation

After blood collection for the permeability assays, mice were sacrificed and tissues were harvested. Whole intestinal pieces from the distal ileum, cecum, proximal colon, and distal colon were harvested were flushed with ice-cold PBS, flash-frozen in liquid nitrogen, and stored in -80°C for protein expression analysis. Frozen tissues were homogenized in RIPA buffer supplemented with protease and phosphatase inhibitors using a bead-beater. Protein concentration was determined, and tissue lysates were subjected to Western blotting, as mentioned above.

For IEC isolation, intestinal pieces were inverted, incubated in Cell Recovery Solution (Corning) on ice for 2 hrs, then vigorously shaken to release IECs. IECs were washed twice with ice-cold PBS then lysed in RIPA supplemented with protease and phosphatase inhibitors, and processed, as mentioned above. Protein concentration was determined and samples were subjected to Western blotting, as mentioned above.

After flushing with ice-cold PBS, intestinal tissues were also fixed in 4% paraformaldehyde in 4°C overnight. Tissues were then washed 3x with PBS, incubated in 30% sucrose in 4°C overnight for cryoprotection, then embedded in optimal cutting temperature (OCT, Sakura) medium and snap-frozen for immunohistochemical analysis.

JAK3 Immunofluorescence in Distal Colons of *Ptpn2*-Deficient Mice

Fixed distal colons from 3 wk old BALB/c wildtype, *Ptpn2* heterozygous and knockout mice embedded in OCT were sectioned and stained with the following primary antibodies at 4°C overnight: phospho-JAK3 (sc-16567, Santa Cruz Biotechnology) and total-JAK3 (sc-513, Santa Cruz Biotechnology). This was followed by incubation with secondary antibodies for 1 hr at room temperature: Cy3-conjugated donkey-anti-goat (Jackson Immunoresearch) and Alexa-Fluor 488-conjugated donkey-anti-rabbit (Jackson Immunoresearch). Slides were mounted using Prolong Gold Antifade Mountant with DAPI (Invitrogen) and visualized with a Leica DM5500 microscope attached with a DFC365 FX camera using the 10x and 63x oil objectives with a 2x zoom. In addition to an image of the entire distal colon cross-section, images from 4-5 fields per tissue were obtained as tiff files using the LAS-AF Lite software.

Assessment of Barrier Function *In Vivo*

Adult mice were food-deprived overnight (3 wk old mice for 2 hrs) then gavaged with either FD4 alone or in combination with creatinine and 70kDa Rhodamine-B (RD70) dissolved in water. Blood was collected after 4-5 hours and fluorescence

intensity was measured in diluted serum using a plate reader (Promega). FD4 and RD70 concentrations were then determined against a standard curve. Creatinine concentration in the serum was measured using the SVT creatinine R1 and R2 reagents. Kinetic absorbance readings were measured at 505nm at 1 min intervals for 30 min using a Synergy HT plate reader (BioTek). ΔOD (OD 6 min – OD 0 min) was determined and creatinine concentrations in the sera were determined against a standard curve. Values from the sera of water-gavaged mice were substracted from those of the samples.

Tofacitinib Citrate Treatment *In Vivo*

Tofacitinib citrate gavage solution was prepared by sonicating tofacitinib citrate powder into a fine suspension in vehicle 0.5% methylcellulose/0.25% Tween 20. To determine the effect of tofacitinib citrate treatment on barrier function, 3wk old or 8wk old BALB/c wildtype and *Ptpn2* heterozygous mice, housed in a conventional vivarium, were orally gavaged with vehicle or tofacitinib citrate solution at a dose of 100mg/kg body weight [137], twice daily for 7d.

Measurement of Intestinal Barrier Function *Ex Vivo*

Electrical resistance (TER), FD4 and RD70 permeability, and change in short-circuit current (ΔI_{sc}) were measured across isolated ceca from 3 week-old BALB/c wildtype (WT), and constitutive *Ptpn2*$^{+/-}$ (Het) and *Ptpn2*$^{-/-}$ (KO) mice using Ussing chambers (Physiologic Instruments). Unstripped ceca were mounted onto paired Ussing chambers maintained at 37°C by heated water jackets and equilibrated in Kreb's Ringer's

buffer (115mM NaCl, 2.4mM K_2HPO_4, 0.4mM KH_2PO_4, 10mM HEPES, 1.2mM $CaCl_2$, 1.2mM $MgCl_2$, 25mM $NaHCO_3$, 10mM glucose) for at least 20 min prior to measurements and treatments. After stabilization, basal TER of the tissues were measured prior to and every hour during a 4-hr exposure to 0.5% DMSO or 50μM tofacitinib administered to the mucosal side of the tissues.

Permeability to FD4 and 70kDa Rhodamine B-dextran (RD70, Sigma) was measured by adding the fluorescent probes to the apical side of the tissues 2 hrs post-treatment then collecting duplicate 50μL samples of the basolateral buffer after a 2 hr incubation. Fluorescence was measured using a microplate reader (Promega) and probe concentrations were determined against a standard curve for FD4 and RD70.

The effects of cAMP and Ca^{2+} stimulation on Cl^- secretion, and viability of the mounted tissues after the 4-hr treatments, were measured after bilateral addition of 20μM forskolin (Fsk) followed by basolateral administration of 300μM carbachol (CCh), respectively. ΔI_{sc} was calculated as the difference between baseline and peak current after stimulation by Fsk or CCh.

Statistical Analysis

All data are expressed as mean ± SD from *n* number of biological replicates. Comparisons between two groups were determined by two-tailed Student t test. Comparisons between three or more groups were analyzed using one-way or two-way analysis of variance (ANOVA), in which Tukey or Holm-Sidak post-test was used to

correct for multiple pairwise comparisons, where appropriate. *P* values ≤ 0.05 were considered significant.

Results

Tofacitinib decreased elevated basal and IFN-γ-stimulated JAK1-STAT1 phosphorylation in IECs lacking PTPN2

For the first time, we show that *PTPN2* KD cells have higher JAK1 phosphorylation compared to CTL cells (Figure 3.1A). In agreement with previous studies [81], *PTPN2* KD cells have increased STAT1 phosphorylation compared to CTL cells (Figure 1A). Following acute treatment with vehicle or tofacitinib for 2 hours, the elevated JAK1 and STAT1 phosphorylation in *PTPN2* KD cells was significantly reduced by tofacitinib (Figure 3.1A). HT-29 CTL and *PTPN2* KD cells were also challenged with IFN-γ with or without the presence of vehicle or tofacitinib, as depicted in Figure 3.1B. JAK1-STAT1 phosphorylation levels potentiated by acute IFN-γ in *PTPN2* KD cells were also significantly reduced by tofacitinib pre-treatment (Figure 3.1B). These results show that tofacitinib can correct basal and IFN-γ-induced JAK-STAT signaling defects in *PTPN2*-deficient IECs *in vitro*.

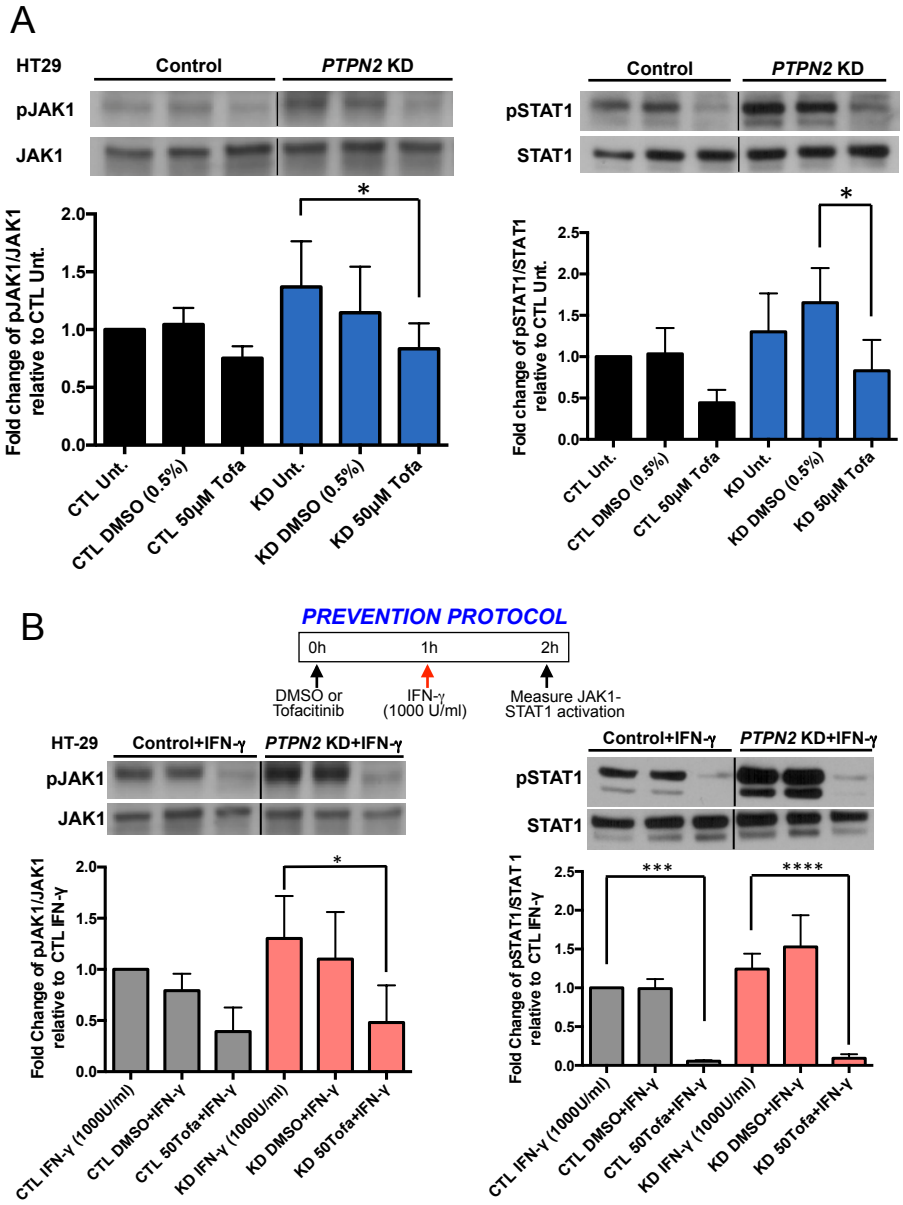

Figure 3.1: Basal and cytokine-induced JAK1-STAT1 phosphorylation elevated in *PTPN2*-deficient IECs is reduced by acute tofacitinib treatment *in vitro*. A) HT29 control (CTL) and *PTPN2* knockdown (KD) cells were treated with vehicle (0.5% DMSO) or tofacitinib (50μM) for 2 hours prior to lysis and Western blot analysis for phosphorylated and total JAK1 and STAT1 expression. B) A schematic of HT29 CTL and *PTPN2* KD cells pre-treated with vehicle (0.5% DMSO) or tofacitinib (50μM) for 1 hour before IFN-g (1000 U/ml; 50ng/ml) for 1 hour before lysis and Western blot analysis for phosphorylated and total JAK1 and STAT1. Representative blots and densitometric analyses are shown. Data are expressed as means ± SEM. *$P < 0.05$, ***$P < 0.001$, ****$P < 0.0001$, $n = 3$-4.

Tofacitinib corrected barrier dysfunction in PTPN2 KD cells before or after IFN-γ exposure

Here we show that tofacitinib rescued the resting lower TER and elevated FD4 permeability observed in *PTPN2*-deficient Caco-2BBe cells (Figure 3.2). Upon IFN-γ-induced decrease in TER and robust increase in FD4 flux, which are potentiated in *PTPN2* KD cells, tofacitinib also normalized TER and FD4 flux in Caco-2BBe or HT29 cells, respectively (Figure 3.2). Barrier defects due to *PTPN2* loss have been described previously in IECs [80]. These results convey the ability of tofacitinib to correct the underlying barrier defect in resting and cytokine-challenged *PTPN2*-deficient cells.

As previously observed [16], DMSO, tofacitinib, and/or IFN-γ did not significantly alter ZO-1 and occludin protein expression in either HT-29 CTL or *PTPN2* KD cell lines (Figure 3.3). Changes in FD4 permeability, are therefore not caused by changes in protein expression of ZO-1 and occludin and may instead be due tight junction protein localization changes.

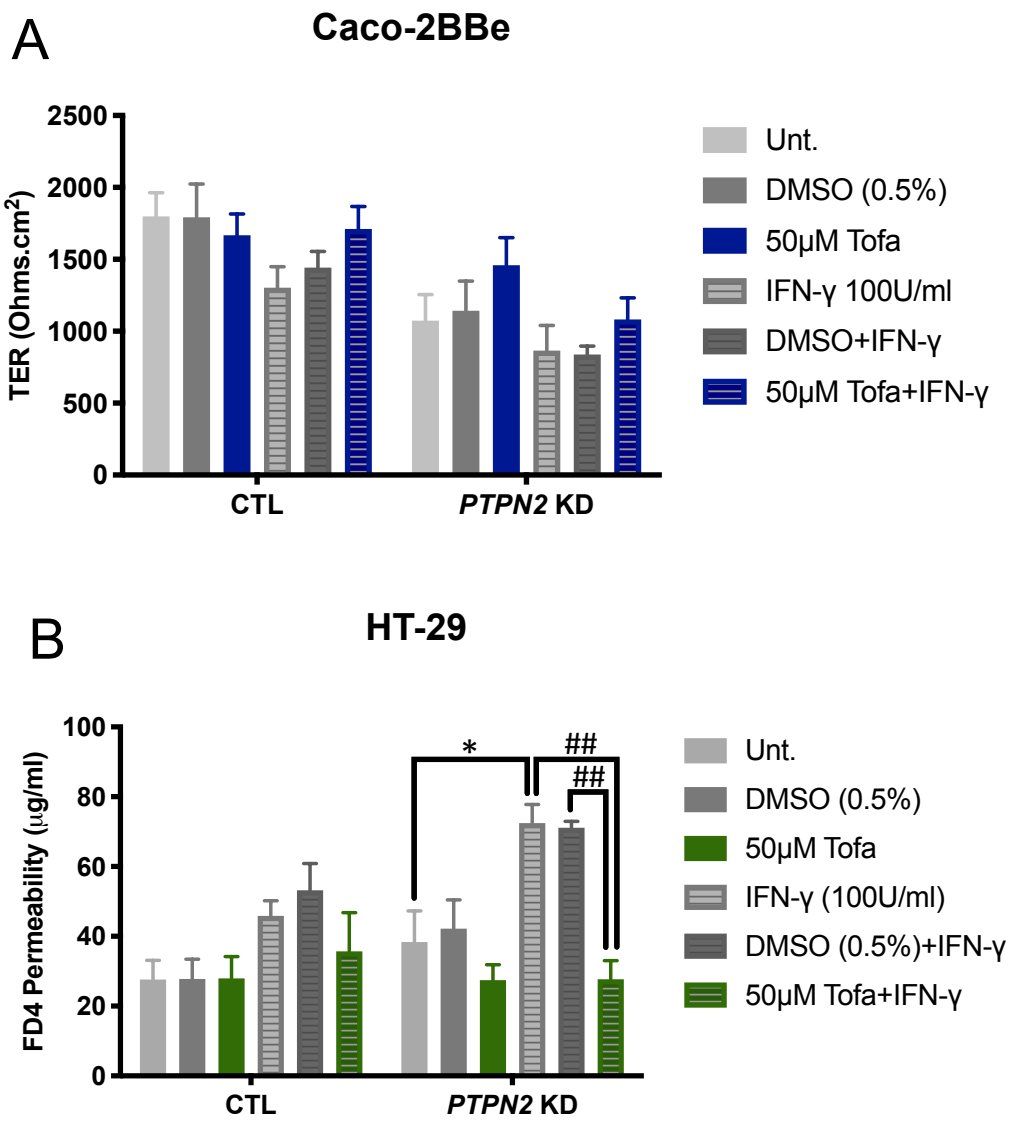

Figure 3.2: Tofacitinib rescues resting and cytokine-induced barrier dysfunction in *PTPN2*-deficient IECs *in vitro*. Control (CTL) and *PTPN2* knockdown (KD) IECs treated with vehicle or tofacitinib for 1 hour with or without subsequent exposure to IFN-γ. After 24 hours, A) TER and B) FD4 permeability were measured. Data are expressed as means ± SEM. *P < 0.05, ##P < 0.01, *n* = 3-4 per group, in duplicates.

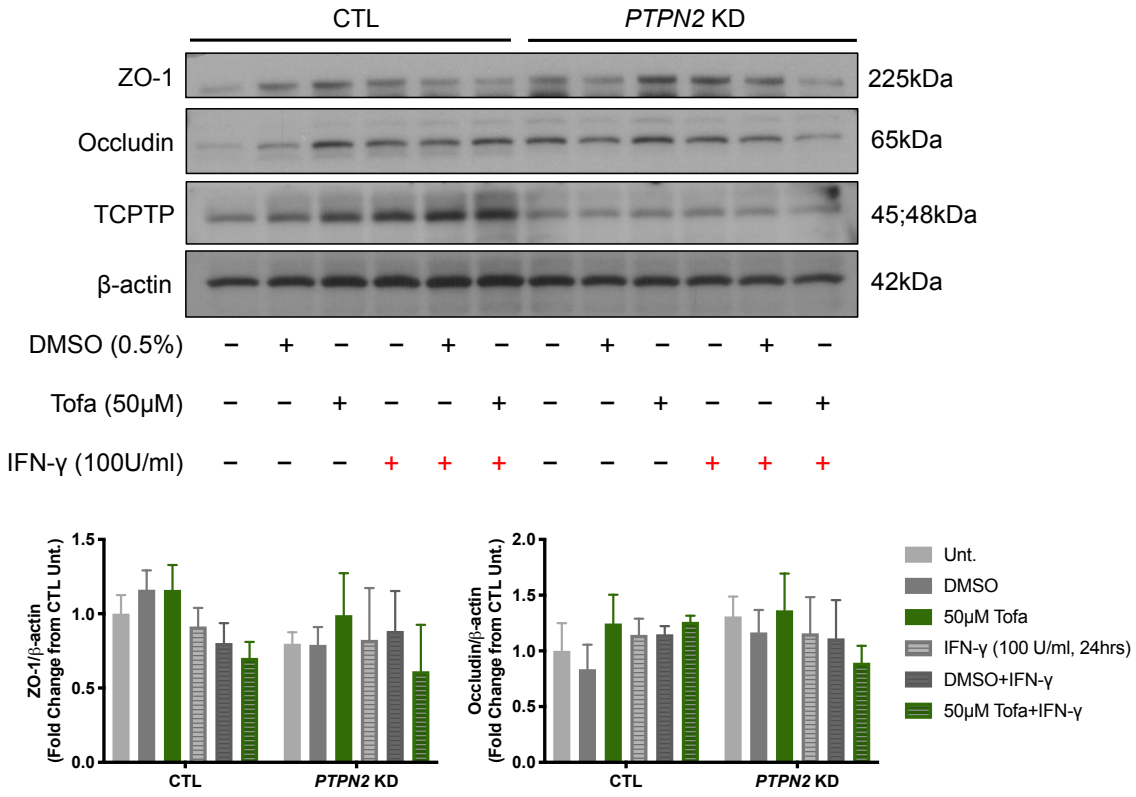

Figure 3.3: ZO-1 and occludin protein expression are unaltered by *PTPN2* deficiency or tofacitinib treatment. HT29 CTL and *PTPN2* KD cells were subjected to vehicle (0.5% DMSO) or tofacitinib (50μM) treatment for 1 hour with or without subsequent exposure to IFN-γ for 24 hours were lysed and subjected to Western blotting. Representative blots are shown for the proteins indicated and densitometric analyses were performed. Data are expressed as means ± SD. $n = 4$ per group, in duplicate.

JAK-STAT activation and macromolecular permeability are elevated in Ptpn2-deficient mice

To determine whether findings from cell culture models are recapitulated *in vivo*, basal levels of JAK-STAT signaling and barrier function were analyzed in BALB/c wildtype (WT) and constitutive *Ptpn2* heterozygous (Het) and knockout (KO) mice. As previously described [82],[138], *Ptpn2* KO mice succumb to systemic inflammation by week 3-5, so to ensure appropriate comparisons with WT and Het littermates, mice were used at 3 weeks of age. As a phosphatase, PTPN2 negatively regulates the JAK-STAT signaling pathway with substrates including JAK1, JAK3, and STAT1. By fluorescence immunohistochemistry, distal colons from *Ptpn2*-deficient mice show elevated JAK3 phosphorylation compared to WT littermates (Figure 3.4). Western blot analysis of whole proximal and distal colons reveal that *Ptpn2*-deficient mice have lower levels of TCPTP and that compared to WT mice, *Ptpn2* Het mice exhibit higher JAK1 and STAT1 phosphorylation. Although the representative blots display robust STAT1 phosphorylation in *Ptpn2* KO mice, higher expression of total STAT were also observed in these tissues, therefore, densitometric analysis reveal pSTAT1/STAT1 levels in *Ptpn2* KO mice that are comparable to WT and *Ptpn2* Het mice. However, isolated distal colon IECs from *Ptpn2* KO mice have significantly higher pSTAT1/STAT1 levels compared to WT and *Ptpn2* Het mice (Figure 3.5).

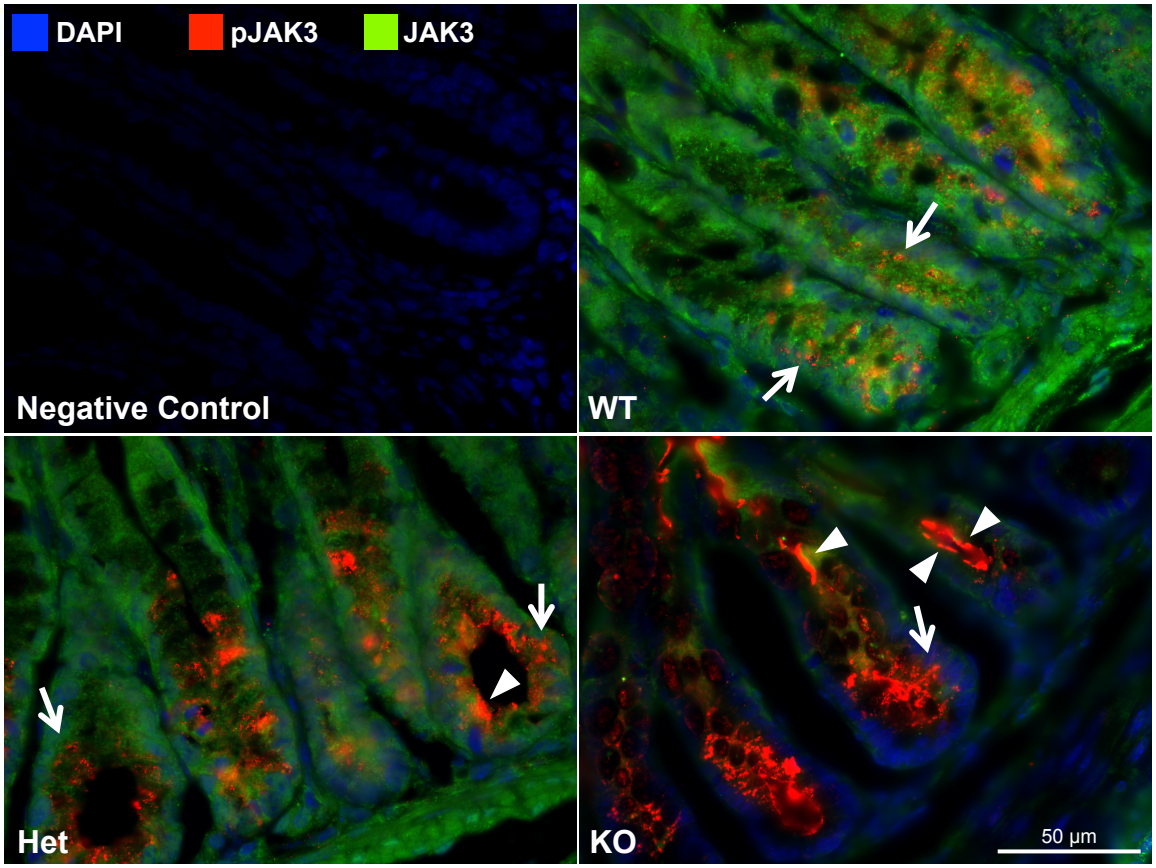

Figure 3.4: Distal colons from *Ptpn2*-deficient mice display elevated levels of JAK3 phosphorylation compared to WT littermates. Representative immunofluorescent images of distal colon crypts from naïve wildtype (WT), constitutive *Ptpn2* heterozygous (Het), and knockout (KO) mice, stained for phospho-JAK3 (red), total JAK3 (green), and DAPI (blue). Images were taken using 10x and 63x objective lenses, and lengths of scalebars are indicated. $n = 5$ per group. Arrows indicate subapical phospho-JAK3 and arrowheads point to intense apical phospho-JAK3 signal detected. *Ptpn2* KO distal colon stained only with fluorophore-conjugated secondary antibodies was used as a negative control.

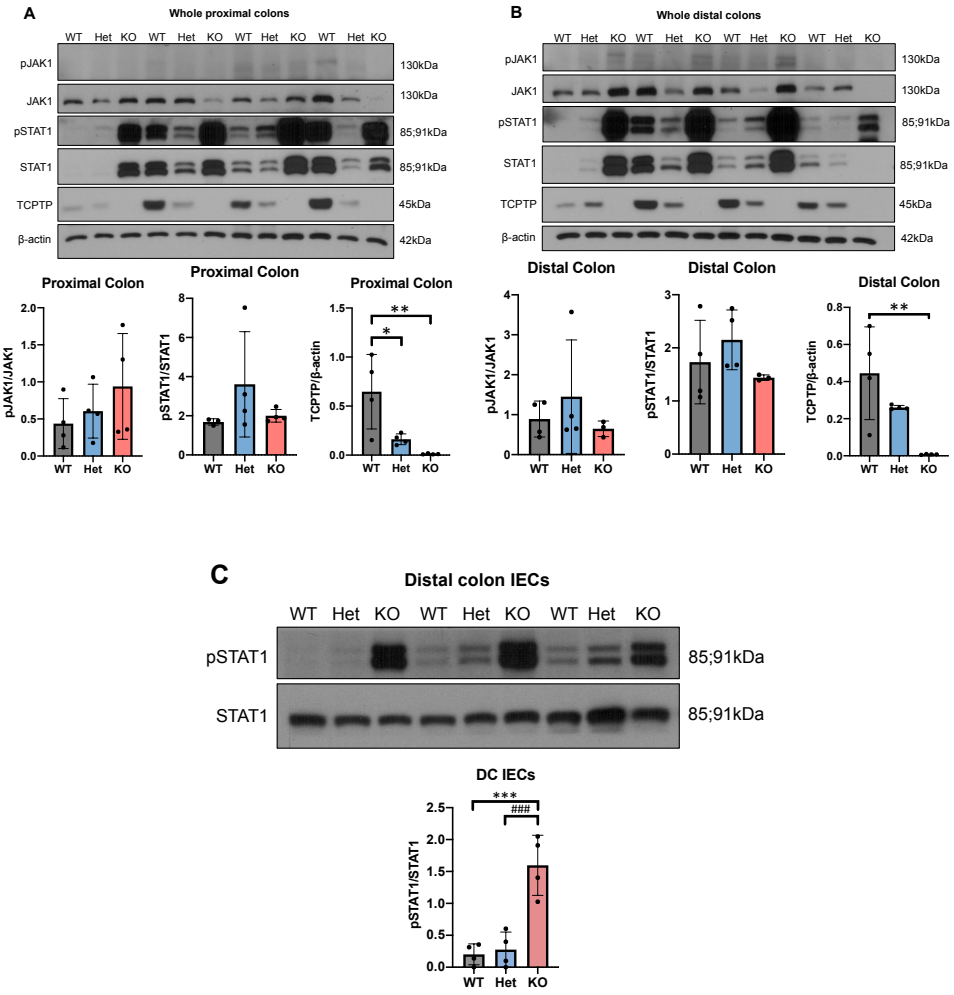

Figure 3.5: Constitutive *Ptpn2*-deficient mice express higher JAK1-STAT1 phosphorylation in intestinal tissues. Representative blots and densitometric analyses of phosphorylated and total JAK1, STAT1, TCPTP, and β-actin are shown from A) whole proximal colons, B) whole distal colons, and C) distal colon IECs isolated from naïve wildtype (WT), constitutive Ptpn2 heterozygous (Het), and knockout (KO) mice. Data are expressed as means ± SD. **P* < 0.05, ***P* < 0.01, ****P* < 0.001, ###*P* < 0.001, *n* = 3-4 per group.

In agreement with findings *in vitro*, *Ptpn2* KO mice display significantly elevated FD4 intestinal permeability compared to WT and *Ptpn2* littermates (Figure 3.6). However, no differences in permeability were seen between WT and Ptpn2 Het mice, as previously observed (unpublished data). Further, neither creatinine and nor RD70 intestinal permeability were altered by *Ptpn2* loss *in vivo* (Figure 3.6). These functional assays suggest that barrier defects associated with loss of *Ptpn2* is recapitulated *in vivo*.

Intestinal permeability was unaffected by tofacitinib citrate treatment in Ptpn2 Het mice in vivo

To determine if tofacitinib affected barrier function *in vivo*, adult WT and *Ptpn2* Het mice were orally gavaged with vehicle or tofacitinib citrate twice daily for 7 consecutive days. Intestinal permeability was assessed before and after tofacitinib treatment. Figure 3.7 shows that naïve weanlings and adult *Ptpn2* Het mice do not display higher intestinal permeability to FD4 compared to WT animals, contrary to previous findings (unpublished). Additionally, tofacitinib citrate treatment did not significantly alter FD4 intestinal permeability compared to vehicle (Figure 3.7). A new animal model was therefore tested for tofacitinib studies *in vivo*.

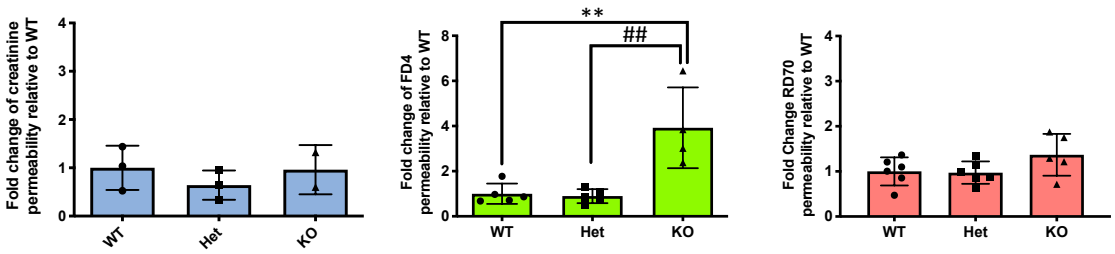

Figure 3.6: *Ptpn2* KO mice have higher macromolecular intestinal permeability than WT and *Ptpn2* Het mice *in vivo*. Intestinal permeability to creatinine, FD4, and RD70 probes were measured in three week-old wildtype (WT), constitutive Ptpn2 heterozygous (Het), and knockout (KO) mice to assess pore, leak, and unrestricted barrier defects, respectively. $**P < 0.01$, $\#\#P < 0.01$, $n = 2$-6 per group.

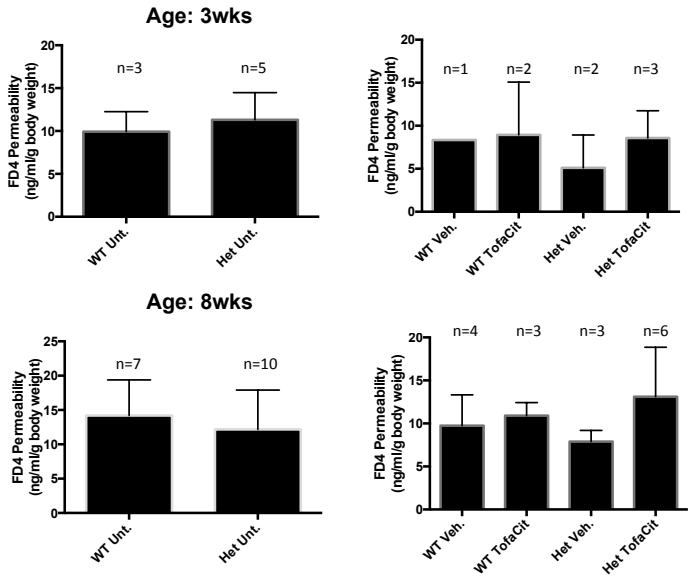

Figure 3.7: Barrier permeability did not differ upon constitutive *Ptpn2* loss or tofacitinib citrate treatment *in vivo*. FD4 permeability in three week-old and adult WT and *Ptpn2* Het mice treated with twice daily oral gavage of vehicle or tofacitinib citrate was measured before and after treatments. Data are expressed as means ± SD.

Ptpn2$^{\Delta IEC}$ mice display higher STAT1 activation, but not barrier permeability, compared to Ptpn2$^{fl/fl}$ mice

To determine if IEC-specific knockout of *Ptpn2* yielded a barrier defect *in vivo*, 3 wk old tamoxifen-inducible villin-Cre-*Ptpn2*$^{fl/fl}$ mice were used. Three weeks after tamoxifen induction, intestinal permeability of *Ptpn2*$^{\Delta IEC}$ and *Ptpn2*$^{fl/fl}$ mice, body weights, spleen weights, and colon lengths showed no change to IEC-specific loss of *Ptpn2* (Figure 3.8). To rule out the potential contribution of an underdeveloped gut, adult tamoxifen-inducible villin-Cre-*Ptpn2*$^{fl/fl}$ mice were also used. Four weeks after tamoxifen induction, barrier permeability studies reveal that compared to *Ptpn2*$^{fl/fl}$ or corn-oil treated mice, *Ptpn2*$^{\Delta IEC}$ mice did not display higher FD4 intestinal permeability (Figure 3.9). Western blot analysis of IECs isolated from both small and large intestines of tamoxifen-treated mice (*Ptpn2*$^{\Delta IEC}$) showed successful knockout of TCPTP in IECs compared to *Ptpn2*$^{fl/fl}$ controls (Figure 3.10). This was correlated with higher STAT1 phosphorylation (Figure 3.10), as seen in the constitutive *Ptpn2* Het and KO mice.

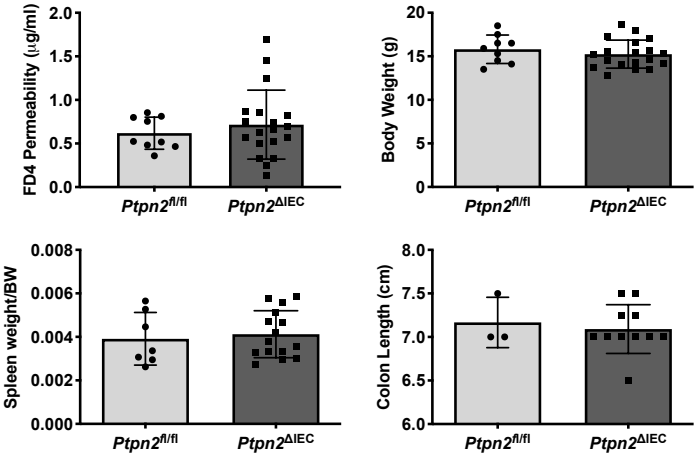

Figure 3.8: Macroscopic measures of inflammation were unaffected by IEC-specific *Ptpn2* loss. Whole intestinal FD4 permeability, body weights, spleen weights, and colon lengths measured three weeks after tamoxifen induction. n = 6-19.

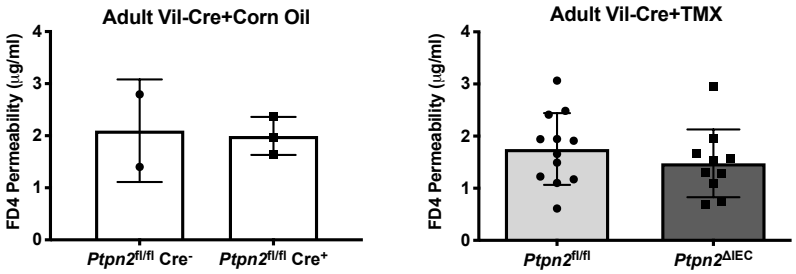

Figure 3.9: Intestinal permeability to FD4 was unaffected by IEC-specific *Ptpn2* loss in adult mice. Four weeks after tamoxifen induction, whole FD4 intestinal permeability was assessed in *Ptpn2*$^{fl/fl}$ and *Ptpn2*$^{\Delta IEC}$ mice. Data are presented as means ± SD. Macromolecular permeability to FD4 was also measured in corn-oil-treated *Ptpn2*$^{fl/fl}$ expressing the Cre-recombinase under the villin promoter (Cre^{+}) or not (Cre^{-}). TMX = tamoxifen. n = 2-12.

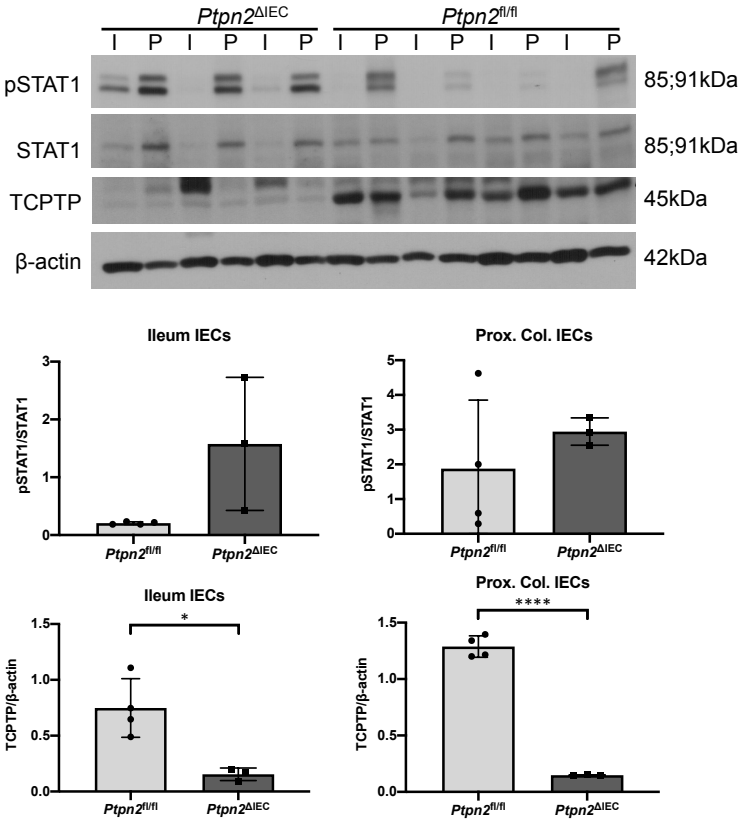

Figure 3.10: IECs from *Ptpn2*$^{\Delta IEC}$ mice displayed higher STAT1 phosphorylation compared to those of *Ptpn2*$^{fl/fl}$ mice. Four weeks after tamoxifen induction, IECs from adult *Ptpn2*$^{\Delta IEC}$ were lysed and subjected to Western blotting. A) Representative blots of ileum (I) and proximal colon (P) IECs from *Ptpn2*$^{\Delta IEC}$ and *Ptpn2*$^{fl/fl}$ mice and B) densitometric analysis of pSTAT1/total STAT1 and TCPTP/β-actin. Data are presented as means ± SD. **P* < 0.05, *****P* < 0.0001, *n* = 3-4.

Acute exposure to tofacitinib prevents time-dependent decrease in TER in ceca of Ptpn2$^{+/-}$ mice ex vivo without affecting macromolecular permeability

Although differences in whole intestinal permeability were not observed in constitutive *Ptpn2* Het or *Ptpn2*$^{\Delta IEC}$ mice with IEC-specific *Ptpn2* loss, region-specific differences may exist. Preliminary studies demonstrated that ceca from *Ptpn2* Het and KO mice displayed lower TER and higher FD4 permeability compared to those of WT mice (unpublished). In order to address whether tofacitinib affected specific regions of the intestinal tract, whole unstripped ceca from WT and constitutive *Ptpn2* Het and KO mice were mounted on Ussing chambers, treated with vehicle or tofacitinib *ex vivo* for a total of 4 hours, and subjected to permeability and ion-transport assays. Over time, TER decreased in vehicle-treated ceca from WT, *Ptpn2* Het, and KO mice (Figure 3.11A). Tofacitinib treatment modestly prevented this decrease in TER in *Ptpn2* Het mice, while no changes in TER were observed in tofacitinib-treated WT or *Ptpn2* KO ceca. FD4 and RD70 fluxes remained unaltered by genotypes or treatments (Figure 3.11B).

Additionally, cAMP-dependent ion transport, induced by forskolin, was significantly higher in vehicle-treated *Ptpn2* Het tissues, compared to those of WT or *Ptpn2* KO, which was unaffected by tofacitinib treatment (Figure 3.12A). Changes in Ca^{2+}-dependent ion transport, induced by carbachol, were not observed among genotypes or treatments (Figure 3.12B).

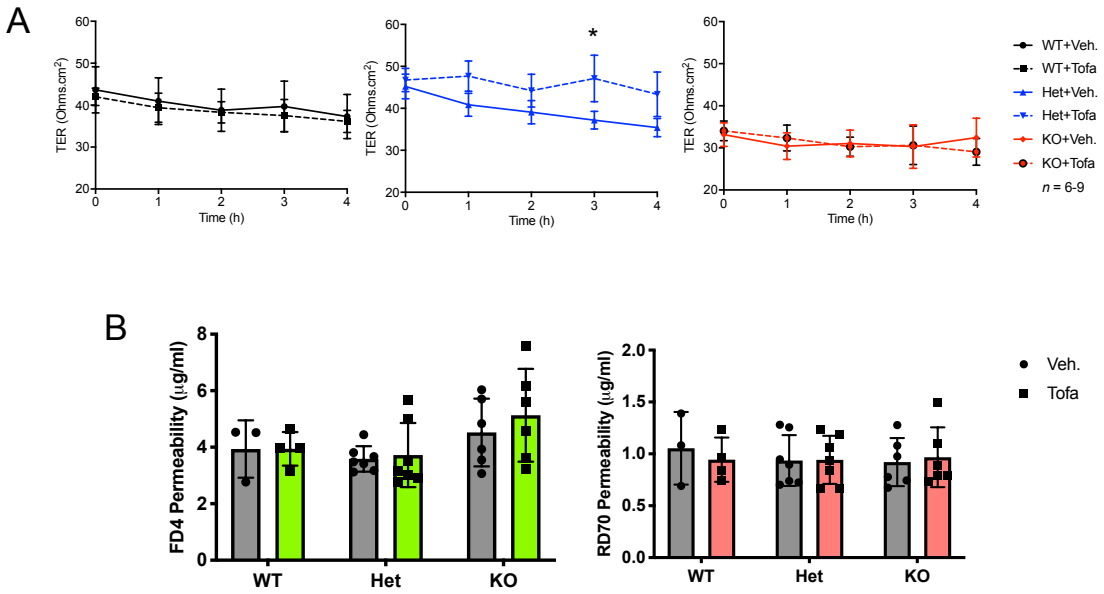

Figure 3.11: Time-dependent decrease in TER (Ohms.cm^2) was prevented by *ex vivo* tofacitinib treatment in *Ptpn2* Het cecum. Isolated ceca from wildtype (WT), constitutive *Ptpn2* heterozygous (Het), and knockout (KO) mice were mounted on Ussing chambers and treated with vehicle (0.5% DMSO) or tofacitinib (50µM) apically for 4 hours. A) TER was measured before, during, and after treatment. At the end of the treatment, B) FD4 and RD70 fluxes were measured and expressed as (µg/ml). Data are presented as means ± SD. *$P < 0.05$, n = 3-7.

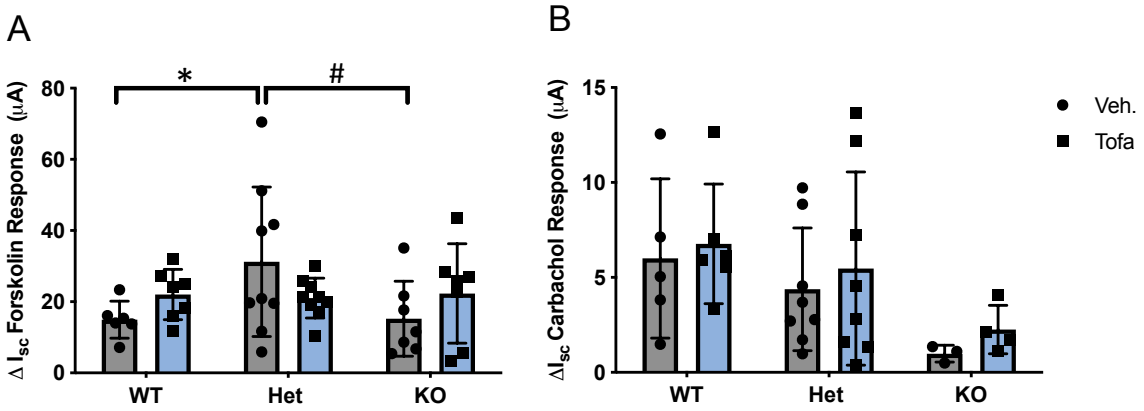

Figure 3.12: Electrogenic ion transport in tofacitinib-treated WT, *Ptpn2* Het, and KO mouse tissues *ex vivo*. Change in short-circuit current (ΔI_{SC}) after (A) bilateral forskolin (20µM) or B) basolateral carbachol (100µM) treatment on vehicle- or tofacitinib-treated ceca of WT, *Ptpn2* Het, and KO mice. Values are presented as means ± SD. * $P < 0.05$, # $P < 0.05$, n = 6-9 per group.

Discussion

In summary, our data show that tofacitinib can correct basal and IFN-γ-induced barrier defect and elevated JAK1 and STAT1 activation in *PTPN2*-deficient IECs. Higher JAK-STAT phosphorylation in epithelial cell lines is consistent with *in vivo* observations in intestinal tissues from *Ptpn2* KO and tamoxifen-inducible *Ptpn2*$^{\Delta IEC}$ mice. In agreement with previous unpublished findings, complete loss of *Ptpn2 in vivo* led to increased FD4 intestinal permeability. However, in these studies, *Ptpn2* Het or *Ptpn2*$^{\Delta IEC}$ mice did not display impaired barrier function, compared to controls. Nevertheless, treatment with tofacitinib *ex vivo* appeared to have a protective effect on time-dependent decrease in TER in *Ptpn2* Het ceca.

For the first time, we show that acute treatment with tofacitinib reduced basal and IFN-γ-stimulated JAK1-STAT1 signaling and barrier dysfunction in *PTPN2* KD cells. This is crucial considering that the lower TER in these are partly due to STAT1-dependent transcription of pore-forming tight junction protein claudin-2 [81]. Future studies will focus on analyzing claudin-2 expression in vehicle vs. tofacitinib-treated CTL and *PTPN2* KD IECs as we have shown in parental T84 cells [16]. The barrier protective effect of tofacitinib on *PTPN2*-deficient cells is likely not mediated through changes in tight junction protein expression, but rather, localization of these proteins, as previously shown in parental T84 cells [16].

Elevated JAK1 and JAK3 phosphorylation levels in *Ptpn2*-deficient mice confirms loss-of-function of the phosphatase *in vivo*. This has previously been demonstrated in immune cells derived from *Ptpn2* KO mice [74], but our results are the

first to show similar effects in IECs and intestinal tissues. As a downstream target of JAK1, STAT1 phosphorylation levels of unchallenged PTPN2 KD cells were also decreased by the acute treatment of tofacitinib. The enhanced activation of JAK1, STAT1, and JAK3 is an indicator of increased production of cytokines which activate these proteins in *Ptpn2*-deficient mice, such as those elevated in IBD [40]. Studies from our lab have shown elevated IFN-γ levels in the serum and intestinal tissues of *Ptpn2*-deficient mice compared to WT controls (unpublished), which may be responsible for the abnormally elevated JAK-STAT phosphorylation in naïve mice. Similar observations are seen in IECs from *Ptpn2*$^{\Delta IEC}$ mice, therefore cytokine profiling of the serum and intestinal tissues from these mice are necessary to delineate what is causing increased JAK-STAT signaling in these mice. Nevertheless, although these results suggest a positive correlation between *Ptpn2* loss and JAK-STAT phosphorylation, not all read-outs reached statistical significance and may require further studies. In addition, the increased total forms of STATs in IBD has been an area of controversy as to whether increased STAT signaling is due to increased total STAT expression overall *vs.* increased phosphorylation (i.e. more STAT proteins available to be phosphorylated and activated rather than an increase in the level of phosphorylation of individual STATs) [108],[139],[140].

Impaired barrier function was observed in *PTPN2*-deficient IECs and *Ptpn2* KO mice, but not in *Ptpn2* Het or *Ptpn2*$^{\Delta IEC}$ mice. This is contradictory to previous findings in our lab that *Ptpn2* Het have significantly higher FD4 permeability compared to WT controls (unpublished). Observed changes in the microbiome of these mice over time may account for the current absence of a difference in barrier phenotype (unpublished)

between WT and *Ptpn2* Het mice. Dramatic changes in bacterial populations, such as those of the pathogenic adherent-invasive *Escherichia coli* (AIEC) involved in IBD pathogenesis [141] and the beneficial segmented filamentous bacteria (SFB) [142] have been observed in small and large intestines of *Ptpn2* KO mice [143]. In addition, lack of barrier defect in $Ptpn2^{\Delta IEC}$ may partly be due to compensation from other protein tyrosine phosphatases [144] or from immune cells in response to *Ptpn2* loss in IECs. This is in agreement with previous work showing that constitutive $Ptpn2^{\Delta IEC}$ mice did not have worse histological scores or response to acute or chronic DSS-induced colitis, respectively [86]. Perhaps an alternative challenge will determine if $Ptpn2^{\Delta IEC}$ mice are more susceptible to barrier dysfunction compared to its $Ptpn2^{fl/fl}$ counterparts. Further, region-specific intestinal permeability in $Ptpn2^{\Delta IEC}$ tissues would need to be analyzed.

Increased creatinine suggests defects in the pore pathway of permeability. No change in creatinine permeability in *Ptpn2* KO mice contradict previous *in vitro* studies that *PTPN2* leads to lower TER [80],[81]. Perhaps region-specific TER measurements will yield more insight into how the pore barrier is affected by *Ptpn2* loss. Indeed, preliminary evidence indicated that vehicle-treated *Ptpn2* KO ceca displayed lower basal TER levels compared to WT and *Ptpn2* Het tissues. RD70 permeability was also unaffected in *Ptpn2*-deficient mice, which reveals that the increase in macromolecular permeability is not due to substantial epithelial damage [145]. Whether other intestinal regions exhibit the same effects will be addressed in further studies.

Ex vivo results on barrier function suggest that during the first 4 hours of treatment, tofacitinib may help preserve the integrity of the barrier, specifically in *Ptpn2*

Het tissues. Indeed, these *ex vivo* studies suggest that tissues need a longer time of exposure to tofacitinib before an impact on barrier function can be observed. Tofacitinib treatment *in vivo*, rather than *ex vivo*, may yield more robust results in its effect in barrier function in *Ptpn2*-deficient mouse models.

Overall, these results demonstrate that tofacitinib may serve as a more effective treatment if genetic profiles of IBD patients are considered and incorporated into patient treatment regimens. Data from clinical trials and retrospective observational studies reveal that tofacitinib induced a clinical response and maintained remission in about 33-40.6% of IBD patients compared to 11% in the placebo groups [58],[146],[147]. It is important to note that increased barrier permeability alone does not cause IBD, as seen in relatives of IBD patients with increased permeability who never develop disease [148], therefore, it should not be the only feature considered in IBD patient care. However, intestinal permeability is still a good indicator of disease as increased permeability occurs prior to the onset of disease [66] and can predict relapse in patients with quiescent Crohn's disease [65]. Tofacitinib treatment should also be taken with caution as increased rates of overall infections, particularly herpes zoster infection, have occurred in patients taking tofacitinib [58]. Recent studies have also shown slightly higher mortality rates in rheumatoid arthritis patients, ages 50 and older, taking tofacitinib with at least one cardiovascular risk factor [59]. These new findings further stress the importance of a personalized medicine approach to IBD treatments, such as tofacitinib for the treatment of UC. With the multi-factorial etiology of IBD, patient genetics should be included in their care plan. Based on results shown here, tofacitinib therefore has the therapeutic

potential to correct signaling and barrier function consequences of *PTPN2* genetic defects as a personalized medicine approach for patients harboring *PTPN2* loss-of-function mutations.

Chapter 4: The JAK-Inhibitor Tofacitinib Rescues Intestinal Barrier Defects and Disrupted Epithelial-Macrophage Crosstalk Caused by Loss of PTPN2 Activity *In Vitro* and *In Vivo*

Introduction

Inflammatory bowel disease (IBD) describes a chronic inflammatory condition affecting the digestive tract, which manifests as diarrhea, abdominal pain, ulcers, and in severe cases anemia. Two main types of IBD are ulcerative colitis and Crohn's disease, which differ in the histopathology and the intestinal sections affected [27],[149],[150]. The etiology of IBD is multi-factorial, in which genetics, environmental factors, the immune system, and the microbiome all contribute to disease manifestation [24]. Because of this, current therapeutics including corticosteroids, prednisone, mesalamine treat symptoms of IBD rather than target specific molecular candidates. Anti-TNF treatment has been shown as an effective treatment option for IBD, but one-third to one-half of anti-TNF-treated IBD patients relapsed after discontinuation unless anti-TNF therapy was re-introduced [151]. Lack or loss of clinical response over time may also occur due to production of antidrug antibodies [152], thus several alternative treatment strategies are currently studied or already approved for the use in IBD.

Tofacitinib (Xeljanz®) is a small-molecule pan-Janus kinase (JAK) inhibitor approved for the treatment of moderate-to-severe ulcerative colitis. Members of the JAK family are the first mediators of pro-inflammatory cytokine signaling associated with inflammation, and tofacitinib has been effective in treating chronic diseases, including

IBD [58],[153],[154]. Although tofacitinib induced higher clinical remission rates than placebo during clinical trials [58], remission at 52 weeks of treatment occurred in only 40.6% of patients. This suggests that there might be select patients with better response to tofacitinib. Primary outcomes for these studies mainly focused on clinical and endoscopic remission [58]thus the effect of tofacitinib in the gut has primarily been interrogated on a macroscopic scale. Recent pre-clinical animal studies with tofacitinib featuring DSS-induced and oxazolone-induced colitis mouse models have yielded great insight into how tofacitinib is acting in the intestinal tract [155],[156]. However, the effect of tofacitinib on specific cell types and the cellular crosstalk involved in intestinal homeostasis has been largely under-studied.

The barrier function of the intestinal epithelium ensures separation of luminal contents from underlying tissues while allowing regulated passage of fluid and electrolytes across the mucosal lining of the gut. The tight junction complex is made up of transmembrane proteins, which help seal the paracellular space between IECs and control the passage of water and ions [157],[158]. The tight junction proteins collectively contribute to the paracellular leakiness of the intestinal epithelium with specific size- and charge-selective properties. Barrier function is essential because increased intestinal permeability, an early feature of IBD [2], has been shown to precede intestinal inflammation in humans and animal models and is a prognostic factor for relapse in Crohn's disease [65],[66],[94],[159],[160]. Disruption of the barrier allows bacterial components to reach immune cells patrolling the lamina propria to initiate an immune response, which in turn, can have detrimental effects to the tight junction complex [96].

How JAK-inhibition by tofacitinib affects barrier function and regulation of tight junction proteins has yet to be identified.

Genome-wide association studies have identified 231 single-nucleotide polymorphisms in 200 gene loci associated with increased risk for IBD [24],[52],[67],[68], including protein tyrosine phosphatase non-receptor type 2 (*PTPN2*). Substrates of PTPN2 include members of the JAK-signal transduction and activators of transcription (STAT) signaling pathway [74],[161]. Constitutive *Ptpn2*$^{-/-}$ mice exhibit intestinal inflammation and succumb to systemic inflammation between 3-5 weeks of age [82]. We have previously shown that knockdown of *PTPN2* in human intestinal epithelial cell cultures cause elevated STAT activation and enhanced barrier defects in the presence of pro-inflammatory cytokine IFN-γ [79]. Colons of RAG2 knockout mice injected with *Ptpn2*-deficient T cells also show increased STAT1 and STAT3 levels [162]. Further, in response to acute DSS-induced colitis, *Ptpn2*$^{fl/fl}$LysMCre mice, which lack *PTPN2* in myeloid cells, have more epithelial damage and worse histopathology scores than their WT counterparts [88] . Whether *PTPN2* loss in macrophages affects IEC properties (i.e. barrier function), or in turn, how *PTPN2*-deficient IECs alter macrophage functions and cytokine secretion, however, is not yet known.

Here, we show that tofacitinib modifies IEC and macrophage function. Co-culture studies reveal that enhanced permeability and JAK-STAT signaling caused by *PTPN2* loss in IECs, macrophages, or both cell types were corrected by tofacitinib. These results translate *in vivo* when *Ptpn2*$^{fl/fl}$LysMCre, which exhibited an underlying permeability defect, were subjected to tofacitinib citrate regimen. Overall, data from these studies

suggest tofacitinib affects crosstalk between IECs and macrophages and that tofacitinib may serve as a 'targeted' therapeutic for a genetic defect associated with IBD. An approach for personalized medicine could lead to greater efficacy of tofacitinib in patients with defects in IBD susceptibility genes such as *PTPN2*.

Materials and Methods

Cell Culture

Human Caco-2BBe intestinal epithelial cells (IECs) were cultured in Dulbecco's Modified Eagle's Medium (DMEM, #15-017-CV, Corning) supplemented with 10% heat-inactivated fetal bovine serum (Gibco, Waltham, MA) and 1% L-glutamine (Lonza, 17-605E, Walkersville, MD). Human THP-1 monocytes were cultured in RPMI 1640 medium (#10-040-CV, Corning) with 10% heat-inactivated fetal bovine serum (Gibco, Waltham, MA). All cells were grown in standard 12-well cell culture plates (#130185, ThermoScientific, Rochester, NY) or transwell membranes (#3460, Corning, Kennebunk, ME) in a humidified incubator at 37°C with 5% CO_2.

Generating Stable shRNA *PTPN2*-Deficient Cell Lines

Cell lines stably expressing *PTPN2* shRNA were generated as previously described [80],[81]. Briefly, Caco-2BBe and THP-1 cells were infected with lentiviral constructs containing either *PTPN2*-specific, or non-targeting scrambled shRNA (Sigma-Aldrich, St. Louis, MO). After 72 hrs of infection, stable cell lines were selected using puromycin (400-128P, Gemini). Stable Caco-2BBe and THP-1 control (CTL) and *PTPN2*

knockdown (KD) cell lines were maintained at 4μg/mL and 0.5μg/ml puromycin, respectively. Knockdown of *PTPN2* was confirmed by Western blotting.

Measurement of Transepithelial Electrical Resistance and 4kDa FITC-Dextran Permeability *In Vitro*

Transepithelial electrical resistance (TER) of Caco-2BBe cells grown on transwells was measured using the EVOM2 Epithelial Voltohmmeter (World Precision Instruments, Sarasota, FL) with the accompanying chopstick electrode set for EVOM2 (World Precision Instruments, Sarasota, FL). The average of three measurements per transwell was calculated, multiplied by the transwell surface area, and expressed as $Ohms.cm^2$.

Permeability to macromolecules was measured as the flux of fluorescein isothiocynate (FITC)-4-kilodalton dextran (FD4, Sigma-Aldrich, St. Louis, MO) across the IEC monolayers. After measurement of TER, cells were washed twice with and equilibrated in 1X PBS with $CaCl_2$ and $MgCl_2$ for 30 min at 37°C. FD4 (at a final concentration of 1mg/mL) was then added to the apical side of the IECs. After 2 hrs at 37°C, duplicate 50μL samples of the basolateral solution were collected, and fluorescence measured using a microplate reader (Promega, Madison, WI). FD4 concentrations were calculated against using a standard curve.

Co-culture Experiments and Tofacitinib Treatments *In Vitro*

Caco-2BBe IECs were seeded at 0.5 x 10^6 cells per well on transwell membranes and cultured for 8 days. Cells were then switched to serum-free media overnight before co-culture with THP-1 cells and/or treated with tofacitinib. Prior to co-cultures with IECs, THP-1 (0.25 x 10^6) monocytes were pulsed for 3 h with PMA to induce macrophage differentiation, seeded on 12-well standard cell culture plates for 48 hrs and then switched to serum-free DMEM the day before the experiment. Prior to start of the co-culture, Caco-2BBe cells were pre-treated apically with vehicle dimethyl sulfoxide (DMSO, 0.5%, Sigma-Aldrich, St. Louis, MO) or tofacitinib (50μM, MedChemExpress, Monmouth Junction, NJ) for 1 hr followed by placing the transwells into the THP-1 cell-containing 12-well plates. After 24 hrs, TER and FD4 permeability were measured, the basolateral media was collected, and protein/RNA from both, Caco-2BBe and THP-1 cells were harvested.

Harvesting and Preparation of Whole Cell Protein Lysates

For protein isolation, cells were washed twice with ice-cold 1X PBS with $CaCl_2$ and $MgCl_2$ (D8662, Sigma, St. Louis, MO) prior to lysis with RIPA lysis buffer (50mM Tris-Cl pH 7.4, 150mM NaCl, 1% NP-40, 0.5% sodium deoxycholate, and 0.1% SDS) supplemented with 1X protease inhibitor (Roche, Mannheim, Germany), 2mM sodium fluoride, 1mM PMSF and phosphatase inhibitors (2mM sodium orthovanadate, Phosphatase Inhibitor Cocktail 2 and 3, Sigma-Aldrich, St. Louis, MO) for 15 min at 4°C. Cells were scraped, transferred into microcentrifuge tubes and homogenized on ice

using the Q125 Sonicator (QSonica Sonicators, Newtown, CT) at 30% amplitude, 10 sec ON/OFF intervals for 40 sec. Cell lysates were then centrifuged at 16, 200 x g at 4°C for 10 min and the supernatants were collected into new microcentrifuge tubes. Protein concentration was determined using the Pierce™ BCA Protein Assay Kit (Thermo Scientific, Rockford, IL). Loading samples were prepared by mixing the same amount of total protein from each sample with Laemmli loading buffer (60mM Tris-Cl pH 6.8, 2% SDS, 5% β-mercaptoethanol, 0.01% bromophenol blue, and 10% glycerol), then boiling the samples at 95°C for 10 min.

Western Blotting

Proteins were separated by SDS-polyacrylamide gel electrophoresis at 60mV for 30min then 150mV for 1 hr, followed by transfer onto polyvinylidene difluoride membranes (Millipore, Tullagreen, Carrigtwohill, Co.) for 1.5 hr at 100mV at 4°C. Membranes were blocked with 3% milk, 1% BSA in TBS-T (Tris-buffered saline with 0.1% Tween-20) for 1 hr at room temperature, followed by incubation with primary antibodies (Table 4.1) at 4°C overnight. The following day, membranes were rinsed 3x with TBS-T and subjected to three 5 min washes with TBS-T. Membranes were then incubated in horseradish peroxidase-conjugated goat anti-mouse (#115-036-062) or goat anti-rabbit (#111-036-045) IgG secondary antibodies (Jackson Immunoresearch Laboratories, Inc. West Grove, PA) diluted at 1:3000 in 3% milk, 1% BSA in TBS-T for 1 hr at room temperature, and again rinsed 3x with TBS-T then subjected to three 5 min washes with TBS-T. Finally, membranes were incubated with SuperSignal™ West Pico

PLUS Chemiluminescent Substrate solution (Thermo Scientific, Rockford, IL) according to manufacturer's directions and immunoreactive proteins were detected by exposing the membranes to film (LabScientific Inc., Highlands, NJ). Densitometric analysis of the blots was performed using ImageJ software [117].

Table 4.1 Primary Antibodies Used for Western Blotting

Antibody	Host	Provider	Catalog No.	Dilution
Claudin-2	Mouse	Thermo Fisher Scientific (Rockford, IL)	32-5600	1:1000
Claudin-4	Mouse	Invitrogen (Camarillo, CA)	32-9400	1:1000
JAM-A	Rabbit	Invitrogen (Camarillo, CA)	36-1700	1:1000
Occludin	Rabbit	Thermo Fisher Scientific (Rockford, IL)	71-1500	1:1000
Tricellulin (MARVELD2)	Rabbit	Abcam (Cambridge, MA)	ab203567	1:1000
TCPTP (anti-mouse)	Mouse	Medimabs (Quebec, Canada)	MM-0018	1:500
TCPTP (anti-human)	Mouse	EMD Millipore (San Diego, CA)	PH03L	1:500
Phospho-JAK1 (Tyr 1022/1023)	Rabbit	Cell Signaling Technology (Danvers, MA)	#3331	1:1000
Total JAK1	Rabbit	Cell Signaling Technology (Danvers, MA)	#3344	1:1000
Phospho-STAT1 (Tyr 701)	Rabbit	Cell Signaling Technology (Danvers, MA)	#9167	1:1000
Total STAT1	Rabbit	Cell Signaling Technology (Danvers, MA)	#9175	1:1000
Phospho-STAT3 (Tyr 705)	Rabbit	Cell Signaling Technology (Danvers, MA)	#9145	1:1000
Total STAT3	Mouse	Cell Signaling Technology (Danvers, MA)	#9139	1:2000
β-actin	Mouse	Sigma Aldrich (St. Louis, MO)	A5316	1:5000

Mice

C57Bl6 male and female mice homozygous for the floxed *Ptpn2* gene were used for these studies, which either did not express LysMCre (*Ptpn2*$^{fl/fl}$) or were heterozygous for the LysMCre construct (*Ptpn2*$^{fl/fl}$LysMCre), as previously described [88],[163]. All animal experiments were conducted with the approval of the Institutional Animal Care and Use Committee at the University of California, Riverside in accordance with the National Institute of Health guidelines for the use of live animals. 8-12 week old male

and female mice housed in a specific pathogen-free (SPF) facility under a 12-hr light, 12-hr dark cycle and food/water *ad libitum* were used for all studies.

Tofacitinib Citrate Treatment *In Vivo*

Vehicle gavage solution was prepared by dissolving methylcellulose (M7027, Sigma-Aldrich, St. Louis, MO) at 1% w/v in PB. Tofacitinib citrate gavage solution was prepared fresh every day by resuspending tofacitinib citrate powder (Selleckchem, Houston, TX) in vehicle. Gavage solutions were sonicated using the Q125 Sonicator (QSonica Sonicators, Newtown, CT) at 30% amplitude for 2 min at 10 sec ON/OFF intervals at room temperature. Mice were orally gavaged with vehicle (50μL per g body weight) or tofacitinib citrate (50mg/kg body weight) twice daily [164] for 7 days.

Measurement of Intestinal Permeability *In Vivo*

On day 7 of treatment, mice were food-deprived for 2 hrs prior to oral administration (200μL) of gavage solution containing three molecular probes: 100mg/mL creatinine (#4255, Sigma-Aldrich, St. Louis, MO), 80mg/mL FD4 (#46944, Sigma-Aldrich, St. Louis, MO) and 20mg/mL Rhodamine B-dextran 70kDa (RD70, #R9379, Sigma-Aldrich, St. Louis, MO Sigma) dissolved in autoclaved MilliQ water and filtered through a 0.2μM syringe filter. A water-gavaged mouse was used as control. After 5 hrs, blood samples were collected via the retro-orbital route, from which serum concentrations of the three probes were determined. At this point, animals were given access to food.

For serum FD4 and RD70 concentration determination, samples were diluted 1:5 in MilliQ water in black 96-well plates. FITC and Rhodamine B fluorescence were measured using a microplate reader (Promega, Madison, WI) at excitation/emission of 490nm/510-570nm and 525nm/580-640nm, respectively. Standards were prepared from the gavage solution. FD4 and RD70 serum concentrations of water-gavaged mice were subtracted from those of the samples to account for autofluorescence in the serum.

For serum creatinine concentration determination, 15 μL of undiluted sera and freshly prepared standards were transferred into a transparent 96-well plate in duplicates. SVT creatinine R1 reagent (100μL; #139-30, Sciteck) was added to each well and allowed to incubate with the samples at room temperature for 5 min. SVT creatinine R2 (50μL; #139-30, Sciteck) reagent was then added to each well and the plate was lightly tapped to mix all components together. Kinetic absorbance readings were measured at 505nm at 1 min intervals for 30 min using a Synergy HT plate reader (BioTek). ΔOD were calculated by subtracting the OD at 0 min from the OD at 6 min and sample concentrations were determined against the standard curve. Values from the sera of water-gavaged mice were subtracted from those of the samples.

Tissue Collection

One day after the intestinal permeability assay, mice were sacrificed and tissues were harvested. Whole intestinal pieces from the distal ileum, cecum, proximal colon and distal colon were flash-frozen in liquid nitrogen and stored at -80°C. Whole intestinal tissues were incubated in Cell Recovery Solution (#354253, Corning, Bedford, MA) on

ice for 2 hrs and subsequently vigorously shaken to collect IECs. IECs were washed twice with PBS and divided into two parts: (1) lysed in RIPA supplemented with protease and phosphatase inhibitors and processed as previously described (see "Harvesting and Preparing Whole Cell Lysates") or (2) snap-frozen in liquid nitrogen and stored at -80°C for subsequent RNA isolation.

RNA Isolation, RT-PCR, and Quantitative PCR

Total RNA was isolated from whole proximal colons from treated mice using RNeasy Mini Kit (Qiagen) per manufacturer's directions. RNA concentration was measured by absorbance at 260 and 280nm using Nanodrop 2000c (Thermo Scientific, Rockford, IL) and reverse transcribed into complementary DNA (cDNA) using qScript cDNA SuperMix (Quantabio, Beverly, MA) and C1000 Touch Thermal Cycler (Bio-Rad, Hercules, CA). qPCR was performed using iQ SYBR Green Supermix (Bio-Rad, Hercules, CA), primers listed in Table 4.2, and the IQ5 Real-Time PCR Thermal Cycler (Bio-Rad, Hercules, CA) with the following protocol: 95 °C for 3 min followed by 45 cycles of denaturation (95 °C for 10 sec), annealing (53°-60°C for 10 sec) and extension (72 °C for 10 sec) steps. Gene expression was calculated using the average C_T values of triplicate readings normalized to the average of housekeeping gene GAPDH C_T values. Results were analyzed using the $\Delta\Delta C_T$ method.

Table 4.2 Murine Primers Used for qPCR

Primers	Forward	Reverse
Il6	AGTCCGGAGAGGAGACTTCA	TTGCCATTGCACAACTCTTT
Il10	CCCAGAAATCAAGGAGCATT	TCACTCTTCACCTGCTCCAC
Il22	GCTCAGCTCCTGTCACATCA	CAGTTCCCCAATCGCCTTGA

Flow Cytometry

After IEC isolation, the remaining whole intestinal tissues were cut into 0.5 cm pieces and digested with Collagenase type IV for 15 min. Digested tissue pieces were then passed three times through a 18.5 G needle and homogenates filtered through a 7 μm cell strainer (BD). Cells were washed once with PBS before re-suspension in 40 μL PBS containing fluorescence-labeled antibodies (Table 4.3) and incubation for 30 min on ice. Samples were washed twice with ice cold PBS, resupended in 200 μL FACS buffer (PBS, 2% FBS) and acquired on an LSR-II flow cytometer from BD.

Table 4.3 Fluorescence-Labeled Antibodies Used for Flow Cytometry

Antibody	Fluorophore	Host, Isotype	Provider	Catalog No.	Clone	Dilution
CD11b (mouse)	BV605	Rat IgG2b κ	Biolegend	101237	M1/70	1:200
Ly-6G (mouse)	BV510	Rat IgG2a κ	Biolegend	127633	1A8	1:100
Ly-6C (mouse)	PerCP/Cy5.5	Rat IgG2c κ	BioLegend	128011	HK1.4	1:200
CD11c (mouse)	PE/Cy7	Hms IgG	Biolegend	117318	N418	1:200
MHC-II (mouse)	AF700	Rat IgG2b κ	Thermo Fisher	56-5321-80	M5/114.15.2	1:100
CD64 (mouse)	PE	Ms IgG1 κ	BioLegend	139303	X54-5/7.1	1:200
CD45 (mouse)	PB	Rat IgG2b κ	BioLegend	103125	30-F11	1:400
F4/80 (mouse)	APC	Rat IgG2a κ	BioLegend	123115	BM8	1:200
CD3 (mouse)	BV650	Rat IgG2b κ	Biolegend	100229	17A2	1:400
NK-1.1 (mouse)	BV650	Ms IgG2a κ	BioLegend	108735	PK136	1:200
CD45R/B220 (mouse/human)	PE/Cy5	Rat IgG2a κ	Biolegend	103209	RA3-6B2	1:400
CD206 (mouse)	PE	Rat IgG2a κ	Biolegend	141705	C068C2	1:100
CD86 (mouse)	AF488	Rat IgG2a κ	Biolegend	105018	GL-1	1:100
Fc block (mouse)	-	several	Miltenyi Biotec	130-092-575	several	1:100

Statistical Analysis

Data are presented as means ± SD for a series of *n* biological replicates or mice. Each *in vitro* condition was performed in duplicate or triplicate. *In vivo* data are represented by one of two independent experiments. Statistical analysis was performed by analysis of variance (ANOVA) followed by Tukey's post-test using GraphPad Prism 8.0 software (GraphPad Software, La Jolla, CA). *P* values < 0.05 were considered statistically significant.

Results

Tofacitinib corrects elevated permeability in IECs lacking PTPN2 and abrogates the effects of macrophages on barrier function

Immune cells in the intestine can manipulate the intestinal epithelial barrier. The close proximity of IEC and intestinal macrophages suggest that macrophages might crucially affect IEC barrier function. Recent publications have shown that tofacitinib affects intestinal macrophage polarization, but it is unknown whether this has an effect on the interaction between macrophages and IECs. To determine how macrophages influence IEC barrier function, and whether tofacitinib influences this cross regulation, THP-1 cells were co-cultured with polarized Caco-2BBe cells that were treated with either vehicle or tofacitinib. In control (CTL) Caco-2BBe cells, co-culture with control THP-1 cells tightened the epithelial barrier as observed by significantly increased TER but reduced FD4 permeability (Figure 4.1), while co-culture with *PTPN2* KD THP-1 cells resulted in a leaky barrier, i.e. reduced TER and increased FD4 flux (Figure 4.1).

Upon treatment with tofacitinib for 24 hrs, both of these effects were prevented (Figure 4.1). As previously shown [80], TER was significantly lower in resting *PTPN2*-deficient IECs compared to CTL IECs. Furthermore, in *PTPN2* KD Caco-2 cells, co-culture with macrophages did not promote barrier tightness (i.e. no induction of TER or reduced FD4 flux), and co-culture with *PTPN2* KD THP-1 further decreased TER while FD4 permeability increased in *PTPN2*-deficient cells (Figure 4.1). Of note, tofacitinib treatment completely abrogated these effects (Figure 4.1). Moreover, tofacitinib rescued the TER of *PTPN2*-deficient Caco-2BBe cells to levels comparable to those of CTL Caco-2BBe cells (Figure 4.1A). These results show that the presence of THP-1 cells induces tightening of the epithelial barrier. On the other hand, *PTPN2*-deficient macrophages cause the barrier to become more leaky to paracellular passage of ions and macromolecules. Both of these effects on the IEC monolayer were abrogated by tofacitinib.

These results demonstrate that JAK inhibition alone can rescue the barrier defect observed in *PTPN2*-deficient IECs. In addition, while macrophages induce barrier tightening to the epithelial monolayer, macrophages lacking *PTPN2* reduce barrier integrity. When the IECs are missing *PTPN2*, the enhancement of the barrier by macrophages is no longer observed. Furthermore, the permeability changes seen in *PTPN2* KD Caco-2BBe cells co-cultured with *PTPN2*-deficient THP-1 cells suggest a synergistic and detrimental effect on epithelial resistance and macromolecular permeability when *PTPN2* is absent in both macrophages and IECs. The key finding of

these results is that tofacitinib can reverse the barrier defect caused by loss of *PTPN2* in either cell type.

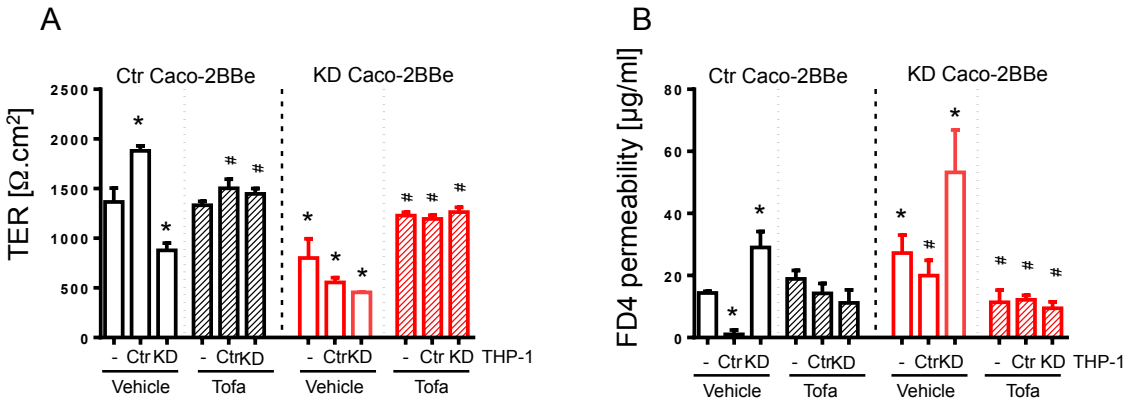

Figure 4.1: Tofacitinib corrects barrier defects in epithelial-macrophage co-cultures caused by *PTPN2* loss in Caco-2BBe or THP-1 cells individually or collectively. A) Transepithelial electrical resistance (TER) values, adjusted for transwell surface area, across Caco-2BBe monolayers pretreated with vehicle (0.5% DMSO) or tofacitinib (tofa, 50µM) for 1 hour prior to co-culture with control (Ctr) or *PTPN2* knockdown (KD) THP-1 cells for 24 hours. B) Concentration of 4kDa fluorescein-dextran (FD4) present in the basolateral compartment of the transwells 2 hours after treatments indicated above. *$P \leq 0.05$ *cf.* untreated Ctr Caco-2BBe; #$P \leq 0.05$ *cf.* vehicle-treated Caco-2BBe; $n = 3$.

Tofacitinib prevents changes in epithelial tight junction protein expression induced by co-culture with PTPN2-deficient macrophages

In order to determine potential mechanisms behind the permeability changes seen with the co-culture studies in the presence or absence of tofacitinib treatment, expression of various tight junction proteins were analyzed. TER can fluctuate in response to the changes in charge-selective claudin proteins, which regulate paracellular passage of fluids and ions. Figure 4.2A and 4.2B show that *PTPN2*-deficient macrophages induced a significant increase in the expression of the pore-forming tight junction protein, claudin-

2, in both control and *PTPN2*-deficient Caco-2BBe cells. Of note, IECs lacking *PTPN2* intrinsically expressed elevated levels of claudin-2 compared to control IECs, which was further enhanced when co-cultured with *PTPN2*-deficient macrophages. Tofacitinib treatment normalized these changes in both control and *PTPN2* KD cells, which imply that the effects of tofacitinib on TER are, at least in part, attributed to normalization of claudin-2. In contrast to claudin-2, overexpression of claudin-4 has been shown to restrict Na^+ permeability [165]. Co-culture with control THP-1 cells increased barrier-sealing molecule claudin-4 expression in control Caco-2BBe cells, while co-culture with *PTPN2*-deficient THP-1 significantly decreased its expression. *PTPN2*-deficient IECs inherently expressed less claudin-4 compared to control IECs, which is further reduced by the presence of *PTPN2*-deficient macrophages. Surprisingly, tofacitinib treatment did not rescue the effects on claudin-4. This demonstrates that the TER changes induced by macrophages are likely caused by a combination of epithelial claudin-2 and claudin-4 protein expression, while the beneficial effect of tofacitinib on barrier resistance is more likely due to decreasing the elevated expression of claudin-2 caused by *PTPN2* deficiency in macrophage-IEC co-cultures.

Macromolecular permeability can be dictated by reduced expression or mislocalization of tight junction proteins regulating the leak pathway (Turner). Expression of barrier-sealing proteins Junctional Adhesion Molecule (JAM-A), occludin, and tricellulin were evaluated (Figure 2A) to determine whether changes in these proteins correspond to the changes in FD4 fluxes. Co-culture with control THP-1 cells induced significant increase in JAM-A and tricellulin levels in CTL Caco-2BBe cells (Figure

4.2D, 4.2F). On the other hand, macrophages deficient in *PTPN2* reduced JAM-A, tricellulin, and occludin below baseline levels of control IECs (Figure 4.2D, 4.2E, 4.2F). With the addition of tofacitinib, the effect of control macrophages on IEC JAM-A expression was reversed, but not the reduction in JAM-A induced by *PTPN2*-deficient macrophages (Figure 4.2D). In control IECs, however, tofacitinib fully restored the reduced levels of occludin and tricellulin caused by macrophages lacking *PTPN2* (Figure 4.2E, 4.2F).

In turn, Caco-2BBe cells lacking *PTPN2* expressed much less occludin compared to control IECs, which is in line with the effects on FD4 permeability. This feature, however, was rescued by tofacitinib treatment (Figure 4.2E). Unlike occludin, levels of JAM-A and tricellulin decreased only when *PTPN2* was absent in macrophages (Figure 4.2D, 4.2F). Moreover, JAM-A and tricellulin expression was not rescued by tofacitinib (Figure 4.2F). TCPTP protein expression remained unchanged by co-culture with macrophages, tofacitinib treatment, or the combination of both (Figure 4.2G).

Collectively, these results suggest that changes in the expression patterns of junctional proteins are individual and distinct. Since epithelial claudin-2, claudin-4, JAM-A, occludin, and tricellulin all changed in response to external cues from macrophages, these tight junction proteins may account for the changes in permeability seen in Caco-2BBe cells during the co-culture studies. Of note, tofacitinib rescued the expression of claudin-2 and occludin in *PTPN2* KD Caco-2BBe cells, implying that tofacitinib rescues the underlying ‘pore’ and ‘leak’ barrier defects in *PTPN2*-deficient IECs, at least in part, through effects on these two tight junction proteins.

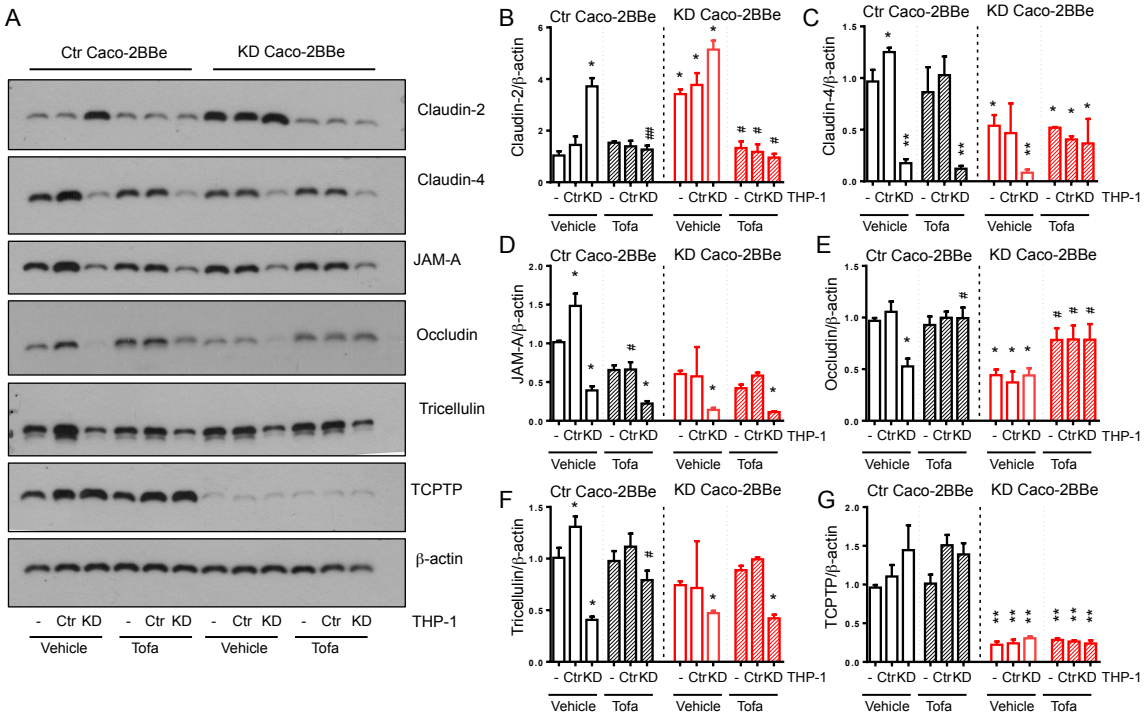

Figure 4.2: Tofacitinib normalizes tight junction protein expression in Caco-2BBe cells due to *PTPN2* loss in IECs, macrophages, or both cell types. Caco-2BBe monolayers pretreated with vehicle (0.5% DMSO) or tofacitinib (tofa, 50μM) for 1 hour prior to co-culture with control (Ctr) or *PTPN2* knockdown (KD) THP-1 cells for 24 hours were lysed and subjected to Western blotting. A) Representative Western blot images of tight junction proteins, TCPTP, and β-actin from Caco-2BBe whole cell lysates. Densitometric analyses of B) claudin-2, C) claudin-4, D) JAM-A, E) occludin, F) tricellulin, and G) TCPTP expression, all normalized to β-actin. **P* ≤ 0.05 *cf.* untreated Ctr Caco-2BBe; #*P* ≤ 0.05 *cf.* vehicle-treated Caco-2BBe; *n* = 3.

Elevated STAT1 and STAT3 phosphorylation in PTPN2-deficient IECs are normalized by tofacitinib

Substrates of *PTPN2* include several members of the JAK-STAT signaling pathway. As a JAK-inhibitor, the effect of tofacitinib on JAK-STAT signaling on IECs lacking *PTPN2* was analyzed. Caco-2BBe cells lacking *PTPN2* had significantly higher STAT1 and STAT3 phosphorylation (Figure 4.3), which was effectively reduced upon

treatment with tofacitinib for 24 hrs. These data show that tofacitinib can correct the elevated JAK-STAT activation in IECs with *PTPN2* loss. Furthermore, co-culture with macrophages significantly increased STAT1 and STAT3 phosphorylation in CTL Caco-2BBe (Figure 4.3), an effect potentiated when the macrophages were lacking *PTPN2* (Figure 4.3), but in both cases, was fully normalized upon tofacitinib treatment (Figure 4.3). Conversely, the elevated phosphorylation of STAT1 and STAT3 in *PTPN2* KD Caco-2BBe cells were unaffected by the presence of macrophages (Figure 4.3). Still, tofacitinib kept STAT activation reduced in *PTPN2*-deficient IECs (Figure 4.3).

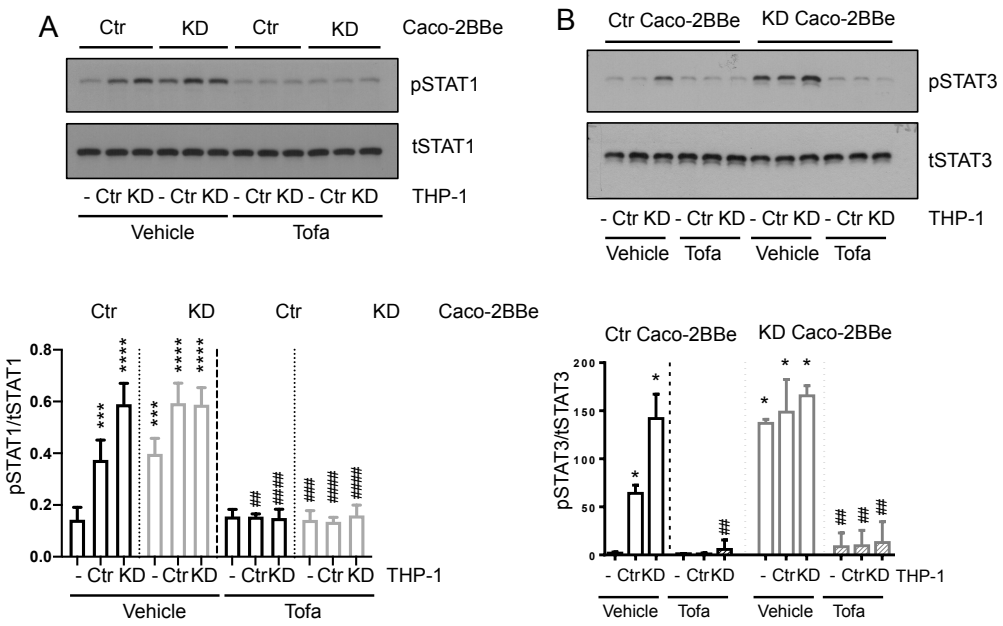

Figure 4.3: Functional inhibition of STAT signaling by tofacitinib in Caco-2BBe cells subjected to co-culture studies. Caco-2BBe monolayers pretreated with vehicle (0.5% DMSO) or tofacitinib (tofa, 50μM) for 1 hour prior to co-culture with control (Ctr) or *PTPN2* knockdown (KD) THP-1 cells for 24 hours. Representative Western blot images and densitometric analyses of A) phospho-STAT1 (pSTAT1) and B) phospho-STAT3 (pSTAT3) normalized to their respective total forms (tSTAT1, tSTAT3) in Caco-2BBe whole cell lysates. **P* ≤ 0.05 *cf.* untreated Ctr Caco-2BBe; #*P* ≤ 0.05 *cf.* vehicle-treated Caco-2BBe; *n* = 3.

JAK-STAT signaling is elevated in macrophages lacking PTPN2, which is reversed by tofacitinib in vitro

To determine how co-culture and tofacitinib affect macrophages, JAK-STAT signaling in THP-1 cells was also analyzed. Consistent with findings among other *PTPN2*-deficient models, macrophages lacking *PTPN2* had elevated JAK1 and STAT1 phosphorylation (Figure 4.4A, 4.4B), an effect fully reversed by tofacitinib (Figure 4.4A, 4.4B). Co-culture of control THP-1 cells with *PTPN2*-deficient Caco-2BBe cells induced JAK1 and STAT1 activation in THP-1 cells (Figure 4.4A, 4.4B). On the other hand, in THP-1 cells lacking *PTPN2*, co-culture with Caco-2BBe cells induced robust induction of JAK1, STAT1 and STAT3 (Figure 4.4A, 4.4B, 4.4C), effects completely negated by tofacitinib treatment. These results suggest that JAK1-STAT1 signaling is activated in control macrophages by the presence of *PTPN2*-deficient IECs alone. Additionally, presence of CTL or *PTPN2*-deficient IECs activated JAK-STAT signaling in *PTPN2*-deficient macrophages. As expected, the administration of tofacitinib completely inhibited this activation of JAK1 and its downstream targets STAT1 and STAT3.

IL-6 and TNF-α secretion is induced by PTPN2 loss in macrophages, IECs, or both, and is suppressed by tofacitinib

A major feature of IBD is a disturbed balance between pro- and anti-inflammatory cytokine secretion. Levels of inflammatory cytokines, such as TNF-α and IL-6 are increased in IBD patients [41]. Of note, co-culture of *PTPN2*-deficient macrophages with

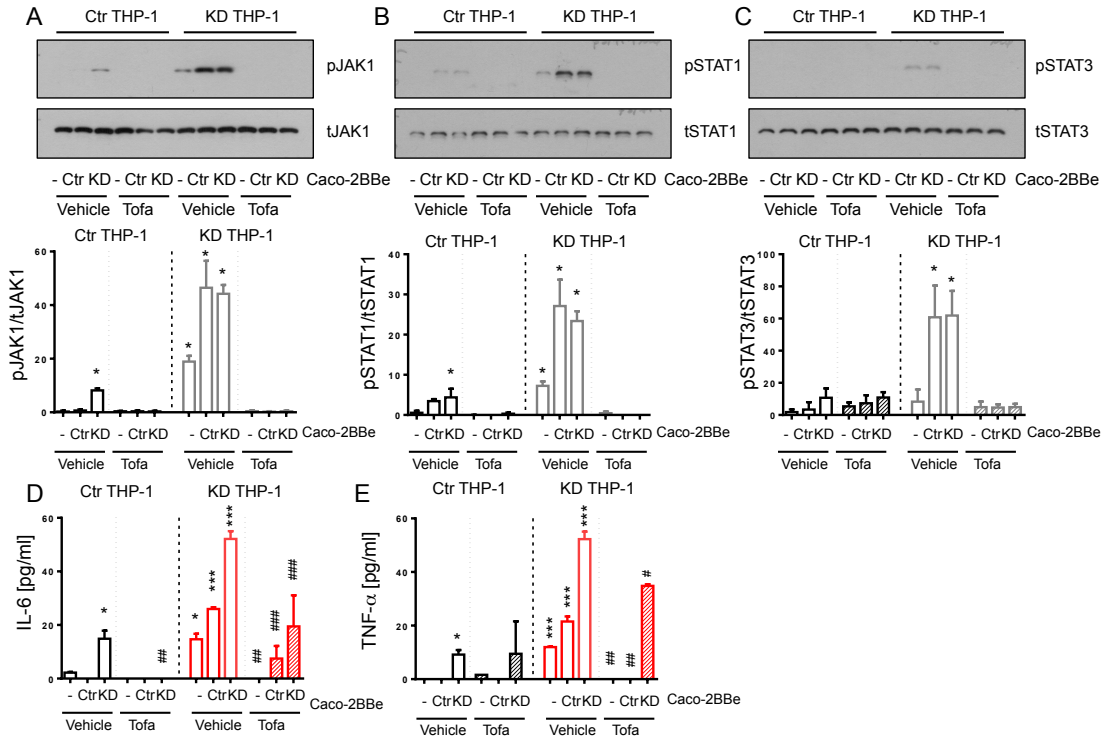

Figure 4.4: Tofacitinib reduces JAK-STAT signaling in THP-1 cells and cytokine IL-6 and TNF-α secretion in co-culture studies. THP-1 cells co-cultured with tofacitinib-treated Caco-2BBe cells for 24 hours were lysed and subjected to Western blotting. Representative Western blot images and densitometric analyses of A) phospho JAK1 (pJAK1), B) phospho-STAT1 (pSTAT1) and C) phospho-STAT3 (pSTAT3) normalized to their respective total forms (tJAK1, tSTAT1, tSTAT3) in THP-1 whole cell lysates. *$P \leq 0.05$ *cf.* untreated Ctr THP-1; $n = 3$. D) IL-6 and TNF-α concentrations present in the culture media after co-culture experiments, measured by ELISA. *$P \leq 0.05$, *** $P \leq 0.001$ *cf.* untreated Ctr THP-1; ##$P \leq 0.01$, ###$P \leq 0.001$ *cf.* vehicle-treated THP-1; $n = 3$.

control Caco-2BBe cells resulted in increased IL-6 and TNF-α release, an effect further increased in the presence of *PTPN2*-deficient Caco-2BBe cells (Figure 4.4D, 4.4E).

Notably, tofacitinib treatment significantly reduced the robust increases in IL-6 (Figure 4.4D) and, to a lesser degree, in TNF-α levels (Figure 4.4E). These results suggest that, at least in *PTPN2*-deficient conditions, JAK-STAT signaling is only partially mediating the release of IL-6 and TNF-α.

Tofacitinib citrate corrected barrier dysfunction observed in Ptpn2$^{fl/fl}$LysMCre mice in vivo

To determine whether the restoration of barrier function by tofacitinib translate *in vivo*, intestinal permeability of three different sized probes were measured in *Ptpn2*$^{fl/fl}$ and *Ptpn2*$^{fl/fl}$LysMCre mice, which lack *PTPN2* in macrophages. Figure 4.5B indicates that *Ptpn2*$^{fl/fl}$LysMCre mice exhibit higher macromolecular permeability compared to their *Ptpn2*$^{fl/fl}$ counterparts, as measured by FD4 flux. Twice daily gavage of tofacitinib citrate for 7d substantially decreased the leaky barrier in *Ptpn2*$^{fl/fl}$LysMCre mice, with virtually no effect in *Ptpn2*$^{fl/fl}$ animals (Figure 4.5B). Creatinine and RD70 fluxes were also evaluated to determine whether the paracellular pore or the unrestricted pathways of permeability were affected by loss of *PTPN2* in macrophages. Figures 4.5A and 4.5C illustrate that the permeability of either pathway was unaltered by *PTPN2*-deficient macrophages and were also unaffected by tofacitinib citrate treatment. Similar to *in vitro* findings, these data suggest that intestinal permeability is elevated by *PTPN2* loss in macrophages *in vivo*, and that this effect can be normalized with JAK-inhibition by tofacitinib citrate.

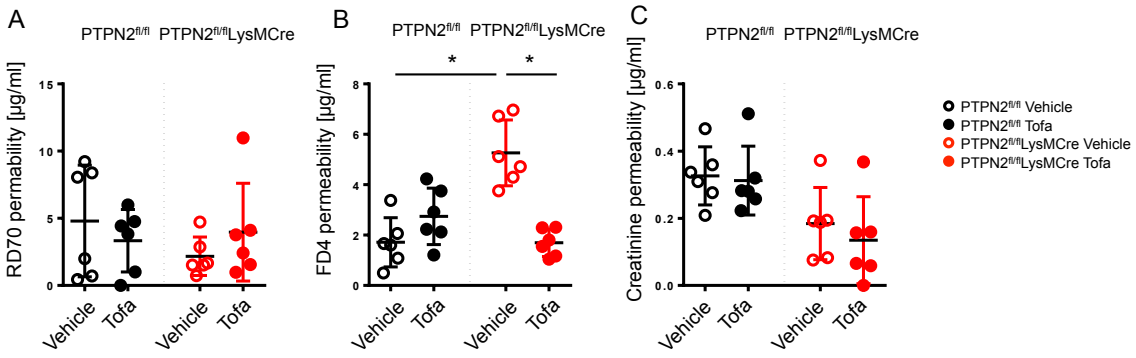

Figure 4.5: Tofacitinib citrate treatment reduced barrier permeability to FD4 *in vivo*. Intestinal permeability to three different-sized probes (creatinine, FD4, RD70) was measured in *Ptpn2*$^{fl/fl}$ and *Ptpn2*$^{fl/fl}$LysMCre mice subjected to twice daily treatment with vehicle (1% methylcellulose in PBS) or tofacitinib citrate (50mg/kg) for 7d. Serum concentrations of A) RD70, B) FD4, and C) creatinine were measured 5 hours post-gavage. *$P \leq 0.05$; $n = 6$.

IECs from Ptpn2$^{fl/fl}$LysMCre mice express reduced levels of barrier-sealing tight junction proteins, which can be rescued by tofacitinib citrate treatment

To delineate the mechanism behind changes in barrier function *in vivo*, the abundance of tight junction proteins regulating the barrier was analyzed in proximal colon IECs from mice subjected to vehicle or tofacitinib citrate treatment. The expression of claudin-2 was significantly increased in IECs from *Ptpn2*$^{fl/fl}$LysMCre mice (Figure 4.6A, 4.6B), while claudin-4, JAM-A, and occludin were all decreased in IECs from *Ptpn2*$^{fl/fl}$LysMCre mice compared to *Ptpn2*$^{fl/fl}$ controls (Figure 4.6A, 4.6C, 4.6D, 4.6E). These effects were corrected by tofacitinib citrate treatment, and expression patterns of these tight junction proteins were all reversed (Figure 4.6A-4.6E). Of note is the induction of occludin expression in *Ptpn2*$^{fl/fl}$ mice by tofacitinib (Figure 4.6E), though this did not result in a functional phenotype of reduced FD4 permeability. In contrast to

co-culture findings *in vitro*, no changes in tricellulin expression were seen as a result of loss of *Ptpn2* in macrophages, while tofacitinib citrate treatment did not have any effect on tricellulin levels in *Ptpn2*$^{fl/fl}$ or *Ptpn2*$^{fl/fl}$LysMCre mice (Figure 4.6F).

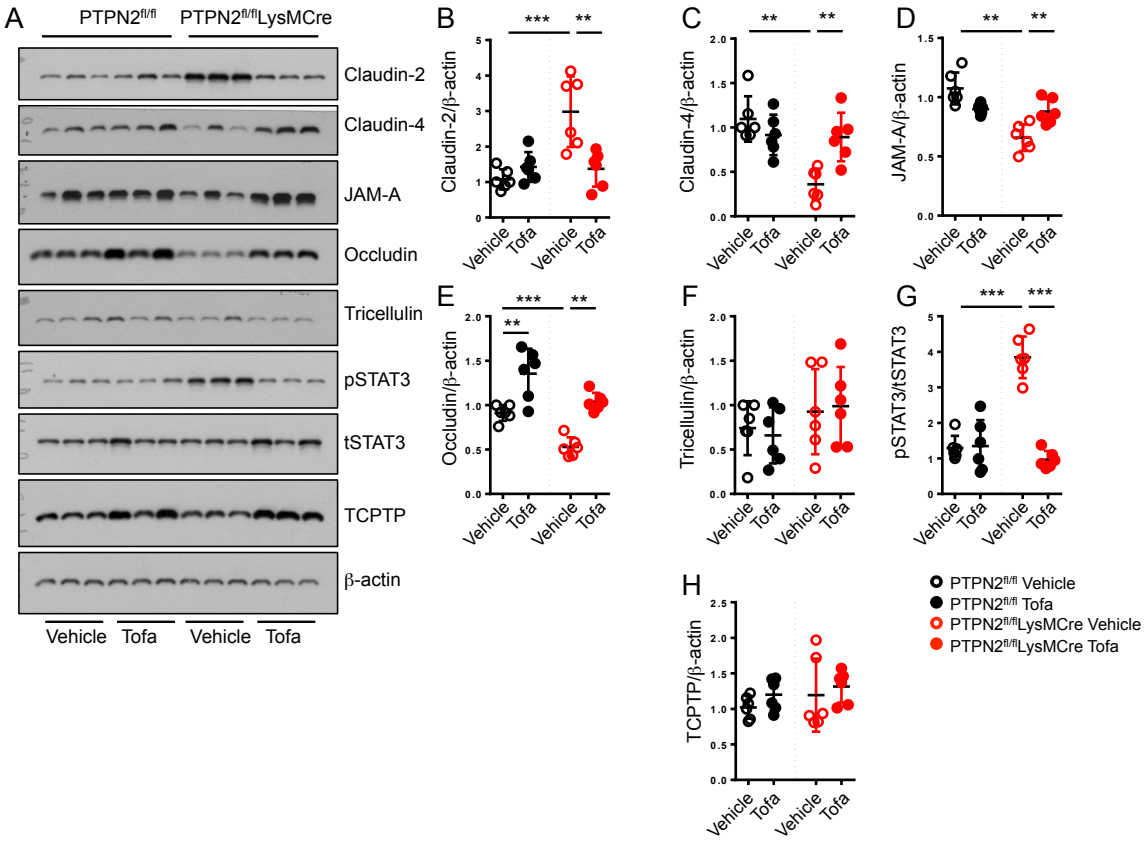

Figure 4.6: Aberrant tight junction protein patterns and elevated STAT3 phosphorylation in *Ptpn2*$^{fl/fl}$LysMCre mice were reversed by tofacitinib citrate treatment *in vivo*. Whole cell lysates of proximal colon IECs isolated from *Ptpn2*$^{fl/fl}$ and *Ptpn2*$^{fl/fl}$LysMCre mice treated with vehicle or tofacitinib citrate were subjected to Western blot analysis. A) Representative Western blot images of the proteins analyzed in proximal colon IECs from experimental mice. Densitometric analyses of B) claudin-2, C) claudin-4, D) JAM-A, E) occludin, F) tricellulin, and H) TCPTP, all normalized to β-actin. G) Densitometric analysis of phospho-STAT3 (pSTAT3) normalized to total STAT3 (tSTAT3) expression. *$P \leq 0.05$, **$P \leq 0.01$, *** $P \leq 0.001$; $n = 6$.

STAT signaling is elevated in IECs of Ptpn2$^{fl/fl}$LysMCre mice and is effectively reduced by tofacitinib citrate administration

STAT phosphorylation in IECs was analyzed to determine how the JAK-STAT signaling was affected in the epithelium of *Ptpn2*$^{fl/fl}$ vs. *Ptpn2*$^{fl/fl}$LysMCre mice treated with vehicle or tofacitinib citrate. *Ptpn2*-deficiency in macrophages increased STAT3 phosphorylation in IECs (Figure 4.6G), an effect significantly reduced with tofacitinib citrate treatment. Of note is the absence of a reduction in STAT3 phosphorylation in *Ptpn2*$^{fl/fl}$ animals (Figure 4.6G). It is also important to note that TCPTP levels remained unchanged in IECs of *Ptpn2*$^{fl/fl}$ vs. *Ptpn2*$^{fl/fl}$LysMCre mice and were unaffected by tofacitinib treatment (Figure 4.6H).

Gene expression profiles of cytokines Il6, Il10, and Il22 in Ptpn2$^{fl/fl}$LysMCre colons are reversed by tofacitinib citrate treatment

Specific cytokines present in tissues can influence epithelial and immune cell processes necessary to manage inflammation in the gut. To determine which cytokines may mediate changes observed *in vivo*, *Il6*, *Il10*, and *Il22* gene expression in proximal colons of *Ptpn2*$^{fl/fl}$ and *Ptpn2*$^{fl/fl}$LysMCre, treated with vehicle or tofacitinib citrate, were determined by qPCR (Figure 4.7A). Both *Il6* and *Il22* expression were significantly elevated, while *Il10* expression was decreased, in vehicle-treated *Ptpn2*$^{fl/fl}$LysMCre mice compared to *Ptpn2*$^{fl/fl}$ mice (Figure 4.7A). With tofacitinib citrate treatment, patterns of *Il6*, *Il10*, and *Il22* were completely reversed (Figure 4.7A).

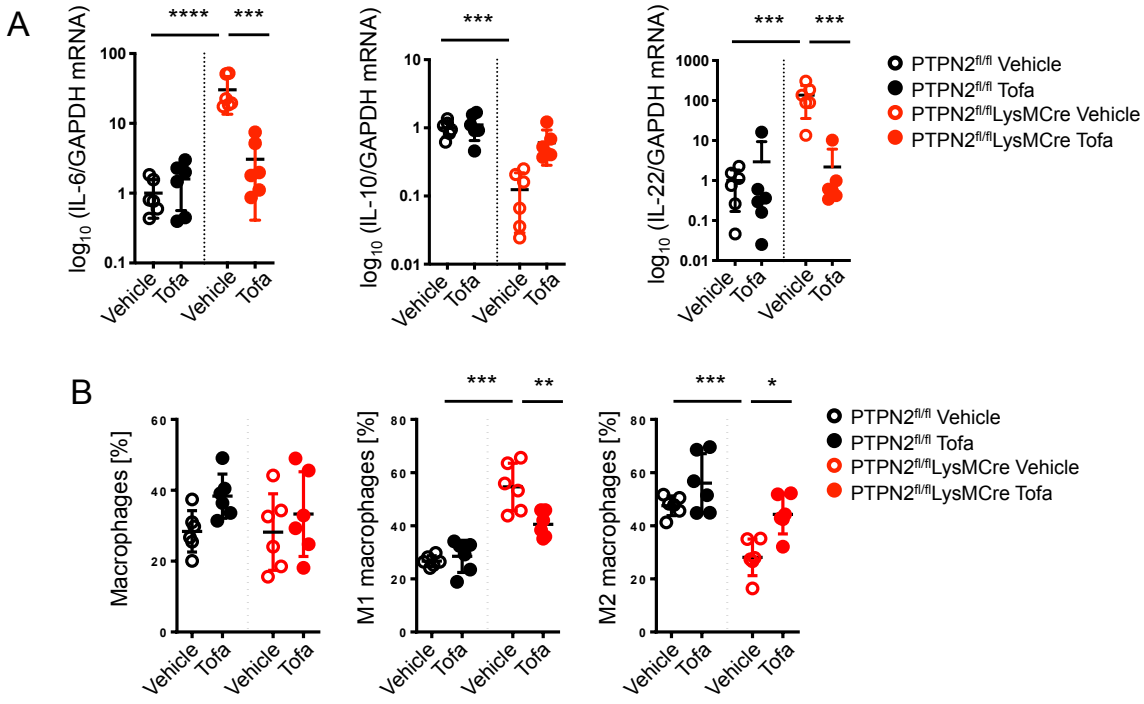

Figure 4.7: Cytokine signatures and proportions of macrophage subpopulations are normalized by tofacitinib citrate treatment in *Ptpn2*$^{fl/fl}$LysMCre mice. A) Gene expression of cytokines IL-6, IL-10, and IL-22 normalized to GAPDH in whole proximal colons of mice treated with vehicle or tofacitinib citrate twice daily for 7 days. B) Proportions of total, M1, and M2 macrophages in whole proximal colons of mice as determined by flow cytometry. *$P \leq 0.05$, **$P \leq 0.01$, *** $P \leq 0.001$; $n = 6$.

Ptpn2*$^{fl/fl}$*LysMCre mice have more M1 macrophages and less M2 macrophages compared to Ptpn2*$^{fl/fl}$ *mice, the proportions of which are normalized by tofacitinib citrate

To determine whether *Ptpn2* loss in macrophages alters macrophage differentiation, M1 and M2 populations in *Ptpn2*$^{fl/fl}$LysMCre vs. *Ptpn2*$^{fl/fl}$ mice were measured by flow cytometry. Figure 7C displays that overall macrophage numbers were unaffected by *Ptpn2* loss in these mice but a significant increase in the proportion of M1 macrophages was observed in *Ptpn2*$^{fl/fl}$LysMCre mice compared to their *Ptpn2*$^{fl/fl}$

counterparts, while M2 macrophages proportions were reduced (Figure 4.7B). These two populations, however, were restored in *Ptpn2*$^{fl/fl}$LysMCre by tofacitinib citrate treatment, which had no effect on M1/M2 macrophage populations in *Ptpn2*$^{fl/fl}$ mice (Figure 4.7B). These results suggest that loss of *Ptpn2* affects macrophage polarization, which can be normalized by tofacitinib administration.

Discussion

In this study, we sought to determine how *PTPN2* plays a role on the effect of macrophages on intestinal epithelial barrier permeability and whether JAK-inhibitor tofacitinib affects this interaction. Our findings show that tofacitinib normalized phenotypes in IECs with *PTPN2* deficiency including barrier dysfunction and tight junction protein expression changes. Through co-culture studies, we also show that loss of *PTPN2* in both IECs and macrophages can have synergistically detrimental effects on these outcomes. Mice with macrophage-specific knockout of *Ptpn2* also had elevated macromolecular permeability as evidenced by significantly higher FD4 whole body permeability compared to controls. STAT3 activation and IL-6 production correlated with these effects, implying that consequences of *PTPN2* deficiency in cell culture and animal models are likely mediated by IL-6-STAT3 signaling. Major findings of this study are that tofacitinib rescued effects on (i) barrier function, (ii) junctional protein regulation, (iii) cytokine production, and (iv) STAT signaling resulting from *PTPN2* deficiency and macrophage-IEC crosstalk.

In agreement with previous data [80], *PTPN2*-deficient Caco-2BBe monolayers display much lower TEER and higher FD4 permeability compared to controls. Our experiments show that tofacitinib can rescue this effect, in part, through expression changes in claudin-2 and occludin. Claudin-2 and occludin were also altered in CTL Caco-2BBe cells when cultured with *PTPN2*-deficient macrophages. These key findings suggest that loss of *PTPN2* in either cell type is sufficient to induce changes on the barrier. These tight junction proteins are clinically relevant considering that claudin-2 is significantly upregulated and occludin is reduced in colonic biopsy samples from patients with active UC compared to non-inflammatory controls [4]. Additionally, tofacitinib reversed the expression of some, but not all, of these tight junction proteins, implying that junctional proteins are selectively regulated by the presence of macrophages and/or JAK-STAT signaling in this co-culture system. Of note, co-culture with control macrophages did not increase TEER in *PTPN2*-deficient IECs, implying that lacking *PTPN2* renders the epithelium insensitive to the barrier promoting effect of non-inflammatory, PTPN2-competent, macrophages. Furthermore, co-culture of *PTPN2* KD IECs with *PTPN2*-deficient macrophages only worsens the already leaky barrier, which demonstrates that consequences from loss of *PTPN2* in both cell types are synergistic.

STAT3 phosphorylation in Caco-2BBe cells correlates well with the changes seen in claudin-2 and occludin expression patterns. STAT3 may be directly involved in alterations of claudin-2 expression since we have previously shown that mutating the STAT-binding motif within the *CLDN2* gene promoter abrogated elevated *CLDN2* promoter activity in *PTPN2* KD IECs [81]. Whether STAT3 directly affects the

transcription of *CLDN2* in IECs also needs to be addressed, while JAK-STAT regulation of occludin is yet to be determined. It was surprising that despite its barrier-tightening properties, the elevated expression of occludin in tofacitinib-treated *Ptpn2*$^{fl/fl}$ mice did not yield a functional decrease in FD4 permeability *in vivo*. The net effect of occludin with JAM-A and tricellulin (both of which were unaffected by tofacitinib in these mice) may contribute to the lack of change in macromolecular permeability observed in these animals after tofacitinib treatment. The status of ZO-1 expression and localization in these mice would also need to be analyzed in future studies, as ZO-1 helps seal the leak barrier.

Our data reveal that IL-6 secretion is stimulated when *PTPN2* is lacking in macrophages, IECs, or both. Increased JAK-STAT activation in both IECs and macrophages may be due to the elevated levels of IL-6, as IL-6 signaling can be mediated by STAT3 [166]. However, the effect of IL-6 on the epithelial barrier is still in debate [105]. While 72-hour IL-6 exposure has been shown to decrease TER and increase mannitol permeability in Caco-2 monolayers [167], IL-6 knockout mice subjected to DSS-induced colitis had greater 4kDa-dextran permeability than controls [168]. This effect, however, may instead be due to the massive epithelial damage induced by DSS, which then disregards the effect of tight junction proteins on barrier function. Further, though pro-inflammatory cytokine TNF-α does not activate JAK-STAT signaling, it is important to note the similar pattern it has with IL-6 during the co-culture studies because TNF-α can induce IL-6 production in Caco-2 cells [169] and, in combination with IFN-γ, in THP-1 cells [170]. IL-6 can be produced by both epithelial and immune cells [171],

therefore, the changes we observed in tight junction proteins and JAK-STAT activation patterns could be due to autocrine or paracrine signaling, or the combination of both.

Further, since tofacitinib treatment did not fully inhibit IL-6 and TNF-α secretion when *PTPN2*-deficient Caco-2BBe and THP-1 cells were co-cultured, these results indicate that in the absence of *PTPN2*, JAK-STAT signaling only has a partial role in mediating IL-6 and TNF-α release. Activation of the mitogen-activated protein kinase (MAPK) pathway, regulated by PTPN2 in both THP-1 cells and IECs [172],[173], may be mediating IL-6 and TNF-α secretion instead. Nevertheless, in our experiments, addition of tofacitinib reduced IL-6 and TNF-α secretion in these co-culture studies. This agrees with recent findings that tofacitinib pretreatment reduced both IL-6 and TNF-α secretion in human peripheral monocytes stimulated by pro-inflammatory stimuli GM-CSF or IFN-γ [174].

The striking reversal of cytokine gene expression profiles of *Il6*, *Il10*, and *Il22* in tofactinib treated *Ptpn2*$^{fl/fl}$LysMCre mice also yields insights into which mediators may be causing the barrier changes observed in these mice. The elevated expression of pro-inflammatory cytokine *Il6* and reduced expression of anti-inflammatory cytokine *Il10* in proximal colons of vehicle-treated *Ptpn2*$^{fl/fl}$LysMCre mice suggest that at basal levels, the intestines are primed towards a pro-inflammatory phenotype. This is in agreement with and supports previous findings that *Ptpn2*$^{fl/fl}$LysMCre mice are more susceptible to DSS-induced colitis [88]. The normalization of these cytokine signatures by tofacitinib treatment for 7d *in vivo* suggests that despite the assessment of clinical outcomes at 8 weeks post-induction of tofacitinib in IBD patients [58], changes in cytokine mRNA

expression in the colon may have already taken place at even earlier time points. Continued release of pro-inflammatory cytokines in the colon may not generate as robust an immune response if the pro-inflammatory characteristic of the tissue has already been inhibited by tofacitinib. Elevated *Il22* expression correlated with increased protein expression of claudin-2 in proximal colons of vehicle-treated *Ptpn2*$^{fl/fl}$LysMCre mice. This is in agreement with findings that Th17 cytokine IL-22 upregulates claudin-2 to increase water efflux for bacterial clearance [175]. IL-22 mRNA expression is also elevated in active CD [176] and UC [177], has been shown to promote epithelial restitution in wound-healing assays [176] and attenuates intestinal inflammation *in vivo* [178]. While IL-22 has been considered to be a protective cytokine of the intestinal mucosa, recent evidence suggests that it can also prove detrimental to colonic epithelial integrity in IBD [179].

When co-cultured with IECs, *PTPN2*-deficient macrophages have higher JAK1, STAT1, and STAT3 phosphorylation. Whether this is in response to factors secreted by the epithelial cells, or if this is activated by autocrine signaling amongst the macrophages will require further study. However, no synergistic effect was observed on STAT phosphorylation (in either cell type) when *PTPN2* was lost in both THP-1 and Caco-2BBe cells. This suggests that secreted factors from *PTPN2*-deficient IECs do not enhance STAT activation in *PTPN2*-deficient macrophages, or vice-versa. Regardless, these data suggest that *PTPN2* deficiency in macrophages or IECs is sufficient to induce detrimental effects to the barrier along with increased JAK-STAT signaling in either cell

type. Most importantly, the key finding here is that one dose of tofacitinib is sufficient to inhibit JAK-STAT signaling in macrophages and IECs lacking *PTPN2*.

The oral gavage of three distinct probes followed by measurement of amount present in the serum allows for size-selective analysis of intestinal permeability *in vivo*. This assay has been used in a previous study [175] and serves as a tool to help tease out the distinct defects in the pore, leak and unrestricted pathways of permeability *in vivo*. Unaltered permeability changes to RD70 were expected since *Ptpn2*$^{fl/fl}$LysMCre mice show no overt signs of mucosal damage in the colon (data not shown). However, it was surprising to see no changes in creatinine permeability considering that changes in claudin-2 and claudin-4 expression patterns were significant in proximal colon IECs of mice treated with tofacitinib citrate. Region-specific TEER across the epithelial barrier may yield a better insight into how tofacitinib influences the pore barrier along the intestinal tract, especially in the colon. Creatinine, FD4, and RD70 are not actively transported by the transcellular pathway, but rather, cross the intestinal epithelium passively through the paracellular pathway. Recovery of these probes in the serum can be affected by overall fluid transport, which can be influenced by distribution within the bloodstream, other tissues, and rate of renal clearance. How these other factors are affected by *PTPN2* loss in macrophages or by tofacitinib are other avenues that could be explored.

The complete rescue of the barrier defect in *Ptpn2*$^{fl/fl}$LysMCre is only one example of the beneficial effects of tofacitinib. In one study, mice treated with tofacitinib (30 mg/kg) during the recovery phase after acute DSS-induced colitis had lower disease

activity and histopathology scores with reduced $CD3^+$ cell infiltrates [155]. Our *in vivo* data on the effect of tofacitinib citrate treatment on reducing M1 while increasing M2 macrophage populations supports findings that tofacitinib pretreatment followed by IFN-γ+LPS stimulation skews murine BMDMs towards a more regulatory, M2-like phenotype [155]. This, however, is not a complete reversal [155], which is evident in our studies that M1/M2 proportions are not normalized by tofacitinib citrate treatment to the same levels as in *Ptpn2*$^{fl/fl}$ vehicle-treated mice. Nevertheless, the effect of tofacitinib on macrophage polarization is significant and indicates a novel mechanism by which JAK inhibition protects the intestinal epithelium.

An important note to mention is that the genetic profiles of the IBD patients included in the tofacitinib clinical studies are unknown. In phase 3 clinical trials, only remission occurred in only 40.6% of UC patients receiving tofacitinib [58] Therefore, it is yet to be determined whether tofacitinib is better at inducing clinical outcomes and sustaining remission at higher rates in patients with certain genetic composition vs. others. The use of tofacitinib in subgroups of patients with distinct genetic profiles, especially those with mutations in IBD candidate genes, such as *PTPN2*, should be more carefully analyzed in order to improve clinical outcomes and remission rates of this drug in IBD patients. Adverse events such as increased rates of overall infections, herpes zoster infections, cardiovascular events, and increased lipid levels were observed in IBD patients taking tofacitinib for 52 weeks [58]. More recently, higher rates of pulmonary embolisms and mortality have occurred in rheumatoid arthritis (RA) patients taking the high dose of 10mg tofacitinib [59]. Although these safety trials are ongoing for patients

with RA with at least one cardiovascular risk factor, the same risks may apply to patients taking tofacitinib for UC [59]. Nevertheless, major potential benefit of our work presented here not only lies in improving response and remission rates in UC patients, but in targeting CD patients with *PTPN2* loss-of-function mutations, as well, as tofacitinib has not been effective in phase 2 clinical trials for the treatment of CD in patients of undetermined *PTPN2* genetic background [115]. Because of these concerns, identifying and specifically targeting select patients who are to receive tofacitinib is crucial.

In summary, these findings reveal that tofacitinib corrected barrier function and tight junction regulation in IECs, cytokine secretion, and macrophage differentiation associated with *PTPN2* deficiency in both co-culture cell system and animal models. Tofacitinib may potentially be a more effective therapeutic for patients harboring *PTPN2* loss-of-function mutations.

Chapter 5: Discussion

Summary

In Chapter 2, we demonstrated the effectiveness of tofacitinib in rescuing the intestinal barrier *in vitro*. In parental IECs and colonoids derived from IBD patients, tofacitinib prevented and rescued cytokine-induced barrier dysfunction. With regards to the pore pathway of permeability, tofacitinib reduces IFN-γ-induced upregulation of claudin-2 on a transcriptional level, without affecting the protein expression of other claudins. Tofacitinib also does not alter expression of tight junction proteins regulating the leak pathway of permeability, ZO-1, occludin, and tricellulin, but rather, exerts its effect on tight junction localization of ZO-1. Here, we provide the first evidence that tofacitinib inhibits JAK1-STAT1 signaling in IECs, and by doing so, protects it from cytokine-induced barrier defects.

Results included in Chapter 3 show how tofacitinib can rescue barrier and JAK-STAT signaling consequences associated with loss of activity of *PTPN2*, an IBD susceptibility gene. Most importantly, we show here that tofacitinib can reverse these consequences to levels comparable to controls even after a cytokine challenge. Robust JAK-STAT phosphorylation and activation are observed in *Ptpn2* KO mice. However, due to the drastic inflammatory phenotype of this mouse model, tofacitinib was unable to reverse any of the consequences resulting from complete *Ptpn2* loss *in vivo*. Therefore, we turned to tissue-specific models to determine if tofacitinib can rescue barrier function *in vivo*. Surprisingly, no barrier defects were seen in young and adult *Ptpn2* Het and $Ptpn2^{\Delta IEC}$ mice, despite observations of higher JAK-STAT phosphorylation and

activation in these mice. Further studies are required to fully tease apart which region(s) in the intestine is most affected by *Ptpn2* loss with regards to barrier function. In addition, identification of a therapeutic effect of tofacitinib in these mice (*Ptpn2*$^{\Delta IEC}$) may only become apparent in the context of an appropriate challenge model leading to a pronounced barrier defect.

Finally, data featured in Chapter 4 highlights the involvement of innate immune cells, specifically macrophages, in intestinal barrier regulation and how tofacitinib modulates the interaction between IECs and macrophages. As mentioned previously, due to the dramatic and robust inflammation in the *Ptpn2* KO mice, mice with cell-specific deletion of *Ptpn2* were used. With myeloid-specific knockout of *Ptpn2*, *Ptpn2*$^{fl/fl}$LysMCre mice exhibited higher intestinal permeability, which coincided with higher expression of claudin-2, and lower expression of claudin-4, occludin, tricellulin, and JAM-A in the colon. These were correlated with higher levels of STAT3 phosphorylation, IL-6, and IL-22 mRNA in the colon. All of these effects, however, were effectively reversed by tofacitinib citrate treatment. *In vitro* studies further help delineate that *PTPN2* loss in macrophages indeed causes barrier dysfunction to CTL IECs and *PTPN2* loss in IECs also promotes release of pro-inflammatory cytokine IL-6 from CTL macrophages. These findings also demonstrate that deficiency in *PTPN2* in IECs and macrophages is synergistic and PTPN2 loss in both cell types further exacerbated the effects seen when *PTPN2* was depleted in either cell type individually. Of note, tofacitinib reversed these effects and corrected the consequences of disrupted macrophage-IEC communication. Further, our mechanistic investigations indicate that

IL-6-STAT3 signaling may be the primary pathway mediating macrophage-epithelial crosstalk in this system.

5.2 Future Studies

While the *in vitro* studies on the effect of tofacitinib on *PTPN2* KD IECs are promising, the rescue in TER with and without cytokine challenge has not yet reached statistical significance. These studies must be completed in full in order to determine if both pore and leak barrier defects arising from PTPN2 loss can be corrected by tofacitinib. Future studies would need to determine if tofacitinib exerts the same effect in claudin-2 expression in *PTPN2* KD cells as they did in parental T84 IECs. *PTPN2*-deficient IECs have been shown to express higher levels of claudin-2, which is partly responsible for the lower TER observed in these cells [81]. We predict that claudin-2 expression changes will correlate to TER results.

Indeed, the cell lines stably expressing shRNA against *PTPN2* used in these studies has led to key findings about the crucial role of *PTPN2* in protecting the intestinal barrier. However, studies on whether specific variants, such as the SNPs leading to loss-of-function mutations associated with CD and UC, cause similar barrier defects in IECs would need to be determined. Suggestions of whether features of variant-carrying IECs can be rescued with vectors containing a WT form of PTPN2 have also been proposed.

Because twice daily oral tofacitinib treatment *in vivo* may be too invasive of a therapeutic strategy for young constitutive *Ptpn2* Het and KO mice, and because a barrier defect was not observed in adult *Ptpn2*-deficient (constitutive *Ptpn2* Het or IEC-specific)

mice *in vivo*, we may need to investigate the effect of tofacitinib on IECs and barrier function using intestinal organoids derived from *Ptpn2*-deficient mice. These models would also help delineate if and how tofacitinib may affect differentiation of epithelial cells into different cell types, in the absence of input from non-epithelial cells. Indeed, region-specific barrier function must be determined in *Ptpn2*$^{\Delta IEC}$ animals to establish whether specific segments of the gut are more affected by IEC-specific deletion of *Ptpn2* compared to others. Depending on these results, tissues from tofacitinib-treated *Ptpn2*$^{\Delta IEC}$ mice would then be subjected to Ussing chambers studies to delineate whether tofacitinib affects barrier function with IEC-specific loss of *Ptpn2*. This would therefore strengthen our *in vitro* findings.

The failure of tofacitinib to induce higher remission rates in CD patients has raised questions about its risk-benefit profiles and has increased the push for clinical studies to test the effectiveness of more selective JAK inhibitors for the treatment of IBD [55]. In particular, more JAK1-selective inhibitors are currently being investigated for treatment of IBD, such as filgotinib and upadacitinib [180]. Filgotinib and upadacitinib clinical studies are ongoing with promising results [180]. Whether these two drugs are as effective at rescuing the barrier as tofacitinib would need to be assessed *in vitro* and *in vivo*. This is a valid experiment considering that PTPN2-deficient cell and animal models have elevated phosphorylation and activation of JAK1 and downstream effectors STAT1, and STAT3.

Lastly, further studies are required to better explain how tofacitinib rescues the leak barrier. *In vitro*, tofacitinib did not change the protein expression of occludin upon

IFN-γ treatment. In contrast, *Ptpn2*$^{fl/fl}$LysMCre mice have lower colonic expression of occludin, JAM-A, and tricellulin, which were reversed by tofacitinib. The discrepancy between data from human and mouse samples may indicate additional cytokine signaling pathways are recruited to remodel tight junction composition *in vivo* compared with the effects of a single cytokine (IFN-γ) *in vitro*. The phosphorylation of the mysosin light chain (MLC) by MLC kinase (MLCK) has been shown to contract the perijunctional actomyosin ring, pulling on the tight junctions proteins to "loosen" the seal between IECs, therefore increasing paracellular permeability [17],[181]. Whether MLC phosphorylation is affected in tofacitinib-treated *PTPN2*-deficient cells would also need to be investigated.

5.3 Conclusions and Implications

Data presented in this dissertation shed light into how tofacitinib exerts its effects on the intestinal epithelium, which is damaged the most in IBD. These studies are the first to show how rescue of barrier function may be contributing to the beneficial effects of tofacitinib treatment seen in IBD patients. Studies in animal models suggest that barrier defects seen in *Ptpn2* KO mice are not entirely due to IECs alone, but that the immune component, particularly the involvement of macrophages, may play a bigger role in causing the barrier defects seen in *Ptpn2* KO mice. In turn, *PTPN2* deficiency in IECs alters macrophage function *in vitro*, however, the mouse model of IEC-specific *Ptpn2* loss has a relatively healthy gut. Compensation by other cell types may be responsible for the lack of a barrier defect in these mice. We predict that this mouse model may be more

susceptible to an appropriate barrier-modifying challenge, as seen in other *Ptpn2* tissue-specific knockout models.

Increased intestinal permeability is a hallmark of IBD and our results show that tofacitinib may be able to alleviate, at least in part, this particular defect. However, tofacitinib treatment does have its disadvantages. As mentioned earlier, the JAK-STAT pathway plays an important role in normal cellular functions [51]. The global and systemic inhibition of this pathway does generate adverse effects, as seen in the tofacitinib clinical trials for IBD patients. These include higher overall infection rates, especially herpes zoster infections, and higher triglyceride levels [58]. Recently, Pfizer, Inc. released results from an ongoing tofacitinib study on patients over the age of 50 with rheumatoid arthritis and at least one cardiovascular risk factor. Increased risk of blood clots (19 cases out of 3,884 patient-years, calculated as # of patients in the study x # of years of participation in the study) and all-cause mortality rates (45 cases out of 3,884 patient-years) were found with the high 10mg twice daily dose of tofacitinib compared to the lower 5mg twice daily dose or anti-TNF blockers [182]. Since tofacitinib is also being used to treat ulcerative colitis, both the FDA and Pfizer, Inc. had issued a warning advising clinicians that the use of tofacitinib to treat UC should be kept at the recommended doses (10mg twice daily as the induction dose for 8 weeks and 5mg twice daily as the maintenance dose) in order to prevent serious, and perhaps, fatal events in patients taking this drug [59],[182]. From this, it makes it even more imperative for IBD therapeutics to be personalized for subgroups of patients likely to be responsive. New therapeutics, such as tofacitinib, have been developed in order to treat IBD patients who

had inadequate or refractory response to anti-TNF therapy or other immunosuppressants. The use of tofacitinib in combination with anti-inflammatory drugs, immunomodulators, and/or anti-TNF has not been recommended until additional safety studies have been conducted. With the multi-factorial etiology of IBD, better incorporation of etiologic factors i.e. genetic polymorphisms into treatment regimen design is warranted.

This study provides a potential role for tofacitinib to reverse specific pathophysiological consequences (increased intestinal permeability) associated with a genetic defect. The ability of tofacitinib to rescue abnormal JAK-STAT signaling, barrier dysfunction, and pro-inflammatory cytokine release observed in *PTPN2*-deficient cell and animal models suggest that patients harboring *PTPN2* loss-of-function mutations may benefit from tofacitinib treatment the most. As mentioned before, the genetic component of IBD has been largely ignored in the process of developing and tailoring therapeutics for IBD patients. There is an increasing amount of evidence as to how IBD candidate genes contribute to IBD pathology. The work presented here provides both an opportunity and a template for more rational treatment regimen design and exploit a personalized medicine approach in treating symptoms of IBD.

References

1. Shen, L., Weber, C. R., Raleigh, D. R., Yu, D. & Turner, J. R. Tight Junction Pore and Leak Pathways: A Dynamic Duo. *Annu. Rev. Physiol.* **73**, 283–309 (2011).

2. Odenwald, M. A. & Turner, J. R. The intestinal epithelial barrier: a therapeutic target? *Nat. Rev. Gastroenterol. Hepatol.* **14**, 9–21 (2017).

3. Günzel, D. & Yu, A. S. L. Claudins and the modulation of tight junction permeability. *Physiol. Rev.* **93**, 525–569 (2013).

4. Heller, F. *et al.* Interleukin-13 is the key effector Th2 cytokine in ulcerative colitis that affects epithelial tight junctions, apoptosis, and cell restitution. *Gastroenterology* **129**, 550–564 (2005).

5. Luettig, J., Rosenthal, R., Barmeyer, C. & Schulzke, J. D. Claudin-2 as a mediator of leaky gut barrier during intestinal inflammation. *Tissue Barriers* vol. 3 (2015).

6. Turner, J. R. Intestinal mucosal barrier function in health and disease. *Nat. Rev. Immunol.* **9**, 799–809 (2009).

7. Fanning, A. S., Jameson, B. J., Jesaitis, L. A. & Anderson, J. M. The tight junction protein ZO-1 establishes a link between the transmembrane protein occludin and the actin cytoskeleton. *J. Biol. Chem.* **273**, 29745–29753 (1998).

8. Van Itallie, C. M., Fanning, A. S., Bridges, A. & Anderson, J. M. ZO-1 stabilizes the tight junction solute barrier through coupling to the perijunctional cytoskeleton. *Mol. Biol. Cell* **20**, 3930–40 (2009).

9. Laukoetter, M. G., Nava, P. & Nusrat, A. Role of the intestinal barrier in inflammatory bowel disease. *World J. Gastroenterol.* **14**, 401 (2008).

10. Furuse, M. *et al.* Direct association of occludin with ZO-1 and its possible involvement in the localization of occludin at tight junctions. *J. Cell Biol.* **127**, 1617–1626 (1994).

11. Ikenouchi, J. *et al.* Tricellulin constitutes a novel barrier at tricellular contacts of epithelial cells. *J. Cell Biol.* **171**, 939–945 (2005).

12. Raleigh, D. R. *et al.* Tight junction-associated MARVEL proteins marveld3, tricellulin, and occludin have distinct but overlapping functions. *Mol. Biol. Cell* **21**, 1200–13 (2010).

13. Krug, S. M. *et al.* Tricellulin forms a barrier to macromolecules in tricellular tight junctions without affecting ion permeability. *Mol. Biol. Cell* **20**, 3713–24 (2009).

14. Ikenouchi, J., Sasaki, H., Tsukita, S., Furuse, M. & Tsukita, S. Loss of occludin affects tricellular localization of tricellulin. *Mol. Biol. Cell* **19**, 4687–4693 (2008).

15. Bruewer, M. *et al.* Interferon-γ induces internalization of epithelial tight junction proteins via a macropinocytosis-like process. *FASEB J.* **19**, 923–933 (2005).

16. Sayoc-Becerra, A. *et al.* The JAK-Inhibitor Tofacitinib Rescues Human Intestinal Epithelial Cells and Colonoids from Cytokine-Induced Barrier Dysfunction. *Inflamm. Bowel Dis.* (2019) doi:10.1093/ibd/izz266.

17. Cunningham, K. E. & Turner, J. R. Myosin light chain kinase: Pulling the strings of epithelial tight junction function. *Ann. N. Y. Acad. Sci.* **1258**, 34–42 (2012).

18. Rosenblatt, J., Raff, M. C. & Cramer, L. P. An epithelial cell destined for apoptosis signals its neighbors to extrude it by an actin- and myosin-dependent mechanism. *Curr. Biol.* **11**, 1847–1857 (2001).

19. Ng, S. C. *et al.* Worldwide incidence and prevalence of inflammatory bowel disease in the 21st century: a systematic review of population-based studies. *Lancet* **390**, 2769–2778 (2017).

20. Knowles, S. R. *et al.* Quality of Life in Inflammatory Bowel Disease: A Systematic Review and Meta-analyses - Part i. *Inflammatory Bowel Diseases* vol. 24 742–751 (2018).

21. Park, K. T. *et al.* The Cost of Inflammatory Bowel Disease: An Initiative From the Crohn's & Colitis Foundation. *Inflamm. Bowel Dis.* (2019) doi:10.1093/ibd/izz104.

22. Ann Shafer, L. *et al.* Association Between IBD Disability and Reduced Work Productivity (Presenteeism): A Population-Based Study in Manitoba, Canada. *Inflamm Bowel Dis* • **25**, (2019).

23. Eloi, C. *et al.* Inflammatory Bowel Diseases and School Absenteeism. *J. Pediatr. Gastroenterol. Nutr.* **68**, 541–546 (2019).

24. Kaser, A., Zeissig, S. & Blumberg, R. S. Inflammatory bowel disease. *Annu. Rev. Immunol.* **28**, 573–621 (2010).

25. Chang, M. D. & Liu, X. Overview of Histopathology of Ulcerative Colitis and Crohn's Disease. in *Interventional Inflammatory Bowel Disease: Endoscopic Management and Treatment of Complications* 49–68 (2018).

26. Feakins, R. M. Ulcerative colitis or Crohn's disease? Pitfalls and problems. *Histopathology* **64**, 317–335 (2014).

27. Baumgart, D. C. & Sandborn, W. J. Crohn's disease. in *The Lancet* vol. 380 1590–1605 (2012).

28. Imam, T., Park, S., Kaplan, M. H. & Olson, M. R. Effector T helper cell subsets in inflammatory bowel diseases. *Frontiers in Immunology* vol. 9 (2018).

29. Moschen, A. R., Tilg, H. & Raine, T. IL-12, IL-23 and IL-17 in IBD: immunobiology and therapeutic targeting. *Nat. Rev. Gastroenterol. Hepatol.* **16**, 185–196 (2019).

30. Kaiko, G. E., Horvat, J. C., Beagley, K. W. & Hansbro, P. M. Immunological decision-making: How does the immune system decide to mount a helper T-cell response? *Immunology* vol. 123 326–338 (2008).

31. Danese, S. & Fiocchi, C. Ulcerative Colitis. *N. Engl. J. Med.* **365**, 1713–1725 (2011).

32. Fuss, I. J. *et al.* Nonclassical CD1d-restricted NK T cells that produce IL-13 characterize an atypical Th2 response in ulcerative colitis. *J. Clin. Invest.* **113**, 1490–1497 (2004).

33. Mamula, P. *et al.* Inflammatory bowel disease in children 5 years of age and younger. *Am. J. Gastroenterol.* **97**, 2005–2010 (2002).

34. Abramson, O. *et al.* Incidence, prevalence, and time trends of pediatric inflammatory bowel disease in Northern California, 1996 to 2006. *J. Pediatr.* **157**, (2010).

35. Rosen, M. J., Dhawan, A. & Saeed, S. A. Inflammatory bowel disease in children and adolescents. *JAMA Pediatrics* vol. 169 1053–1060 (2015).

36. Paganelli, M. *et al.* Inflammation is the main determinant of low bone mineral density in pediatric inflammatory bowel disease. *Inflamm. Bowel Dis.* **13**, 416–423 (2007).

37. MacKner, L. M. *et al.* Psychosocial issues in pediatric inflammatory bowel disease: Report of the north american society for pediatric gastroenterology, hepatology, and nutrition. *J Pediatr Gastroenterol Nutr*. **56**, 449–458 (2013).

38. Engström, I. Mental Health and Psychological Functioning in Children and Adolescents with Inflammatory Bowel Disease: a Comparison with Children having Other Chronic Illnesses and with Healthy Children. *J. Child Psychol. Psychiatry* **33**, 563–582 (1992).

39. Coskun, M., Salem, M., Pedersen, J. & Nielsen, O. H. Involvement of JAK/STAT signaling in the pathogenesis of inflammatory bowel disease. *Pharmacol. Res.* **76**, 1–8 (2013).

40. Neurath, M. F. Cytokines in inflammatory bowel disease. *Nature Reviews Immunology* vol. 14 329–342 (2014).

41. Sanchez-Muñoz, F., Dominguez-Lopez, A. & Yamamoto-Furusho, J. K. Role of cytokines in inflammatory bowel disease. *World Journal of Gastroenterology* vol. 14 4280–4288 (2008).

42. Fuss, I. J. *et al.* Disparate CD4+ lamina propria (LP) lymphokine secretion profiles in inflammatory bowel disease. Crohn's disease LP cells manifest increased secretion of IFN-gamma, whereas ulcerative colitis LP cells manifest increased secretion of IL-5. *J. Immunol.* **157**, 1261–70 (1996).

43. Fais, S. *et al.* Spontaneous release of interferon γ by intestinal lamina propria lymphocytes in Crohn's disease. Kinetics of in vitro response to interferon γ inducers. *Gut* **32**, 403–407 (1991).

44. Breese, E., Braegger, C. P., Corrigan, C. J., Walker-Smith, J. A. & MacDonald, T. T. Interleukin-2- and interferon-gamma-secreting T cells in normal and diseased human intestinal mucosa. *Immunology* **78**, 127–31 (1993).

45. Smith, P. D. *et al.* Intestinal macrophages and response to microbial encroachment. *Mucosal Immunology* vol. 4 31–42 (2011).

46. Bain, C. C. & Mowat, A. M. Macrophages in intestinal homeostasis and inflammation. *Immunological Reviews* vol. 260 102–117 (2014).

47. Murai, M. *et al.* Interleukin 10 acts on regulatory T cells to maintain expression of the transcription factor Foxp3 and suppressive function in mice with colitis. *Nat Immunol* **10**, 1178–1184 (2009).

48. Zigmond, E. & Jung, S. Intestinal macrophages: Well educated exceptions from the rule. *Trends in Immunology* vol. 34 162–168 (2013).

49. Fernando, M. R., Reyes, J. L., Iannuzzi, J., Leung, G. & McKay, D. M. The pro-inflammatory cytokine, interleukin-6, enhances the polarization of alternatively activated macrophages. *PLoS One* **9**, (2014).

50. Al-Ghadban, S., Kaissi, S., Homaidan, F. R., Naim, H. Y. & El-Sabban, M. E. Cross-talk between intestinal epithelial cells and immune cells in inflammatory bowel disease. *Sci. Rep.* **6**, (2016).

51. Shuai, K. & Liu, B. Regulation of JAK-STAT signalling in the immune system. *Nat. Rev. Immunol.* **3**, 900–911 (2003).

52. Jostins, L. *et al.* Host-microbe interactions have shaped the genetic architecture of inflammatory bowel disease. *Nature* **491**, 119–124 (2012).

53. Christophi, G. P., Rong, R., Holtzapple, P. G., Massa, P. T. & Landas, S. K. Immune markers and differential signaling networks in ulcerative colitis and Crohn's disease. *Inflamm. Bowel Dis.* **18**, 2342–2356 (2012).

54. Löwenberg, M. & D'Haens, G. Next-Generation Therapeutics for IBD. *Current Gastroenterology Reports* vol. 17 (2015).

55. Ma, C. *et al.* Systematic review with meta-analysis: efficacy and safety of oral Janus kinase inhibitors for inflammatory bowel disease. *Aliment. Pharmacol. Ther.* **50**, 5–23 (2019).

56. Fernández-Clotet, A., Castro-Poceiro, J. & Panés, J. JAK Inhibition: The Most Promising Agents in the IBD Pipeline? *Curr. Pharm. Des.* **25**, 32–40 (2019).

57. Soendergaard, C., Bergenheim, F. H., Bjerrum, J. T. & Nielsen, O. H. Targeting JAK-STAT signal transduction in IBD. *Pharmacology and Therapeutics* vol. 192 100–111 (2018).

58. Sandborn, W. J. *et al.* Tofacitinib as induction and maintenance therapy for ulcerative colitis. *N. Engl. J. Med.* **376**, 1723–1736 (2017).

59. Pfizer. Highlights of Prescribing Information: Xeljanz/Xeljanz XR. http://labeling.pfizer.com/ShowLabeling.aspx?id=959 (2019).

60. Michielan, A. & D'Incà, R. Intestinal Permeability in Inflammatory Bowel Disease: Pathogenesis, Clinical Evaluation, and Therapy of Leaky Gut. *Mediators of Inflammation* vol. 2015 (2015).

61. Smecuol, E. *et al.* Gastrointestinal permeability in celiac disease. *Gastroenterology* **112**, 1129–36 (1997).

62. McCole, D. F. IBD candidate genes and intestinal barrier regulation. *Inflamm. Bowel Dis.* **20**, 1829–1849 (2014).

63. Weber, C. R. & Turner, J. R. Inflammatory bowel disease: Is it really just another break in the wall? *Gut* **56**, 6–8 (2007).

64. Arnott, I. D. R., Kingstone, K. & Ghosh, S. Abnormal intestinal permeability predicts relapse in inactive Crohn disease. *Scand. J. Gastroenterol.* **35**, 1163–1169 (2000).

65. Wyatt, J., Vogelsang, H., Hübl, W., et al. Intestinal permeability and the prediction of relapse in Crohri's disease. *Lancet* **341**, 1437–1439 (1993).

66. Irvine, E. J. & Marshall, J. K. Increased intestinal permeability precedes the onset of Crohn's disease in a subject with familial risk. *Gastroenterology* **119**, 1740–1744 (2000).

67. Wellcome Trust Case Control Consortium. Genome-wide association study of 14,000 cases of seven common diseases and 3,000 shared controls. *Nature* **447**, 661–678 (2007).

68. Liu, J. Z. *et al.* Association analyses identify 38 susceptibility loci for inflammatory bowel disease and highlight shared genetic risk across populations. *Nat. Genet.* **47**, 979–986 (2015).

69. Franke, A. *et al.* Genome-wide meta-analysis increases to 71 the number of confirmed Crohn's disease susceptibility loci. *Nat. Genet.* **42**, 1118–1125 (2010).

70. McCole, D. F. Phosphatase regulation of intercellular junctions. *Tissue Barriers* vol. 1 (2013).

71. Glas, J. *et al.* PTPN2 Gene Variants Are Associated with Susceptibility to Both Crohn's Disease and Ulcerative Colitis Supporting a Common Genetic Disease Background. *PLoS One* **7**, e33682 (2012).

72. Lorenzen, J. A., Dadabay, C. Y. & Fischer, E. H. COOH-terminal sequence motifs target the T cell protein tyrosine phosphatase to the ER and nucleus. *J. Cell Biol.* **131**, 631–643 (1995).

73. ten Hoeve, J. *et al.* Identification of a Nuclear Stat1 Protein Tyrosine Phosphatase. *Mol. Cell. Biol.* **22**, 5662–5668 (2002).

74. Simoncic, P. D., Lee-Loy, A., Barber, D. L., Tremblay, M. L. & McGlade, C. J. The T cell protein tyrosine phosphatase is a negative regulator of Janus family kinases 1 and 3. *Curr. Biol.* **12**, 446–453 (2002).

75. Tiganis, T., Bennett, A. M., Ravichandran, K. S. & Tonks, N. K. Epidermal Growth Factor Receptor and the Adaptor Protein p52 Shc Are Specific Substrates of T-Cell Protein Tyrosine Phosphatase . *Mol. Cell. Biol.* **18**, 1622–1634 (1998).

76. Galic, S. *et al.* Regulation of Insulin Receptor Signaling by the Protein Tyrosine Phosphatase TCPTP. *Mol. Cell. Biol.* **23**, 2096–2108 (2003).

77. Lu, X. *et al.* T-Cell Protein Tyrosine Phosphatase, Distinctively Expressed in Activated-B-Cell-Like Diffuse Large B-Cell Lymphomas, Is the Nuclear Phosphatase of STAT6. *Mol. Cell. Biol.* **27**, 2166–2179 (2007).

78. Yamamoto, T. *et al.* The nuclear isoform of protein-tyrosine phosphatase TC-PTP regulates interleukin-6-mediated signaling pathway through STAT3 dephosphorylation. *Biochem. Biophys. Res. Commun.* **297**, 811–7 (2002).

79. Scharl, M. *et al.* Protection of epithelial barrier function by the Crohn's disease associated gene protein tyrosine phosphatase n2. *Gastroenterology* **137**, 2030-2040.e5 (2009).

80. Krishnan, M., Penrose, H. M., Shah, N. N., Marchelletta, R. R. & McCole, D. F. VSL#3 probiotic stimulates T-cell protein tyrosine phosphatase-mediated recovery of IFN-γ-induced intestinal epithelial barrier defects. *Inflamm. Bowel Dis.* **22**, 2811–2823 (2016).

81. Krishnan, M. & McCole, D. F. T cell protein tyrosine phosphatase prevents STAT1 induction of claudin-2 expression in intestinal epithelial cells. *Ann. N. Y. Acad. Sci.* **1405**, 116–130 (2017).

82. You-ten, K. E. *et al.* Impaired Bone Marrow Microenvironment and Phosphatase – deficient Mice. *J Exp Med* **186**, 683–693 (1997).

83. Doody, K. M., Bourdeau, A. & Tremblay, M. L. T-cell protein tyrosine phosphatase is a key regulator in immune cell signaling: lessons from the knockout mouse model and implications in human disease. *Immunol. Rev.* **228**, 325–341 (2009).

84. Okayasu, I. *et al.* A novel method in the induction of reliable experimental acute and chronic ulcerative colitis in mice. *Gastroenterology* **98**, 694–702 (1990).

85. Hassan, S. W. *et al.* Increased susceptibility to dextran sulfate sodium induced colitis in the T cell protein tyrosine phosphatase heterozygous mouse. *PLoS One* **5**, (2010).

86. Kasper, S. H. *et al.* Deficiency of Protein Tyrosine Phosphatase Non-Receptor Type 2 in Intestinal Epithelial Cells Has No Appreciable Impact on Dextran Sulphate Sodium Colitis Severity But Promotes Wound Healing. *Digestion* **93**, 249–259 (2016).

87. Spalinger, M. R. *et al.* PTPN2 controls differentiation of CD4+ T cells and limits intestinal inflammation and intestinal dysbiosis. *Mucosal Immunol.* **8**, 918–929 (2015).

88. Spalinger, M. R. *et al.* PTPN2 Regulates Inflammasome Activation and Controls Onset of Intestinal Inflammation and Colon Cancer. *Cell Rep.* **22**, 1835–1848 (2018).

89. Zeissig, S. *et al.* Changes in expression and distribution of claudin 2, 5 and 8 lead to discontinuous tight junctions and barrier dysfunction in active Crohn's disease. *Gut* **56**, 61–72 (2007).

90. Turner, J. R. *et al.* Physiological regulation of epithelial tight junctions is associated with myosin light-chain phosphorylation. *Am. J. Physiol. - Cell Physiol.* **273**, (1997).

91. Bruewer, M., Samarin, S. & Nusrat, A. Inflammatory bowel disease and the apical junctional complex. *Ann. N. Y. Acad. Sci.* **1072**, 242–252 (2006).

92. Anderson, J. M. & Van Itallie, C. M. Tight junctions and the molecular basis for regulation of paracellular permeability. *Am. J. Physiol. - Gastrointest. Liver Physiol.* **269**, 467–475 (1995).

93. Anbazhagan, A. N., Priyamvada, S., Alrefai, W. A. & Dudeja, P. K. Pathophysiology of IBD associated diarrhea. *Tissue Barriers* **6**, (2018).

94. Olson, T. S. *et al.* The primary defect in experimental ileitis originates from a nonhematopoietic source. *J. Exp. Med.* **203**, 541–552 (2006).

95. Su, L. *et al.* Targeted Epithelial Tight Junction Dysfunction Causes Immune Activation and Contributes to Development of Experimental Colitis. *Gastroenterology* **136**, 551–563 (2009).

96. Clayburgh, D. R., Shen, L. & Turner, J. R. A porous defense: The leaky epithelial barrier in intestinal disease. *Lab. Investig.* **84**, 282–291 (2004).

97. Rosenthal, R. *et al.* Claudin-2, a component of the tight junction, forms a paracellular water channel. *J. Cell Sci.* **123**, 1913–1921 (2010).

98. Amasheh, S. *et al.* Claudin-2 expression induces cation-selective channels in tight junctions of epithelial cells. *J. Cell Sci.* **115**, 4969–4976 (2002).

99. Prasad, S. *et al.* Inflammatory processes have differential effects on claudins 2, 3 and 4 in colonic epithelial cells. *Lab. Investig.* **85**, 1139–1162 (2005).

100. Heller, F. *et al.* Interleukin-13 Is the Key Effector Th2 Cytokine in Ulcerative Colitis That Affects Epithelial Tight Junctions, Apoptosis, and Cell Restitution. *Gastroenterology* **129**, 550–564 (2005).

101. Weber, C. R. *et al.* Epithelial myosin light chain kinase activation induces mucosal interleukin-13 expression to alter tight junction ion selectivity. *J. Biol. Chem.* **285**, 12037–12046 (2010).

102. Ikenouchi, J. *et al.* Tricellulin constitutes a novel barrier at tricellular contacts of epithelial cells. *J. Cell Biol.* **171**, 939–945 (2005).

103. Nusrat, A. *et al.* The coiled-coil domain of occludin can act to organize structural and functional elements of the epithelial tight junction. *J. Biol. Chem.* **275**, 29816–29822 (2000).

104. Van Itallie, C. M. & Anderson, J. M. Occludin confers adhesiveness when expressed in fibroblasts. *J. Cell Sci.* **110**, 1113–1121 (1997).

105. Al-Sadi, R., Boivin, M. & Ma, T. Mechanism of cytokine modulation of epithelial tight junction barrier. *Front. Biosci.* **14**, 2765–2778 (2009).

106. Marchiando, A. M. *et al.* Caveolin-1-dependent occludin endocytosis is required for TNF-induced tight junction regulation in vivo. *J. Cell Biol.* **189**, 111–126 (2010).

107. Van Itallie, C. M., Fanning, A. S., Holmes, J. & Anderson, J. M. Occludin is required for cytokine-induced regulation of tight junction barriers. *J. Cell Sci.* **123**, 2844–2852 (2010).

108. Mudter, J. *et al.* Activation pattern of signal transducers and activators of transcription (STAT) factors in inflammatory bowel diseases. *Am. J. Gastroenterol.* **100**, 64–72 (2005).

109. Penrose, H. M., Marchelletta, R. R., Krishnan, M. & McCole, D. F. Spermidine stimulates T cell protein-tyrosine phosphatasemediated protection of intestinal epithelial barrier function. *J. Biol. Chem.* **288**, 32651–32662 (2013).

110. Watson, C. J., Hoare, C. J., Garrod, D. R., Carlson, G. L. & Warhurst, G. Interferon-γ selectively increases epithelial permeability to large molecules by activating different populations of paracellular pores. *J. Cell Sci.* **118**, 5221–5230 (2005).

111. Beaurepaire, C., Smyth, D. & McKay, D. M. Interferon-γ regulation of intestinal epithelial permeability. *J. Interf. Cytokine Res.* **29**, 133–143 (2009).

112. Bruewer, M. *et al.* Proinflammatory Cytokines Disrupt Epithelial Barrier Function by Apoptosis-Independent Mechanisms. *J. Immunol.* **171**, 6164–6172 (2003).

113. Utech, M. *et al.* Mechanism of IFN-gamma-induced endocytosis of tight junction proteins: myosin II-dependent vacuolarization of the apical plasma membrane. *Mol. Biol. Cell* **16**, 5040–52 (2005).

114. Hodge, J. A. *et al.* The mechanism of action of tofacitinib - an oral Janus kinase inhibitor for the treatment of rheumatoid arthritis. *Clinical and Experimental Rheumatology* vol. 34 318–328 (2016).

115. Panés, J. *et al.* Tofacitinib for induction and maintenance therapy of Crohn's disease: Results of two phase IIb randomised placebo-controlled trials. *Gut* **66**, 1049–1059 (2017).

116. Pfizer Inc. *Pfizer Announces U.S. FDA Approves XELJANZ® (tofacitinib) for the Treatment of Moderately to Severely Active Ulcerative Colitis | Pfizer*. https://www.pfizer.com/news/press-release/press-release-detail/pfizer_announces_u_s_fda_approves_xeljanz_tofacitinib_for_the_treatment_of_moderately_to_severely_active_ulcerative_colitis-0.

117. Schneider, C. A., Rasband, W. S. & Eliceiri, K. W. NIH Image to ImageJ: 25 years of image analysis. *Nature Methods* vol. 9 671–675 (2012).

118. Sato, T. *et al.* Long-term expansion of epithelial organoids from human colon, adenoma, adenocarcinoma, and Barrett's epithelium. *Gastroenterology* **141**, 1762–1772 (2011).

119. Stelzner, M. *et al.* A nomenclature for intestinal in vitro cultures. *Am. J. Physiol. - Gastrointest. Liver Physiol.* **302**, 1359–1363 (2012).

120. Xu, P., Becker, H., Elizalde, M., Masclee, A. & Jonkers, D. Intestinal organoid culture model is a valuable system to study epithelial barrier function in IBD. *Gut* vol. 67 1905–1906 (2018).

121. Van Itallie, C. M. & Anderson, J. M. Claudins and Epithelial Paracellular Transport. *Annu. Rev. Physiol.* **68**, 403–429 (2006).

122. Spence, J. R. *et al.* Directed differentiation of human pluripotent stem cells into intestinal tissue in vitro. *Nature* **470**, 105–110 (2011).

123. Foulke-Abel, J. *et al.* Human enteroids as an ex-vivo model of host–pathogen interactions in the gastrointestinal tract. *Exp. Biol. Med.* **239**, 1124–1134 (2014).

124. Zachos, N. C. *et al.* Human enteroids/colonoids and intestinal organoids functionally recapitulate normal intestinal physiology and pathophysiology. *Journal of Biological Chemistry* vol. 291 3759–3766 (2016).

125. Yu, H. *et al.* The Contributions of Human Mini-Intestines to the Study of Intestinal Physiology and Pathophysiology. *Annu. Rev. Physiol.* **79**, 291–312 (2017).

126. Smyth, D., Phan, V., Wang, A. & McKay, D. M. Interferon-γ-induced increases in intestinal epithelial macromolecular permeability requires the Src kinase Fyn. *Lab. Investig.* **91**, 764–777 (2011).

127. Rosen, M. J. *et al.* STAT6 activation in ulcerative colitis: A new target for prevention of IL-13-induced colon epithelial cell dysfunction. *Inflamm. Bowel Dis.* **17**, 2224–2234 (2011).

128. Rosen, M. J. *et al.* STAT6 Deficiency Ameliorates Severity of Oxazolone Colitis by Decreasing Expression of Claudin-2 and Th2-Inducing Cytokines. *J. Immunol.* **190**, 1849–1858 (2013).

129. McKay, D. M., Botelho, F., Ceponis, P. J. & Richards, C. D. Superantigen immune stimulation activates epithelial STAT-1 and PI 3-K: PI 3-K regulation of permeability. *Am. J. Physiol. Gastrointest. Liver Physiol.* **279**, G1094-103 (2000).

130. Watson, J. L. *et al.* Green tea polyphenol (-)-epigallocatechin gallate blocks epithelial barrier dysfunction provoked by IFN-γ but not by IL-4. *Am. J. Physiol. - Gastrointest. Liver Physiol.* **287**, (2004).

131. McKay, D. M. *et al.* Phosphatidylinositol 3′-kinase is a critical mediator of interferon-γ-induced increases in enteric epithelial permeability. *J. Pharmacol. Exp. Ther.* **320**, 1013–1022 (2007).

132. Yoshida, H. *et al.* Low dose CP-690,550 (tofacitinib), a pan-JAK inhibitor, accelerates the onset of experimental autoimmune encephalomyelitis by potentiating Th17 differentiation. *Biochem. Biophys. Res. Commun.* **418**, 234–240 (2012).

133. Rosengren, S., Corr, M., Firestein, G. S. & Boyle, D. L. The JAK inhibitor CP-690,550 (tofacitinib) inhibits TNF-induced chemokine expression in fibroblast-like synoviocytes: Autocrine role of type I interferon. *Ann. Rheum. Dis.* **71**, 440–447 (2012).

134. Sandborn, W. J. *et al.* Tofacitinib, an oral Janus kinase inhibitor, in active ulcerative colitis. *N. Engl. J. Med.* **367**, 616–624 (2012).

135. Shen, L. *et al.* Myosin light chain phosphorylation regulates barrier function by remodeling tight junction structure. *J. Cell Sci.* **119**, 2095–2106 (2006).

136. Liu, J., Walker, N. M., Cook, M. T., Ootani, A. & Clarke, L. L. Functional Cftr in crypt epithelium of organotypic enteroid cultures from murine small intestine. *Am. J. Physiol. - Cell Physiol.* **302**, 1492–1503 (2012).

137. Dowty, M. E. *et al.* Preclinical to clinical translation of tofacitinib, a janus kinase inhibitor, in rheumatoid arthritis. *J. Pharmacol. Exp. Ther.* **348**, 165–173 (2014).

138. Doody, K. M., Bourdeau, A. & Tremblay, M. L. T-cell protein tyrosine phosphatase is a key regulator in immune cell signaling: Lessons from the knockout mouse model and implications in human disease. *Immunol. Rev.* **228**, 325–341 (2009).

139. Schreiber, S. *et al.* Activation of signal transducer and activator of transcription (STAT) 1 in human chronic inflammatory bowel disease. *Gut* **51**, 379–385 (2002).

140. Zundler, S. & Neurath, M. F. Integrating immunologic signaling networks: The JAK/STAT pathway in colitis and colitis-associated cancer. *Vaccines* **4**, (2016).

141. Shawki, A. & McCole, D. F. Mechanisms of Intestinal Epithelial Barrier Dysfunction by Adherent-Invasive Escherichia coli. *CMGH* vol. 3 41–50 (2017).

142. King, S. J. & McCole, D. F. Epithelial-microbial diplomacy: escalating border tensions drive inflammation in inflammatory bowel disease. *Intest. Res.* **17**, 177–191 (2019).

143. Shawki, A. *et al.* 694 – The IBD Candidate Gene, Ptpn2, Regulates Segmented Filamentous Bacteria Mediated Th17 Response and Intestinal Barrier Protection Against Adherent-Invasive E. Coli. *Gastroenterology* **156**, S-151-S-152 (2019).

144. Ulugöl, S. *et al.* Deletion of Protein Tyrosine Phosphatase Nonreceptor Type 2 in Intestinal Epithelial Cells Results in Upregulation of the Related Phosphatase Protein Tyrosine Phosphatase Nonreceptor Type 23. *Inflamm. Intest. Dis.* **4**, 14–26 (2019).

145. France, M. M. & Turner, J. R. The mucosal barrier at a glance. *J. Cell Sci.* **130**, 307–314 (2017).

146. Weisshof, R. *et al.* Real-World Experience with Tofacitinib in IBD at a Tertiary Center. *Dig. Dis. Sci.* **64**, 1945–1951 (2019).

147. D'Amico, F., Parigi, T. L., Fiorino, G., Peyrin-Biroulet, L. & Danese, S. Tofacitinib in the treatment of ulcerative colitis: efficacy and safety from clinical trials to real-world experience. *Therap. Adv. Gastroenterol.* **12**, (2019).

148. Peeters, M. *et al.* Clustering of increased small intestinal permeability in families with Crohn's disease. *Gastroenterology* **113**, 802–7 (1997).

149. Adams, S. M. & Bornemann, P. H. Ulcerative colitis. *Am. Fam. Physician* **87**, 699–705 (2013).

150. Ordás, I., Eckmann, L., Talamini, M., Baumgart, D. C. & Sandborn, W. J. Ulcerative colitis. in *The Lancet* vol. 380 1606–1619 (2012).

151. Gisbert, J. P., Marín, A. C. & Chaparro, M. Systematic review: factors associated with relapse of inflammatory bowel disease after discontinuation of anti-TNF therapy. *Aliment. Pharmacol. Ther.* **42**, 391–405 (2015).

152. Baert, F. *et al.* Influence of immunogenicity on the long-term efficacy of infliximab in Crohn's disease. *N. Engl. J. Med.* **348**, 601–608 (2003).

153. Dhillon, S. Tofacitinib: A Review in Rheumatoid Arthritis. *Drugs* **77**, 1987–2001 (2017).

154. Berekmeri, A., Mahmood, F., Wittmann, M. & Helliwell, P. Tofacitinib for the treatment of psoriasis and psoriatic arthritis. *Expert Rev. Clin. Immunol.* **14**, 719–730 (2018).

155. De Vries, L. C. S. *et al.* A Jak1 selective kinase inhibitor and tofacitinib affect macrophage activation and function. *Inflamm. Bowel Dis.* **25**, 647–660 (2019).

156. Beattie, D. T. *et al.* Intestinally-restricted Janus Kinase inhibition: A potential approach to maximize the therapeutic index in inflammatory bowel disease therapy. *J. Inflamm. (United Kingdom)* **14**, 1–11 (2017).

157. Garcia-Hernandez, V., Quiros, M. & Nusrat, A. Intestinal epithelial claudins: Expression and regulation in homeostasis and inflammation. *Ann. N. Y. Acad. Sci.* **1397**, 66–79 (2017).

158. Buckley, A. & Turner, J. R. Cell biology of tight junction barrier regulation and mucosal disease. *Cold Spring Harb. Perspect. Biol.* **10**, (2018).

159. D'Incà, R. *et al.* Intestinal Permeability Test As A Predictor of Clinical Course in Crohn's Disease. *Am. J. Gastroenterol.* **94**, 2956–2960 (1999).

160. Hollander, D. *et al.* Increased intestinal permeability in patients with Crohn's disease and their relatives: A possible etiologic factor. *Ann. Intern. Med.* **105**, 883–885 (1986).

161. McCole, D. F. Regulation of epithelial barrier function by the inflammatory bowel disease candidate gene, PTPN2. *Ann. N. Y. Acad. Sci.* **1257**, 108–114 (2012).

162. Spalinger, M. R., McCole, D. F., Rogler, G. & Scharl, M. Role of protein tyrosine phosphatases in regulating the immune system: Implications for chronic intestinal inflammation. *Inflamm. Bowel Dis.* **21**, 645–655 (2015).

163. Clausen, B. E., Burkhardt, C., Reith, W., Renkawitz, R. & Förster, I. Conditional gene targeting in macrophages and granulocytes using LysMcre mice. *Transgenic Res.* **8**, 265–277 (1999).

164. Ghoreschi, K. *et al.* Modulation of Innate and Adaptive Immune Responses by Tofacitinib (CP-690,550). *J. Immunol.* **186**, 4234–4243 (2011).

165. Van Itallie, C., Rahner, C. & Anderson, J. M. Regulated expression of claudin-4 decreases paracellular conductance through a selective decrease in sodium permeability. *J. Clin. Invest.* **107**, 1319–1327 (2001).

166. Wang, Y., Van Boxel-Dezaire, A. H. H., Cheon, H., Yang, J. & Stark, G. R. STAT3 activation in response to IL-6 is prolonged by the binding of IL-6 receptor to EGF receptor. *Proc. Natl. Acad. Sci. U. S. A.* **110**, 16975–16980 (2013).

167. Tazuke, Y., Drongowski, R. A., Teitelbaum, D. H. & Coran, A. G. Interleukin-6 changes tight junction permeability and intracellular phospholipid contentin a human enterocyte cell culture model. *Pediatr. Surg. Int.* **19**, 321–325 (2003).

168. Wang, L., Srinivasan, S., Theiss, A. L., Merlin, D. & Sitaraman, S. V. Interleukin-6 Induces Keratin Expression in Intestinal Epithelial Cells: Potential Role of Keratin-8 in Interleukin-6-Induced Barrier Function Alterations. **282**, 8219–8227 (2007).

169. Vitkus, S. J. D., Hanifin, S. A. & McCee, D. W. Factors affecting Caco-2 intestinal epithelial cell interleukin-6 secretion. *Vitr. Cell. Dev. Biol. - Anim.* **34**, 660–664 (1998).

170. Sanceau, J., Wijdenes, J., Revel, M. & Wietzerbin, J. IL-6 and IL-6 receptor modulation by IFN-gamma and tumor necrosis factor-alpha in human monocytic cell line (THP-1). Priming effect of IFN-gamma. *J. Immunol.* **147**, 2630–7 (1991).

171. Song, M. & Kellum, J. A. Interleukin-6. *Crit. Care Med.* **33**, S463–S465 (2005).

172. Scharl, M., Hruz, P. & McCole, D. F. Protein tyrosine phosphatase non-receptor Type 2 regulates IFN-γ-induced cytokine signaling in THP-1 monocytes. *Inflamm. Bowel Dis.* **16**, 2055–2064 (2010).

173. Scharl, M. *et al.* Protein tyrosine phosphatase N2 regulates TNFα-induced signalling and cytokine secretion in human intestinal epithelial cells. *Gut* **60**, 189–197 (2011).

174. Cordes, F. *et al.* Tofacitinib Reprograms Human Monocytes of IBD Patients and Healthy Controls Toward a More Regulatory Phenotype. *Inflamm. Bowel Dis.* (2019).

175. Tsai, P. Y. *et al.* IL-22 Upregulates Epithelial Claudin-2 to Drive Diarrhea and Enteric Pathogen Clearance. *Cell Host Microbe* **21**, 671-681.e4 (2017).

176. Brand, S. *et al.* IL-22 is increased in active Crohn's disease and promotes proinflammatory gene expression and intestinal epithelial cell migration. *Am. J. Physiol. - Gastrointest. Liver Physiol.* **290**, (2006).

177. Yamamoto-Furusho, J. K. *et al.* Colonic epithelial upregulation of interleukin 22 (IL-22) in patients with ulcerative colitis. *Inflamm. Bowel Dis.* **16**, 1823 (2010).

178. Sugimoto, K. *et al.* IL-22 ameliorates intestinal inflammation in a mouse model of ulcerative colitis. *J. Clin. Invest.* **118**, 534–544 (2008).

179. Powell, N. *et al.* Interleukin-22 orchestrates a pathological endoplasmic reticulum stress response transcriptional programme in colonic epithelial cells. *Gut* (2019)

180. Pérez-Jeldres, T. *et al.* Targeting cytokine signaling and lymphocyte traffic via small molecules in inflammatory bowel disease: JAK inhibitors and S1PR agonists. *Frontiers in Pharmacology* vol. 10 (2019).

181. Blander, J. M. A new approach for inflammatory bowel disease therapy. *Nature Medicine* vol. 25 545–546 (2019).

182. FDA approves Boxed Warning about increased risk of blood clots and death with higher dose of arthritis and ulcerative colitis medicine tofacitinib (Xeljanz, Xeljanz XR) | FDA. https://www.fda.gov/drugs/drug-safety-and-availability/fda-approves-boxed-warning-about-increased-risk-blood-clots-and-death-higher-dose-arthritis-and.